GEOCHEMISTRY AND ORIGIN OF IGNEOUS ROCKS FROM THE ARCHEAN BEIT
BRIDGE COMPLEX, LIMPOPO BELT, SOUTH AFRICA

by
Mark D. Boryta

*Submitted in partial fulfillment
of the requirements for the degree of*
Master of Science in Geology

New Mexico Institute of Mining and Technology
Socorro, New Mexico
June 7, 1988

Abstract

The Archean Beit Bridge Complex (BBC) in the Central
Zone (CZ) of the Limpopo Belt of southern Africa is com-
prised of granulite-facies metasediments (quartzites,
pelites, rare carbonates), amphibolites (mainly dikes and
sills) and quartzofeldspathic gneisses (chiefly granitic
intrusives). Radiometric dates constrain the age of the
BBC to 3300-3500 Ma.

Amphibolites have relatively flat REE patterns with
slight negative Eu anomalies. Depletion of Th, U and Cs in
a few samples probably occurred during granulite-facies
metamorphism. These rocks also exhibit a strong subduction
zone component (Nb-Ta depletion relative to LILE) as well
as incompatible element ratios (e.g., La/Yb, Ti/Y, Zr/Nb)
that compare favorably with modern basalts from arc-related
tectonic settings. Trace element modeling suggests that
BBC amphibolites may be derived by 10-20% batch melting of
an LILE-enriched lherzolite source, followed by 5-20%
fractional crystallization of olivine, clinopyroxene and
magnetite. BBC granitic gneisses range in composition from
tonalite to granite. Previous studies have interpreted
most of the gneisses as metasediments, but their major and
trace element distributions strongly suggest an igneous
parentage. The gneisses have REE distributions ranging
from strongly to slightly LREE-enriched, with both positive
and negative Eu anomalies. These rocks also have
subduction zone geochemical signatures, similar to arc-
related dacites and rhyolites.

A new model, consistent with geochemical and geologic
data and with radiometric dates, adopts a dual collision
scenario. The Kaapvaal/Limpopo collision at about 3200 Ma
involves partial subduction of the BBC to lower crustal
levels where it undergoes high-pressure granulite-facies
metamorphism and is intruded by arc-related magmas,
followed by rapid uplift and erosion. A second collision,
at about 2800 Ma, involves the Zimbabwe craton and results
in a second granulite-grade metamorphic event, and crustal
shortening by thickening.

Acknowledgements

Table of Contents

List of Figures

List of Figures (continued)

List of Tables

Introduction

The Limpopo Mobile Belt of southern Africa is an ENE-trending zone
of Archean high-grade para- and orthogneisses which separates the
Kaapvaal craton to the south from the Zimbabwe craton to the north
(Fig. 1). It is exposed along a length of about 600 km and reaches
about 300 km in width, disappearing under Kalahari sands in the west
(in Botswana) and under other younger igneous and sedimentary
formations in the east (in Mozambique). The Belt is divided into three
zones (the Central Zone (CZ) and bordering Northern and Southern
Marginal Zones (NMZ and SMZ)) on the basis of lithologies and
structural trends. The NMZ and SMZ are metamorphic equivalents of
granite-greenstone lithologies of the Zimbabwe and Kaapvaal cratons,
respectively (Tankard et al., 1982; Barton, 1983b), while the CZ
represents its own unique lithologic package.

The purpose of this study is to examine the geochemical evidence
from major lithologies of the CZ which are well exposed in the Messina
area (Fig. 2). Geochemical interpretations can be combined with struc-
tural and metamorphic histories that have been previously outlined
(e.g. Robertson, 1968; Coward et al., 1973; Mason, 1973; Horrocks,
1980; Du Toit et al., 1983; Watkeys et al., 1983) and many geochronolo-
gical studies that have been completed (e.g. Barton et al., 1979;
Barton et al., 1983a-c). By doing so it may be possible to constrain
the tectonic setting of this complex terrain. This is important to our
understanding of the origin and early development of the earth's crust.

Figure 1

Generalized geology of southern Africa and location of study area.
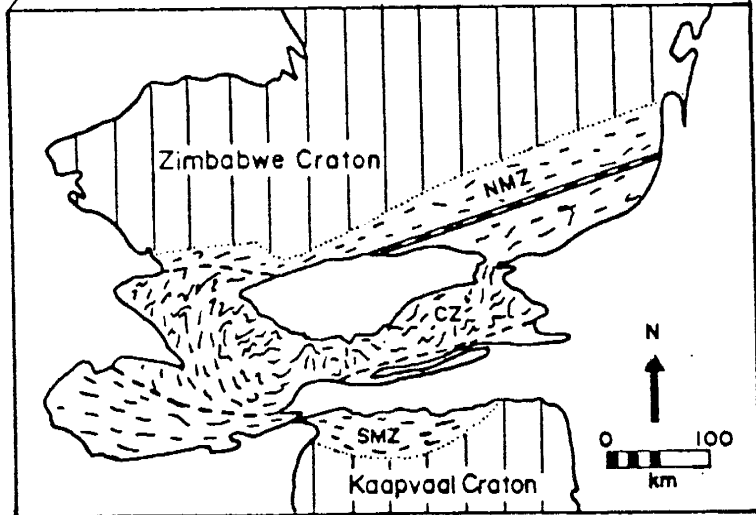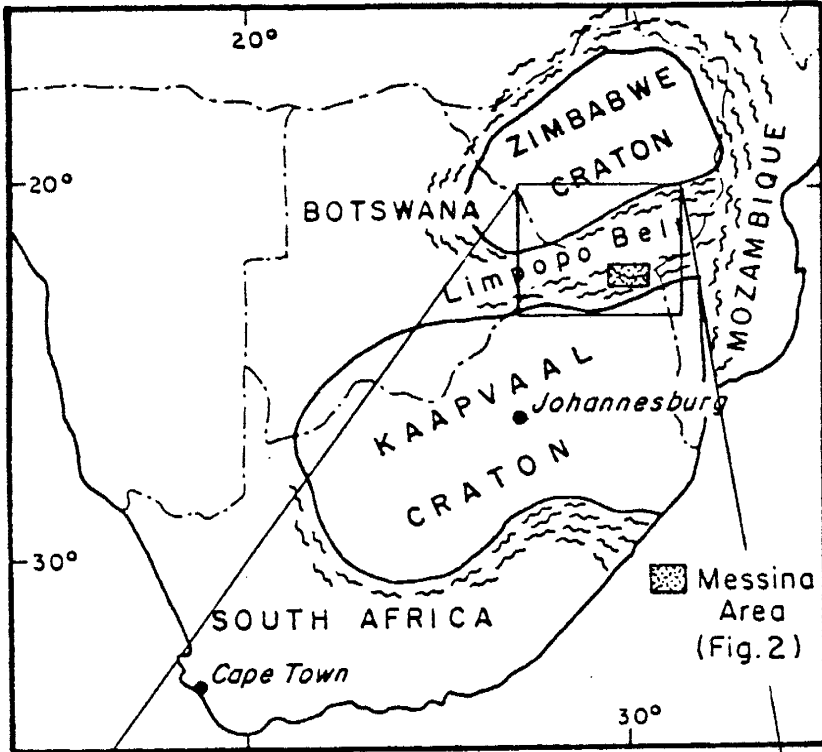
Structural trends in the zones of the
Limpopo Mobile Belt
(after Watkeys et al., 1983)

Figure 2
Geologic and structural map of the study area with sample locations.
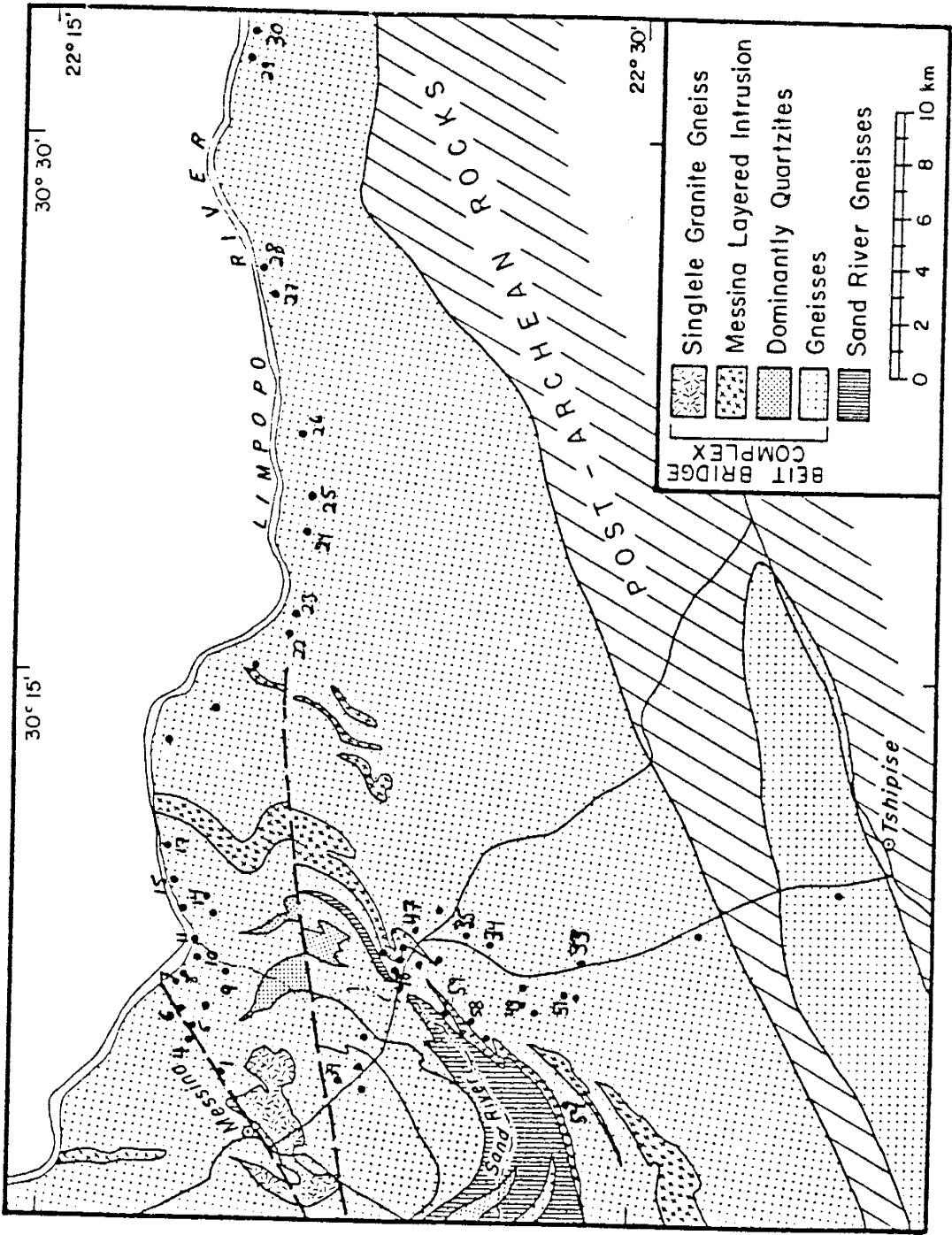
The few studies that include chemical compositions of Limpopo rocks are limited in scope and base conclusions on generally accepted interpretations of others (i.e. Brandl, 1983). Some workers introduce major element analyses of the 'supracrustal rocks' of the Beit Bridge Complex, plot these limited data on a few diagrams and leave interpretations to the reader. Others base their interpretations on rock associations without considering the chemical compositions of the rocks. None has paid attention to the trace element characteristics of the series.

Several authors base their interpretations of the evolution of the Limpopo Belt on the assumption that felsic rocks of the Beit Bridge Complex are metasediments. Light (1982, p. 329) has interpreted these rocks as volcanics and Shackleton (1986, p. 343) refers to them as a 'metasedimentary cover sequence' overlying the Sand River Gneisses. Burke et al. (1985, p. 18) refer to the Beit Bridge Complex as a 'carbonate shelf facies' and other authors consider these rocks as a combination of para- and orthogneisses. Major and trace element characteristics suggest that at least some of the felsic rocks in the study area have igneous rather than sedimentary protoliths. Such a conclusion has an obvious bearing on interpretations regarding the tectonic evolution of the Limpopo Belt.

Geology of the Limpopo Belt

The general geology of the Limpopo Belt is summarized here from the works of several others. A more detailed summary of the geology of the field area follows based mostly on the work of Horrocks (1983) and Fripp (1983).

The Northern Marginal Zone

The NMZ is characterized by multiply-deformed isoclinal folds and by a variably developed coarse foliation which is not found in the cratonic environment to the north. The foliation and the major fold axes trend generally ENE (Mason, 1973). Some of the later deformational structures have been traced from the NMZ into the Zimbabwe Craton (Coward et al., 1976).

Metamorphism in the NMZ has been studied by Robertson (1968) and an overview is presented by Mason (1973). Mason divides the NMZ into three subzones on the basis of metamorphic grade: a well-preserved granulite-charnockite terrain nearest to the craton, a sheared retrograde granulite terrain, and the Tuli-Sabi shear belt, which separates the NMZ from the CZ. Robertson (1968) reports evidence for potassium metasomatism in portions of the NMZ but does not speculate as to when this occurred in relation to the various metamorphic events.

The granulite-charnockite terrain contains a complete range of rock compositions, from acid to ultramafic granulites (Robertson, 1968; Mason, 1973). Charnockitic gneisses are widespread. Pyroxene granulites and associated basic granulites are interlayered with

gneissic granulites and magnetite quartzites. This assemblage is the metamorphic equivalent of lower grade greenstone belt material of the Zimbabwe Craton.

The retrograded granulite subzone is similar to the granulite-charnockite terrain, but a greater amount of shearing has facilitated the introduction of late metamorphic fluids into the rocks. The shearing (and associated retrogression) is probably related to the events forming the Tuli-Sabi shear belt (Mason, 1973).

The Tuli-Sabi shear belt, extending over the entire length of the Limpopo Belt, is one of the largest features of its kind on the African continent. Its width varies from about 5 to 50 km. The shear belt is characterized by thin flinty crush bands which occur as curvilinear features separating strongly sheared segments of the country rocks (mainly flaser gneisses and mylonitic gneisses), thus imparting a distinctly braided character to the belt (Mason, 1973). Barton (1983b) notes that in a single locality, fabric evidence for right-lateral, left-lateral, normal, and reverse motions may be seen; shearing has induced widespread retrogression from higher grades of metamorphic mineral assemblages, and movement has occurred repeatedly into the Phanerozoic.

The Southern Marginal Zone

Mason (1973) maintains that the SMZ is a mirror image of its northern counterpart. He divides it into two subzones: a granulite subzone adjacent to the Kaapvaal craton and the Soutpansberg (or Palala) fault zone which separates the SMZ from the CZ. Proterozoic

and younger sedimentary rocks cover much of the SMZ, but extensive granulite terrains are exposed in some portions of the area.

A detailed overview of the SMZ is presented by Du Toit et al. (1983). They show that the SMZ is very different from the NMZ. Structures in the SMZ are indicative of a complex deformational history, and thus the zone cannot be characterized by a single structural orientation. It appears that there is an arcuate grain with dominantly ENE-trending structures in the east, E-trending structures in the central portion and WNW- to NW-trending structures in eastern Botswana (Du Toit et al., 1983; Key et al., 1983).

Du Toit et al. (1983) propose three metamorphic events for the SMZ. M_1 is an inferred event of granulite-facies conditions and M_2 is a low-pressure granulite-facies overprinting of M_1. These two events are distinguished from one another by the presence of two generations of orthopyroxene. M_1 is characterized by the stable coexistence of garnet + orthopyroxene + biotite while M_2 is characterized by replacement of garnet by hypersthene + cordierite. M_3 is a retrogressive event related to shearing and hydration in the southern part of the granulite terrain, and is responsible for the relative positions of the orthoamphibole and orthopyroxene isograds in the SMZ. Metamorphic conditions during the granulite facies events are as follows: M_1 peaks at $>800^{\circ}C$ and at least 9.5 Kb, and M_2 peaks at pressures of 7.2 - 8.2 Kb and temperatures between $780-820^{\circ}C$. The authors suggest that the second event represents rapid erosion of an overthickened tectonic pile.

The Central Zone

The lithologies present in the marginal zones appear to be the metamorphic equivalents of those on the adjoining cratons. Greenstone belt successions on the Kaapvaal and Zimbabwe cratons have been traced through the isograds into the SMZ and NMZ, respectively (Du Toit et al., 1983; Mason, 1973). The Central Zone contains its own distinctive lithologic package as well as its own structural style.

The dominant structural trend in the CZ is approximately N-S. Dome and basin structures and intricate folding and refolding are evident on all scales. Watkeys et al. (1983) distinguish six deformational events. D_0 affects the basement lithologies only (the Sand River Gneisses). The subsequent five deformations also affect the Beit Bridge Complex. The style of deformation is terminated by the bounding shear zones mentioned above so that correlation of units between the CZ and either the NMZ or SMZ is not possible.

Watkeys et al. (1983) also outline three distinct regional metamorphic events and three later localized events in the CZ. M_1, which is coeval with D_1, is characterized by pressures in excess of 11 Kb and temperatures above $830^{\circ}C$. This metamorphism outlasted the deformation and ended with a rapid decrease in pressure to about 10.2 Kb. The second metamorphic event (M_2) is also of granulite facies, and mineral assemblages (kornerupine + corundum) indicative of high temperatures ($840 - 910^{\circ}C$) and pressures ($8.7 - 10.2$ Kb) are overprinted by assemblages indicative of temperatures above $740^{\circ}C$ and pressures constrained between $4.9 - 8.7$ Kb. M_2 is correlated with D_2. The conditions of the M_3 event are not well constrained, but are estimated at

about 625 - 750°C and about 6 - 7 Kb. This event may have lasted from the end of D_2 into the beginning of D_4. The timing of each of these events is given in Table I.

Table I
Summary of the Geologic Events occurring in the Limpopo Belt

Age[*]	SMZ	Age	CZ	Age	NMZ
(M3)[+] 750°C, 8 Kb (wet)					
2480 | | 2600	Bandelierkop post-tectonic monzonites and related plutons, trending NE and extending from Kaapvaal through SMZ and into CZ (includes Matok's Pluton)				
		2605	Pikwe area Met. (eastern CZ) (M2) metamorphic event 870°C, 8.7-10.2 Kb		
2650	Retrograde Granulite metamorphic event (M2) 800°C, 7.6-8.5 Kb				
		2693	Emplacement (?) of Bulai Gneiss	2700	M2?
				2870	Bangala Granulite facies (M1) > 750°C, > 5Kb
2960 | 3000	dike emplacement near Zanzibar, eastern SMZ				
		3060 M1r	Stockford dikes 840°C, 10.2-11 Kb		
M1?	800°C, > 9Kb				
		3150 M1p	Rb/Sr Met age, > 830°C, > 11 Kb		
3230	Def. of Zanzibar Gneiss (Bots)				
		3270	MLI Pb-Pb emplacement age		
3295	Baviaanskloof (Kaapvaal)	3567	Causeway Dikes		
		3786	Sand River Gneisses		

[*] Age in Ma. Events marked by ? or in parentheses are not well constrained.

[+] Metamorphic temperatures and pressures are given in °C and kilobars.

Data Sources: Cahen et al., 1984, p. 52; Barton, 1983b; Barton et al., 1983a; Watkeys et al., 1983.

Geology of the Study Area

The geology of the area of this report has been studied in detail by Horrocks (1983). Major rock types include the basement or Sand River gneisses (SRG); the Beit Bridge Complex (BBC); the Messina Layered Intrusion (MLI); two units of lesser extent which are the Singelele and Bulai Gneisses; and mafic dikes of different ages.

Rock Types

Rock types exposed in the CZ are predominantly metamorphic rocks of Archean age. An overlying succcession of Karroo sediments (late Paleozoic, Fig. 2) is not discussed in this report.

The Sand River Gneisses, which Barton et al. (1983c) dated at 3790 Ma, are a group of banded and migmatitic gray granodioritic gneisses. These are some of the oldest rocks known on the African continent, and may have been the basement upon which the supracrustal rocks of the BBC were deposited. Mafic dikes dated at 3570 Ma (Barton et al., 1977) are recognized only within the SRG.

The Beit Bridge Complex is composed of six rock types: garnet-iferous paragneisses (metapelites), quartzofeldspathic gneisses, calc-silicate gneisses, magnetite-quartzites, quartzites, and amphibolites. As part of this study, major and trace element analyses were made of each of these rock types. Interpretations based on the analyses of the amphibolites and the granitic gneisses form the bulk of the research presented here. According to Horrocks (1983), the most abundant rocks

in the Messina area are granitic gneisses, which range in composition from tonalite to granite. Mafic dikes cutting the Sand River Gneisses, the BBC, and the MLI are dated at 3000 Ma by Barton et al. (1983b) by the Rb-Sr method.

The Messina Layered Intrusion has been studied by Barton et al. (1979). It cross-cuts and is complexly infolded with the SRG and the rocks of the BBC. The MLI consists of anorthositic and gabbroic gneisses and was emplaced at about 3270 Ma (Barton, 1983a). Barton et al. (1979) believe that the intrusion was emplaced at a high crustal level (<12 km depth) at the contact between the SRG and the BBC and within the BBC itself. The chemical compositions of their samples form a weak calc-alkaline trend, but Barton et al. (1979) conclude that the composition of the parent magma is a quartz tholeiite. They suggest that the calc-alkaline trend reflects the abundance of cumulus plagioclase in the exposed rock types and that the volume of the parent magma greatly exceeds the volume of the cumulus crystals. They envision the MLI as having formed from a dry and reasonably unoxidized magma in a continental environment. The Fiskenaesset Complex of southwest Greenland, in contrast, appears to have formed from a wet, oxidized basaltic magma, possibly in a back arc environment.

The Singelele Gneiss is an orange-weathering, quartzofeldspathic gneiss interlayered with the BBC. Contacts can be found that indicate both conformable and discordant relationships with the supracrustal rocks. Of several varieties, a heterogeneous banded type is most common (Watkeys et al., 1983). The origin of the Singelele Gneiss is uncertain, and Watkeys et al. (1983) review a number of current

hypotheses. It could be derived from an anatectic melt, a restite, a metamorphosed felsic volcanic or an arkosic sediment. Efforts to determine an age for this unit have failed. Watkeys et al. (1983) prefer to interpret the Singelele Gneiss as a granitic melt, possibly associated with the MLI, which was injected into the BBC and subsequently underwent anatexis during regional high-grade metamorphism.

The Bulai Gneiss crops out northwest of Messina. This body ranges from trondhjemitic to adamellitic in composition, and is interpreted to be intrusive in two stages: as a syntectonic igneous magma and then as a solid diapir (Watkeys et al., 1983).

Structure

Structural studies of the Messina area by Horrocks (1983) and Fripp (1983) indicate that several events involving intense folding affected the rocks (Fig. 2). The SRG underwent at least one and probably two deformational events prior to the emplacement of the BBC (Fripp, 1983).

In the northwest section of the study area (Fig. 2), folding is visible at the scale of the mapping, while towards the southeast attenuation of the units has resulted in a strong ENE orientation (Horrocks, 1983). Horrocks reports evidence for at least two and possibly three events of fold closure and speculates that these may be the result of continuous deformation. Fripp (1983) describes dome-basin type interference patterns and relates them to a D_5 overprinting of D_4 folds. His outline of deformational events is not equivalent to

that of Watkeys et al. (1983).

Faults occur in two sets, trending NNW and NNE, with evidence for vertical and transcurrent movements occurring repeatedly from the late Proterozoic into the Phanerozoic (Mason, 1973; Watkeys et al., 1983).

Metamorphism

Mineral assemblages indicative of the granulite facies are described by Fripp (1983), Horrocks (1983), and Brandl (1983). Assemblages in the SRG are not suitable for determination of the temperatures and pressures of metamorphism. Two units in the BBC, however, contain abundant geothermobarometers. Data from amphibolites and metapelites result in pressures and temperatures of about 10 Kb and 900°C for the highest grade of metamorphism. Horrocks (1983) reports assemblages from the metapelites that record a lower-grade event of 6-7 Kb and 700°C. Such conditions are preserved in the amphibolites by the assemblage orthopyroxene + clinopyroxene + hornblende + plagioclase + quartz + magnetite, and in the metapelites by garnet + cordierite + biotite + sillimanite + plagioclase + quartz.

Analytical Procedures

Rocks were collected by K. C. Condie, H. C. Crow, and D. J. Wronkiewicz from outcrops east and south of Messina in the Republic of South Africa (Fig. 2). Three hand specimens of each sample, collected from the locations shown in the Figure, are used as follows: one is kept for reference, one is used for geochemical analysis, and one is cut for a thin section. Thin sections are prepared and stained with sodium cobaltinitrate to facilitate the identification of potassium feldspars. Samples used for chemical analyses are powdered in three steps. A chipmunk jaw crusher reduces the rock to pieces approximately the size of pebbles and a rotary porcelain disc grinder reduces the sample to a powder. Powders are further pulverized to -200 mesh with a mechanical agate mortar and pestle. These techniques are expected to produce very little contamination.

X-Ray Fluorescence

Major and trace elements Y, Zr, Nb, Rb, Sr, Ba, Pb, V, and Ni are determined by X-ray fluorescence (XRF) using an automated Rigaku 3064 XRF spectrometer coupled with a PDP-11 computer and in-house software at the New Mexico Bureau of Mines and Mineral Resources. Two techniques are involved, following the methods of Norrish and Hutton (1969) and Norrish and Chappel (1977). Fusion discs are made for major element analysis and trace elements are determined using pressed powder pellets. Precision and accuracy tables for XRF are given in Appendix A.

Fusion discs are made by fusing a fixed proportion of sample powder and a flux composed of lithium borate and lanthanum oxide. The ratio used is 0.5 grams of powder to 2.7 grams of flux. The procedure involves mixing the powder and flux with ammonium nitrate (an oxidant which is lost upon heating) in a Pt (5% Au) crucible. The mixture is heated over an open flame until molten for about 15 minutes. This liquid is quenched in an aluminum platten, and the resulting glass disc is allowed to cool. Standards for calibration are prepared in the same manner.

Pressed powder pellets are made by adding one drop of polyvinyl alchohol (a binder) per gram of sample powder to about 8 grams of powder; this mixture is pressed with a boric acid backing to 20 tons per square inch for about one minute. Quartz-rich samples are pressed to 10 tons per square inch to reduce the possibility of exfoliation.

Instrumental Neutron Activation Analysis

Cs, Th, U, Sc, Cr, Co, Hf, Ta, La, Ce, Sm, Eu, Tb, Yb, and Lu are determined by INAA using methods similar to those described by Jacobs et al. (1977) and Gibson and Jagam (1980). Approximately 300 milligrams of powder are sealed in polyethylene vials and irradiated in the Annular Core Research Reactor at Sandia National Laboratory in Albuquerque, New Mexico. The vials are subjected to a neutron flux estimated at 2.7×10^{13} for ten thousand seconds. An air hose attached to the container in the irradiation chamber assures an even flux on all samples. Gamma ray counts are conducted after about 7 and 40 days with a coaxial intrinsic Ge-crystal detector using a Nuclear Data 6600

multichannel analyser coupled with an LSI-11 computer. Three vials containing approximately 200 mg of fly ash standard NBS-1633a are irradiated with the samples for use as reference standards using methods similar to those of Korotev (1987). Other international rock standards are included to aid in the determination of accuracy. Data are reduced by computer using TEABAGS (Trace Element Analysis By Automated Gamma-ray Spectrometry, Lindstrom and Korotev, 1982) software. Precision and accuracy tables for INAA are given in Appendix A.

Mafic Rocks

Field Relationships

Condie (personal communication, 1986) maintains that the amphibolites, or mafic rocks, intruded into the surrounding lithologies as hypabyssal sills and/or dikes. Crosscutting relationships are not well exposed and it is possible that at least a few of the units are extrusive. Many of the amphibolite units appear to be conformable. Pre-metamorphic textures are not preserved. One sample (MS-5), collected for a previous study, may be from a dike related to the MLI. The other mafic rocks are from the BBC. The mafic units make up a minor proportion of the Archean terrain of the study area.

Petrography

The relative proportions of major phases are highly variable in the mafic rocks. Intermediate plagioclase is the most abundant mineral, comprising from 3 to 70% with anorthite contents ranging from An_{30} to An_{60}. Twinning is common and some twin lamellae are bent. Clinopyroxene ranges from 5 to 60%, averaging about 20 to 25%. Orthopyroxene is also common in all but one sample (LMP-51), and ranges from 5 to 30%, averaging about 10 to 15%. Amphibole is present in the form of either reddish-brown or green hornblende; one sample contains only 2% (LMP-1) and one sample contains 80% (LMP-10). In the other samples the abundance is variable, usually between 10 and 50%. The remainder of the mode consists of either garnet or quartz varying from 0 to 10%; if garnet is present then quartz is not, and vice versa.

The relative proportions of trace minerals also vary and include, in order of decreasing abundance: opaque minerals, zircon, apatite, and sphene (and possibly zoisite in one sample); calcite is rarely present as vein filling. One sample (LMP-49) is composed of about 60% clinopyroxene and 25% hornblende, contains a negligible proportion of opaque minerals, and up to 1% sphene and appreciable amounts of both zircon and apatite.

Textures are generally polygonal equigranular granoblastic, with amphiboles showing a weak preferred alignment. Grain sizes vary but average about 1 to 3 mm.

A detailed description of each sample appears in Appendix B.

Chemical Composition

Major and trace element data for the mafic rocks are presented in Table II. In order to use geochemical characteristics to classify metamorphic rocks one must first determine whether those characteristics are original or whether they are the result of mobilization. Several studies suggest that mobilization may or may not occur on a regional or outcrop scale (for examples, see Sheraton, 1985; Lamb et al., 1986; Fowler, 1986; and Fernandes, 1987), and Condie and Allen (1984) have shown that depletions in K_2O, Rb, Cs, Th, U, and Pb may be associated with the passage of a fluid phase.

There are relatively few methods that delineate the effects of high-grade metamorphism on rock compositions. One method involves tracing rock units across metamorphic isograds while assuming chemical homogeneity or continuity within the unit.

Table II
Chemical Compositions of BBC Mafic Rocks

SAMPLE	LMP-1	LMP-10	LMP-14	LMP-22	LMP-23	LMP-25	LMP-45	LMP-51
SiO_2	49.65	44.43	48.72	49.94	50.47	52.40	47.86	53.30
TiO_2	1.19	1.16	0.85	1.02	0.76	0.43	1.10	0.69
Al_2O_3	17.76	14.35	16.09	15.27	14.76	16.88	16.07	16.27
Fe_2O_3T	9.31	16.08	10.51	12.51	11.35	8.02	11.83	10.11
MnO	0.18	0.22	0.11	0.18	0.15	0.16	0.16	0.14
MgO	5.43	8.84	8.61	7.48	8.25	5.67	8.26	7.15
CaO	14.88	12.22	10.41	9.60	11.16	11.38	11.42	9.63
Na_2O	2.70	1.66	3.00	2.94	2.31	3.64	2.69	2.76
K_2O	0.16	0.80	0.83	0.94	0.33	1.49	0.78	0.90
P_2O_5	0.12	0.07	0.08	0.10	0.07	0.05	0.09	0.08
LOI	0.19	0.29	1.07	0.56	0.59	1.17	0.79	0.54
Total	101.57	100.12	100.28	100.54	100.20	101.29	101.05	101.57
Rb	5.3	10	13	26	16	57	19	18
Cs	< 0.10	< 0.10	0.13	< 0.10	0.19	0.25	0.14	0.30
Sr	166	78	123	159	115	111	129	113
Ba	53	74	229	552	105	187	66	371
Th	0.67	0.48	0.61	0.74	1.1	0.51	0.42	1.2
U	0.21	0.28	0.46	0.18	0.28	0.42	0.17	1.2
Pb	12	9.0	17	11	25	16	9.9	16
Sc	44	55	33	33	38	39	40	32
Y	30	30	18	23	17	13	24	18
Zr	82	53	58	71	52	40	68	66
Hf	2.6	1.8	1.6	2.0	1.5	1.2	2.0	2.1
Nb	4.8	4.3	4.3	4.4	4.2	4.1	4.3	4.6
Ta	0.27	0.13	0.20	0.18	0.21	0.24	0.17	0.28
La	6.9	4.0	4.7	5.6	5.5	4.5	5.0	9.3
Ce	17	11	12	15	13	10	14	19
Sm	3.9	2.9	2.3	2.7	2.2	1.2	2.8	2.6
Eu	1.2	0.94	0.81	0.90	0.81	0.38	0.91	0.87
Tb	0.83	0.80	0.43	0.57	0.41	0.29	0.63	0.57
Yb	3.0	3.5	1.8	2.3	1.9	1.4	2.4	2.0
Lu	0.48	0.58	0.28	0.38	0.31	0.24	0.37	0.31
V	296	418	254	297	245	253	341	247
Cr	366	255	354	237	296	254	365	236
Co	55	68	46	48	52	45	47	43
Ni	160	166	160	137	90	128	115	114
Mg #	57	55	65	57	62	61	61	61

Major elements in wt. %; trace elements in ppm. Fe_2O_3T = total Fe as Fe_2O_3. Mg # is $[MgO/(MgO+FeO*)] * 100$, oxides in mol. proportions.

Table II (continued)

SAMPLE	LMP-6	LMP-54	LMP-34	LMP-47	MS-5	LMP-49	LMP-58
SiO_2	56.16	52.72	50.40	48.57	46.91	47.86	54.55
TiO_2	0.62	0.79	1.15	0.87	1.38	1.26	1.72
Al_2O_3	7.18	6.08	13.59	16.76	15.46	13.44	13.18
Fe_2O_3T	11.21	14.12	14.02	9.91	15.17	10.90	15.48
MnO	0.22	0.24	0.19	0.17	0.19	0.20	0.18
MgO	12.01	12.97	7.20	8.86	9.03	7.28	2.69
CaO	12.26	12.24	10.72	12.51	11.20	15.79	6.87
Na_2O	1.31	1.17	3.05	2.08	0.97	1.86	3.03
K_2O	0.28	0.37	0.61	0.74	0.44	1.59	1.19
P_2O_5	0.05	0.07	0.09	0.07	0.29	0.32	0.39
LOI	0.07	0.00	0.00	0.85	0.00	0.74	0.94
Total	101.37	100.77	101.02	101.39	101.04	101.24	100.22
Rb	5.7	7.4	6.8	38	7.5	56	36
Cs	< 0.10	< 0.10	< 0.10	0.13	< 0.10	0.20	0.88
Sr	78	136	114	117	89	344	154
Ba	294	147	124	30	24	402	417
Th	0.66	0.18	0.24	< 0.10	0.26	13	4.9
U	0.29	< 0.05	0.23	< 0.05	0.07	2.9	0.77
Pb	10	8.4	14	10	13	13	15
Sc	28	31	40	39	50	28	28
Y	15	19	22	19	48	36	70
Zr	62	70	66	48	128	144	281
Hf	1.8	2.1	2.3	1.3	4.0	4.6	8.0
Nb	4.5	5.2	4.6	4.1	5.7	39	16
Ta	0.23	0.36	0.20	0.10	0.45	1.7	0.86
La	8.7	10	4.6	2.6	14	94	26
Ce	21	27	12	7.1	40	207	62
Sm	2.8	4.4	2.8	2.0	7.7	20	9.8
Eu	0.74	1.0	0.93	0.70	2.2	3.3	2.7
Tb	0.45	0.70	0.57	0.48	1.4	1.5	2.0
Yb	1.4	1.8	2.1	1.9	4.9	3.4	6.5
Lu	0.23	0.28	0.33	0.32	0.74	0.53	1.0
V	196	209	353	262	297	264	177
Cr	1392	588	71	832	334	298	10
Co	60	87	54	46	56	52	35
Ni	261	333	90	160	129	186	17
Mg #	71	67	54	67	57	60	28

Another method is to plot elements on igneous variation diagrams. To use this method one must assume that elements behave in a systematic manner during igneous processes, and that such processes were similar in the Archean to those operating today. It is also assumed that the BBC mafic rocks are all genetically related. This postulation is supported by the presence of trends indicative of magmatic processes on several geochemical plots.

The samples are classified according to three different schemes, involving both major and trace elements, in Figures 3 through 5. The majority of the samples fall in the subalkaline mafic fields on the discrimination diagrams of Winchester and Floyd (1977). Most samples fall in the subalkaline basalt field on the SiO_2 vs. Nb/Y and SiO_2 vs. Zr/TiO_2 diagrams (Fig. 3) and in the basaltic andesite field on the Zr/TiO_2 vs. Nb/Y diagram (Fig. 4). On the classification scheme of Bavington and Taylor (1980), the samples fall in the tholeiite field (Fig. 5). Several of the samples are anomalous because they plot in different fields on different diagrams. Comparison of the SiO_2-Zr/TiO_2-Nb/Y plots reveals that SiO_2 may have been mobile in samples 25, 51, 6, and 54. Indeed, a quartz vein is observed in the thin section of LMP-6. It is possible, therefore, that samples 6 and 54 are derived from rocks similar in composition to basaltic komatiites. Relative to the high-magnesium andesites (boninites) of Hickey and Frey (1982), the BBC samples are poor in Al_2O_3 and rich in CaO, Y, Zr, Hf, and REE; however, these authors suggest that there is a wider range in these elements than their data indicate due to our poor understanding of mantle metasomatism associated with subduction zones.

Figure 3

Classification of BBC Rocks according to SiO_2 vs. Zr/TiO_2. Fields from Winchester and Floyd (1977). Open circles, granites; filled squares, tonalitic to granodioritic gneisses; +, amphibolites; x, altered amphibolites; open squares, anomalous mafic rocks. See text for further descriptions.
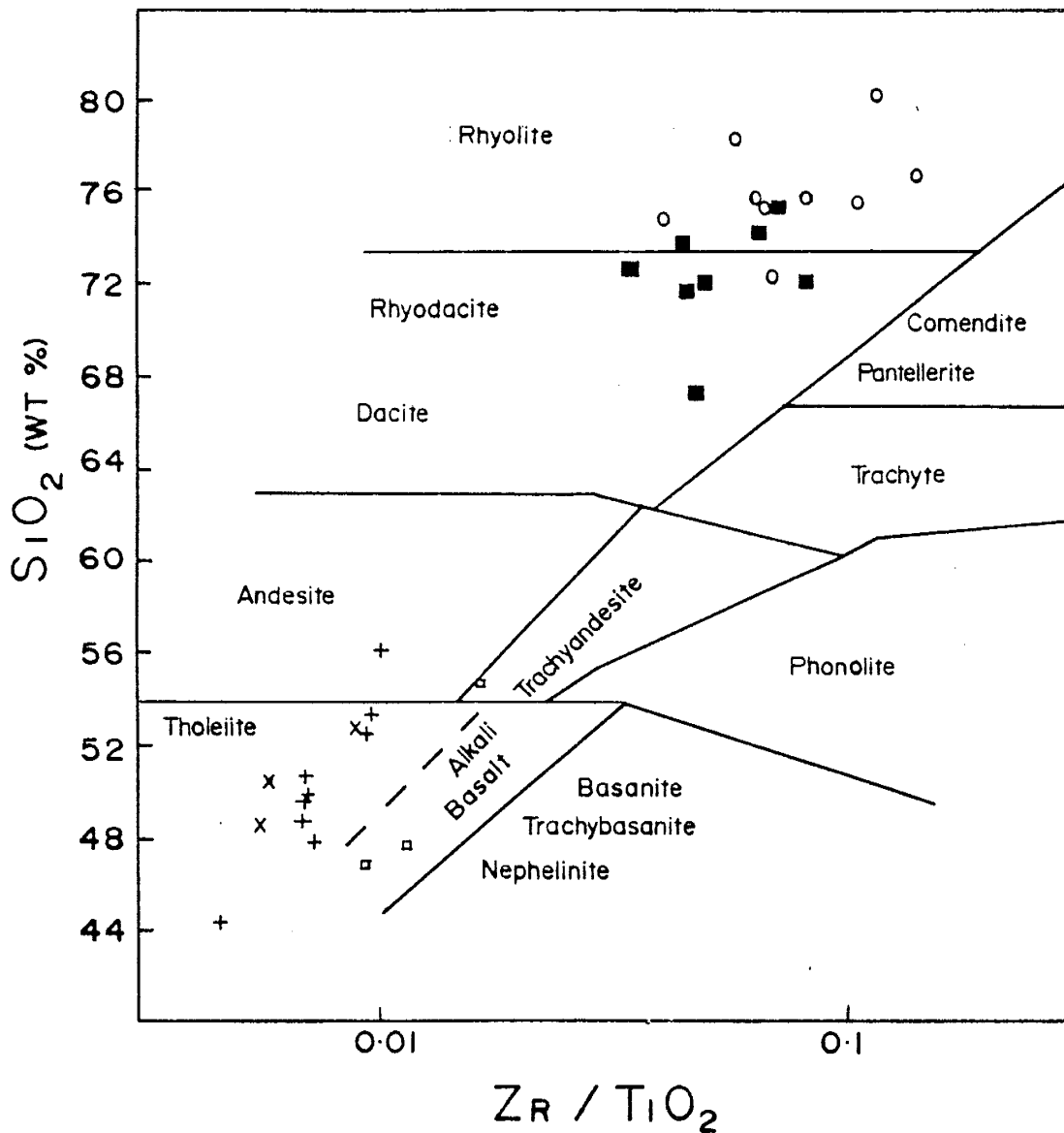
Figure 4
Classification of BBC Rocks according to Nb/Y vs. Zr/TiO_2. Fields
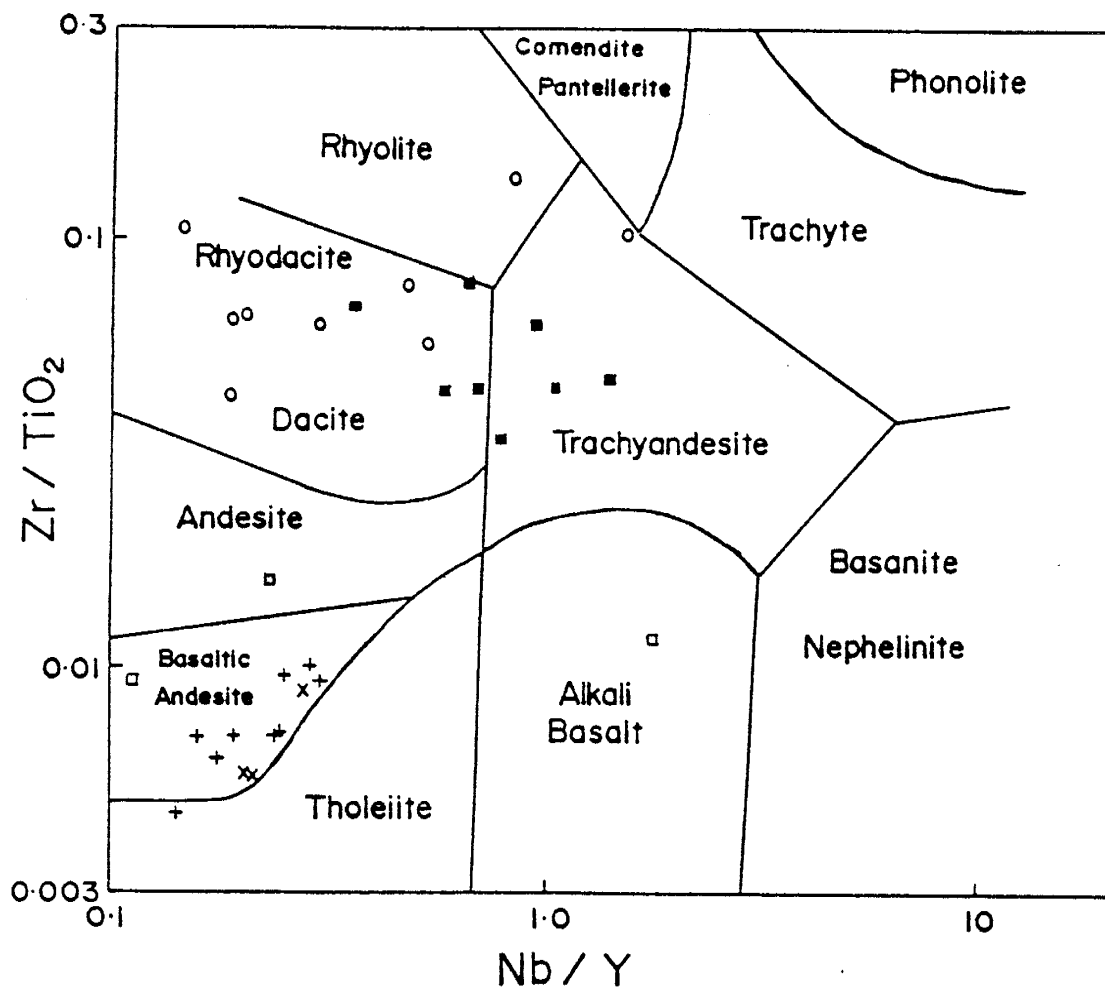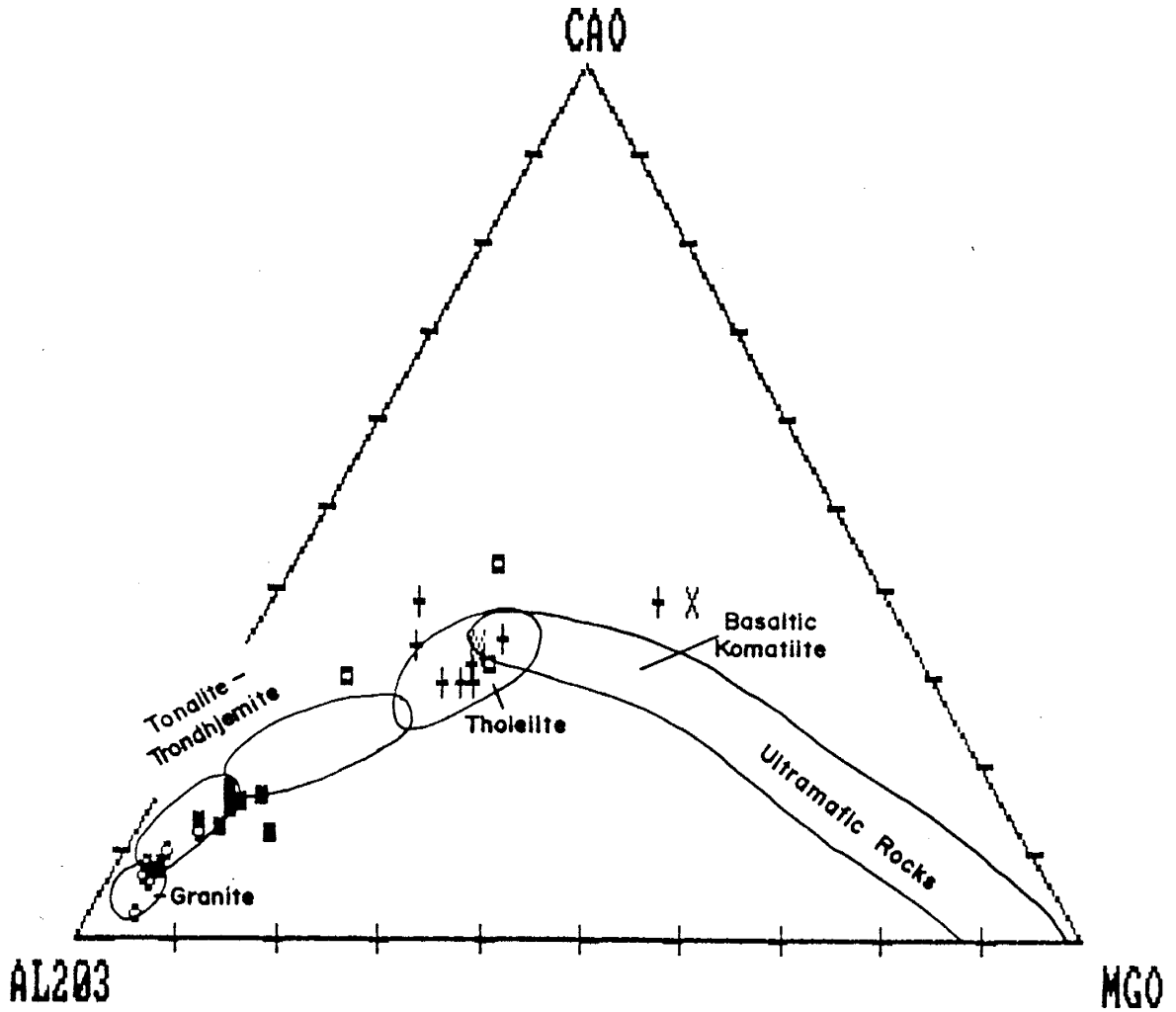from Winchester and Floyd (1977). Symbols as in Figure 3.

Figure 5
Classification of BBC Rocks according to CaO-Al$_2$O$_3$-MgO. Fields from
Bavington and Taylor (1980). Symbols as in Figure 3.

Plots of major elements versus SiO_2 (Fig. 6a-h) show some covariations within the mafic group which may represent igneous fractionation trends. A negative correlation exists for Fe_2O_3T, MgO, and TiO_2 vs. SiO_2, and a positive correlation is exhibited by Na_2O vs. SiO_2. Other major elements show considerable scatter. It is not clear what this scatter indicates, but three explanations are possible: 1) they represent the original compositional variation of the suite; 2) they represent a pre- or synmetamorphic contamination, or 3) they represent minor amounts of mobilization of certain elements during metamorphism. Of course any combination of the above cannot be ruled out. The mobilization hypothesis is favored because calcium and potassium are known to be both sensitive indicators of igneous fractionation processes and readily mobilized during metamorphic processes. Al_2O_3 is not readily mobilized but does not always reflect the evolution of igneous processes between 45 and 65% SiO_2. An alteration screen, designed by Davis et al. (1979) for volcanic rocks, indicates that if these rocks are of volcanic origin, then some have undergone varying but rather small degrees of alteration, possibly by gaining or losing small amounts of CaO.

The mafic rocks straddle the boundary between the tholeiitic and calc-alkaline suites on many variation diagrams. On the AFM diagram of Irvine and Baragar (1971) they fall mainly in the tholeiite field, but no obvious trend emerges. On the cation plot by Jensen (1976), samples lie in the field of high-Mg tholeiites, but pass into the calc-alkaline basalt field (Fig. 7). On plots by Miyashiro and Shido (1975) the

Figure 6a,b

SiO$_2$ vs. TiO$_2$ and Al$_2$O$_3$ for all BBC Rocks. Symbols as in Figure 3
except: *, anomalous mafic rocks; ¤ , tonalitic to granodioritic rocks;
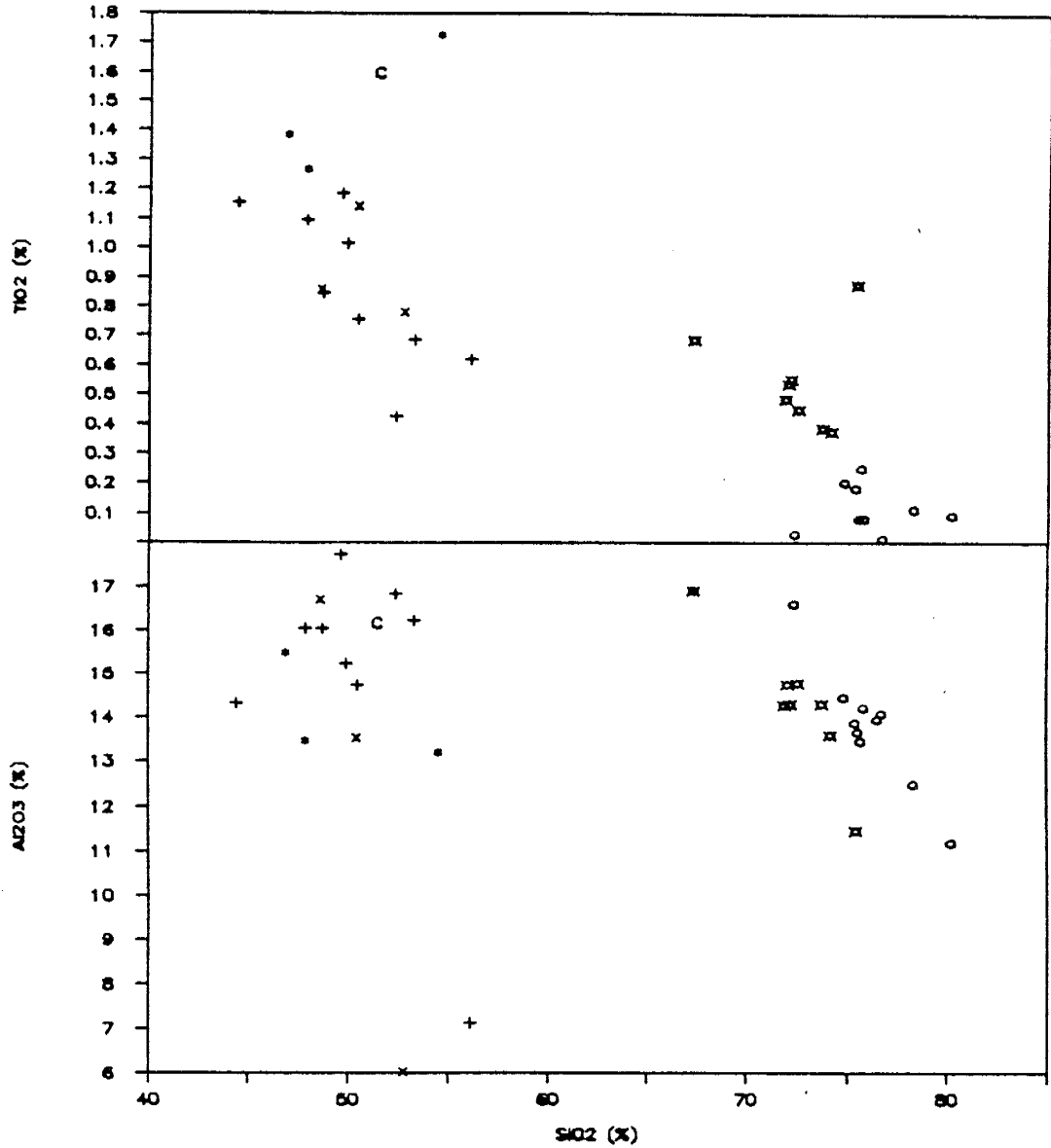and C, NMORB of Condie (1985).

28

Figure 6c-e
SiO$_2$ vs. Fe$_2$O$_3$T, MgO, and CaO for all BBC Rocks.
Symbols as in Figure 6a.
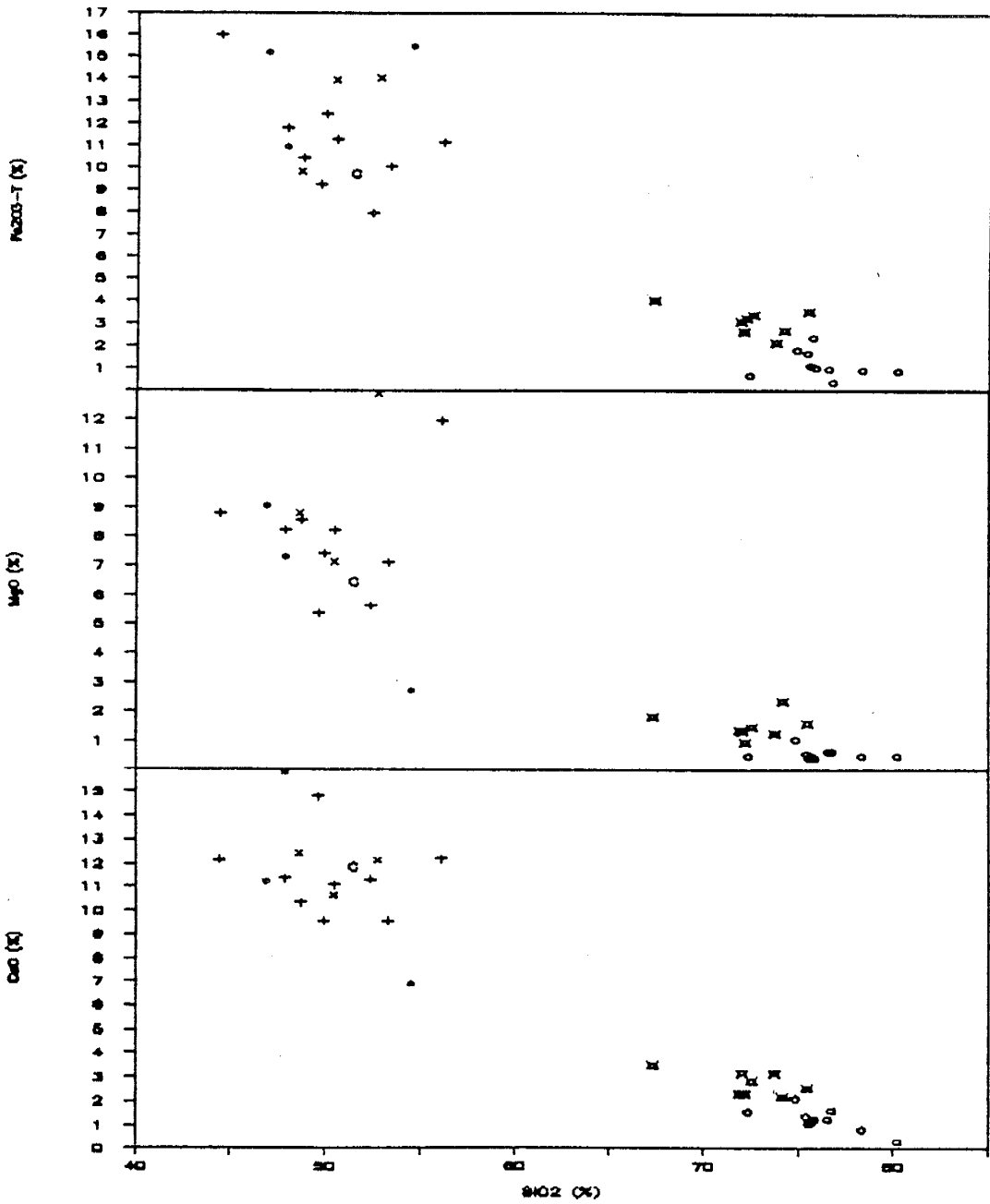
Figure 6f-h
SiO_2 vs. Na_2O, K_2O, and P_2O_5 for all BBC Rocks.
Symbols as in Figure 6a.
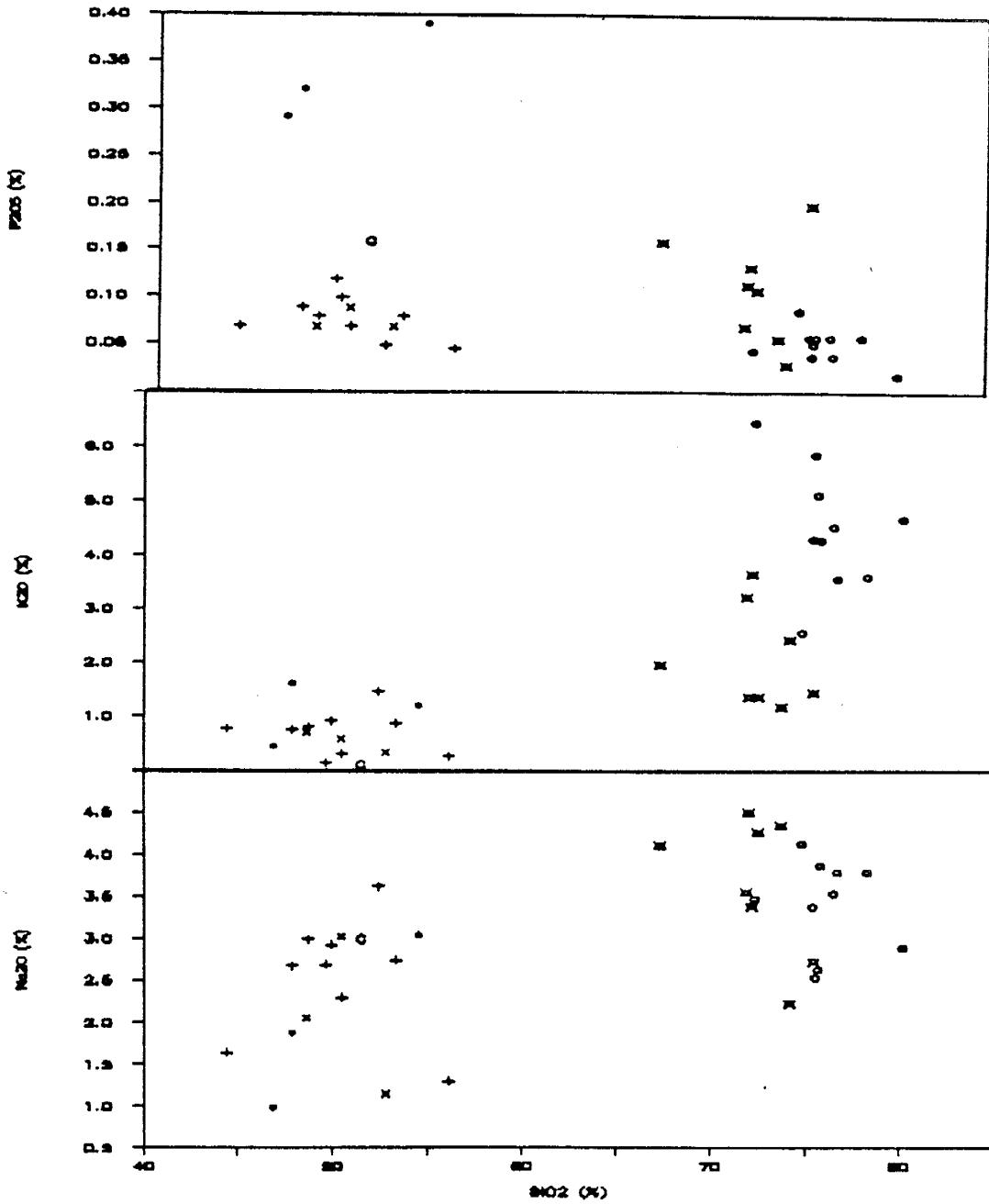
samples straddle the boundary, and a plot of MgO against Fe_2O_3T also demonstrates the transitional character of the mafics.

The major element plots suggest that there has been only a relatively small fluctuation among highly mobile elements, and most of the amphibolites have apparently maintained a close resemblance to the chemical compositions of their igneous precursors. The precursors are basaltic in composition, with a few exceptions: that of LMP-58 is andesitic, and those of LMP-6 and -54 are perhaps more ultramafic than basalt. Igneous trends suggestive of cogenetic relationships are vaguely represented.

Trace elements show relatively mobile or immobile characteristics. It is generally believed that most trace elements can be classified into groups which behave differently under various geologic conditions. Large ion lithophile elements (LILE) are more easily mobilized than the high field strength elements (HFSE) and rare earth elements (REE), which are more or less immobile, during metamorphic processes (Tatsumi et al., 1986).

Most samples exhibit some degree of LILE mobility. Variable depletions in Rb, Ba, U, and especially Th (Table II) are found in samples 34, 47, 54, and MS-5 (although 47 is enriched in Rb) relative to other samples. Other samples show slight depletion or enrichment in one or more of these elements and so care must be exercised when interpreting diagrams that use these elements. As the four samples mentioned above plot with the others on all diagrams except those involving Th, Th in the samples may have been mobilized during metamorphism. Plots of TiO_2 vs. the LILE for the mafic rocks reveal a

Figure 7

AFM Cation plot of Jensen (1976). A $-$ Al_2O_3; F $-$ (FeO $+$ Fe_2O_3 $+$ TiO_2);
M $-$ MgO; oxides are in molar proportions. Symbols as in Figure 3.
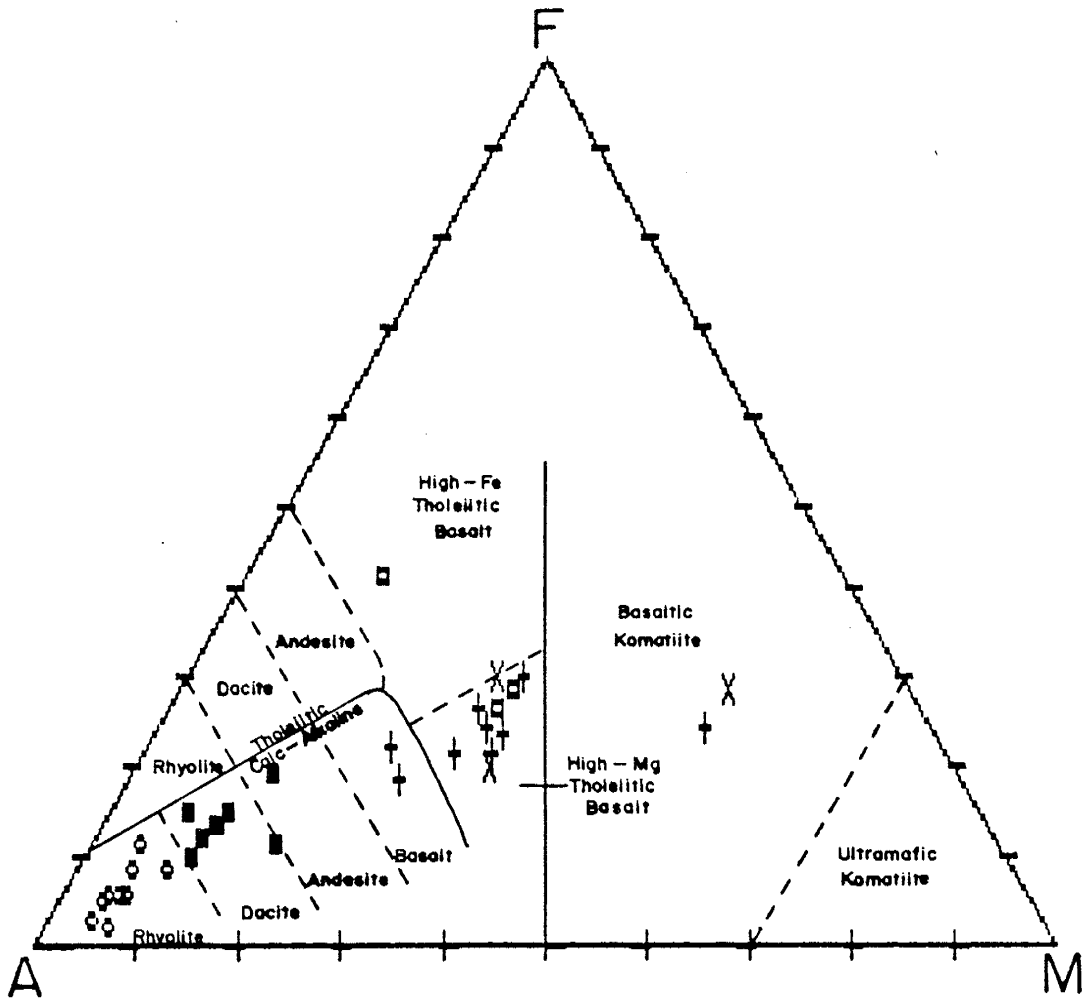
lack of covariance, further demonstrating LILE mobility in the Messina area.

Variable mobility of the HFSE and REE may or may not occur in the granulite facies (Sheraton, 1985; Weaver and Tarney, 1980; Condie and Allen, 1984; Muecke et al., 1979). Finlow-Bates and Stumpfl (1981) and Vance and Condie (1987) have demonstrated that few elements (only Zr and TiO_2 and possibly Ce) are immobile during the intense hydrothermal alteration that accompanies the formation of volcanogenic massive sulphide deposits. These authors believe that such mobilization can be easily recognized by comparing element ratios. The linear trends defined in plots of TiO_2 vs. various HFSE and REE suggest that 1) the HFSE have not been mobilized to any significant degree, and 2) the mafic samples may be genetically related to one another.

Chondrite-normalized REE plots (Fig. 8a-c) show flat to gently sloping patterns with slightly negative or no Eu anomalies. Exceptions are the strongly enriched patterns exhibited by the three samples mentioned earlier (LMP-49, -58, and MS-5). Two samples (47 and 54) have REE patterns similar to an average mid-ocean ridge basalt (NMORB), with LREE depletion and no Eu anomaly. The remaining samples appear to have patterns intermediate between average island arc basalts (IAB) and continental arc basalts (CAB), excepting the Eu anomalies: the patterns are not fractionated enough to be similar to most extensional or intraplate-related basalts.

There are two ways of providing an analogy that may lead to a better understanding of the evolution of the Limpopo Belt. These are 1) sample distributions on tectonic discrimination diagrams, and 2)

Figure 8a-c
Chondrite-normalized REE distrubutions.   8a,b for amphibolites;
8c for Low-Th and other amphibolites.
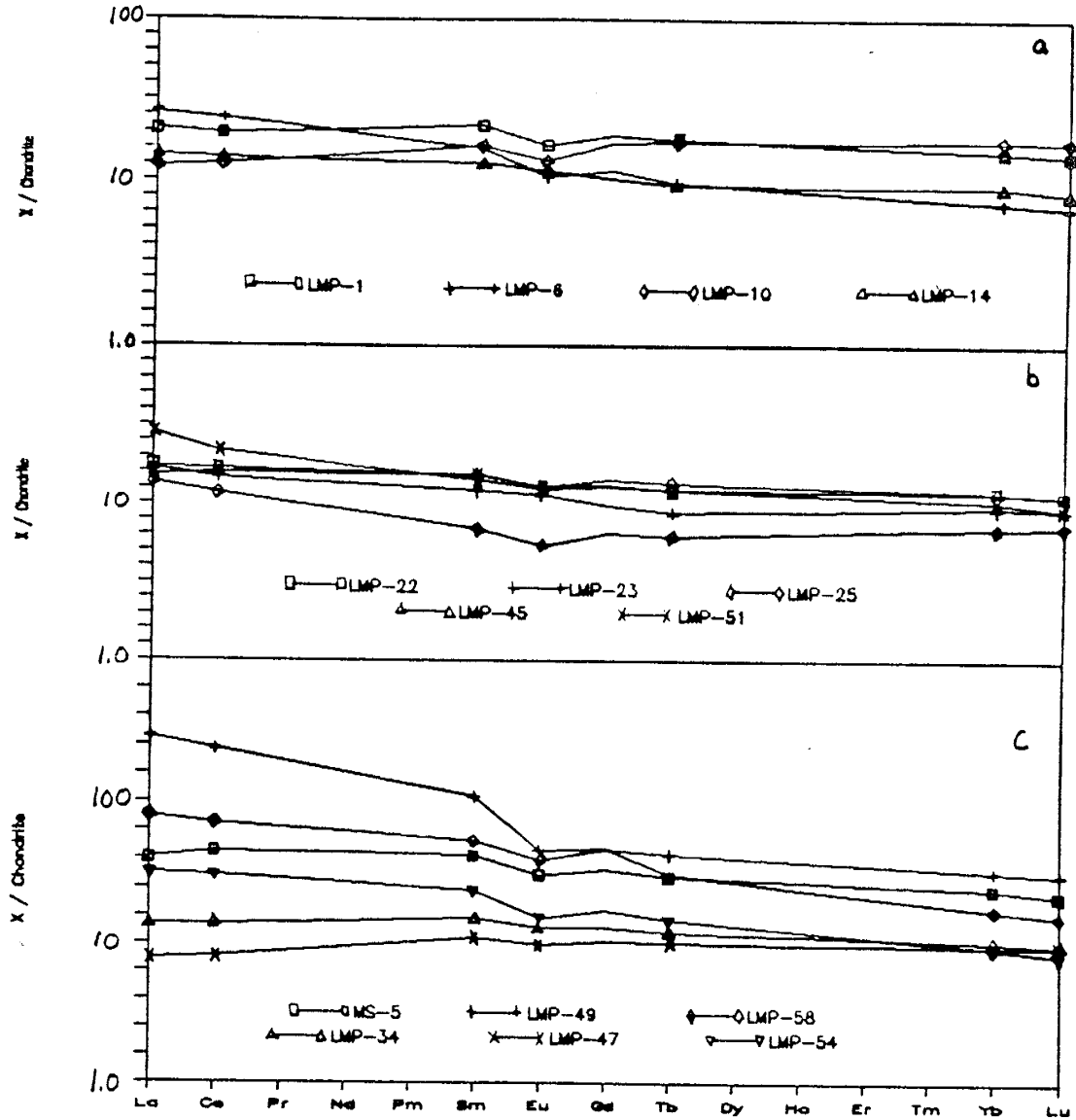
comparison of element ratios with samples from known tectonic settings. Overlaps may be caused by similarities between rocks from known tectonic settings and by variable mobilities, however small, of some of the elements during metamorphism.

Several diagrams suggest that the rocks are not related to continental rifting. An example is that of Nb vs. La (Fig. 9). A diagram which also illustrates that the three unusual samples mentioned above (LMP-49, -58, and MS-5) do not fit with the others is the ternary plot of Mullen (1983), involving TiO_2, MnO x 10 and P_2O_5 x 10. Most of the samples plot in an arc-related cluster, without overlapping the fields of within-plate basalts. Samples 49, 58, and MS-5 are highly enriched in P_2O_5. This enrichment, along with other anomalous element concentrations, may be related to the presence of an excessive amount of a minor phase such as apatite, although this phase is sparsely distributed in thin section.

In other plots involving titanium, samples scatter across the boundary between arc- and MORB-related fields. Examples are diagrams of Garcia (1978) (Ti vs. Cr and TiO_2 vs. Zr); Pharoah and Pearce (1984) (TiO_2 vs. Zr, Fig. 10); Condie (unpublished) (Ti/Zr vs. Zr/Y, Fig. 11); and Pearce and Cann (1973) (Ti/100-Zr-Y*3, Fig. 12). The plot of Nb*2, Zr/4, and Y (Fig. 13) by Meschede (1986) shows that the samples again fall in a nonspecific field but are not related to rifting and cannot be associated with a mantle plume. These diagrams help refute origins in a rift environment, which is suggested by various authors (e.g. Fripp, 1983). It is still not clear, however, to which tectonic setting these rocks belong.

Figure 9
Nb vs. La, BBC mafic rocks. Symbols as in Figure 6a; also,
W: NMORB, and P: Primordial Mantle, both of Wood (1979).
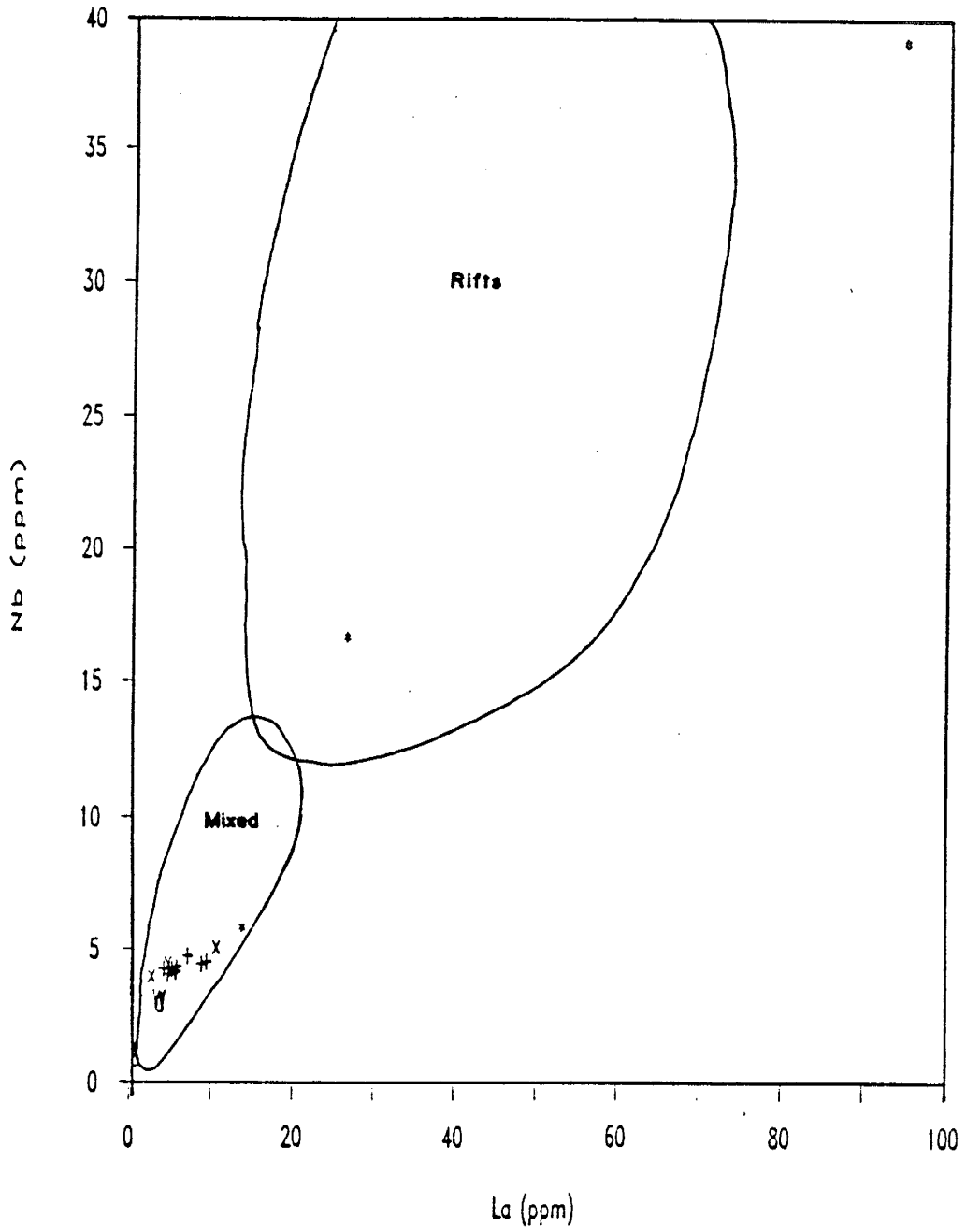
Figure 10
TiO$_2$ vs. Zr (log scale), BBC rocks. Fields from Pharoah
and Pearce, 1984. Symbols as in Figure 3.
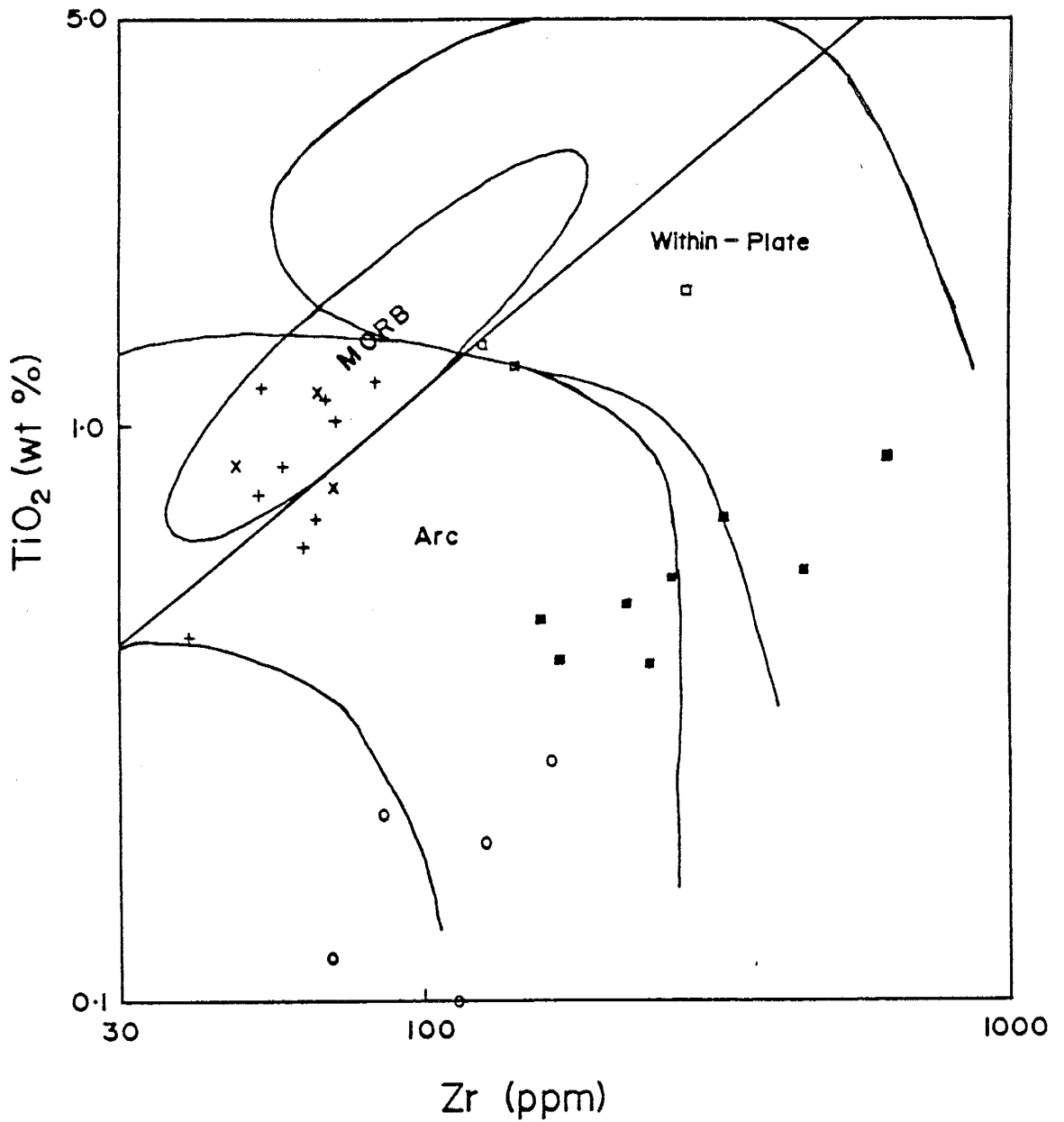
Figure 11
Ti/Zr vs. Zr/Y, BBC mafics. Fields after Condie (unpub.).
Symbols as in Figure 9.
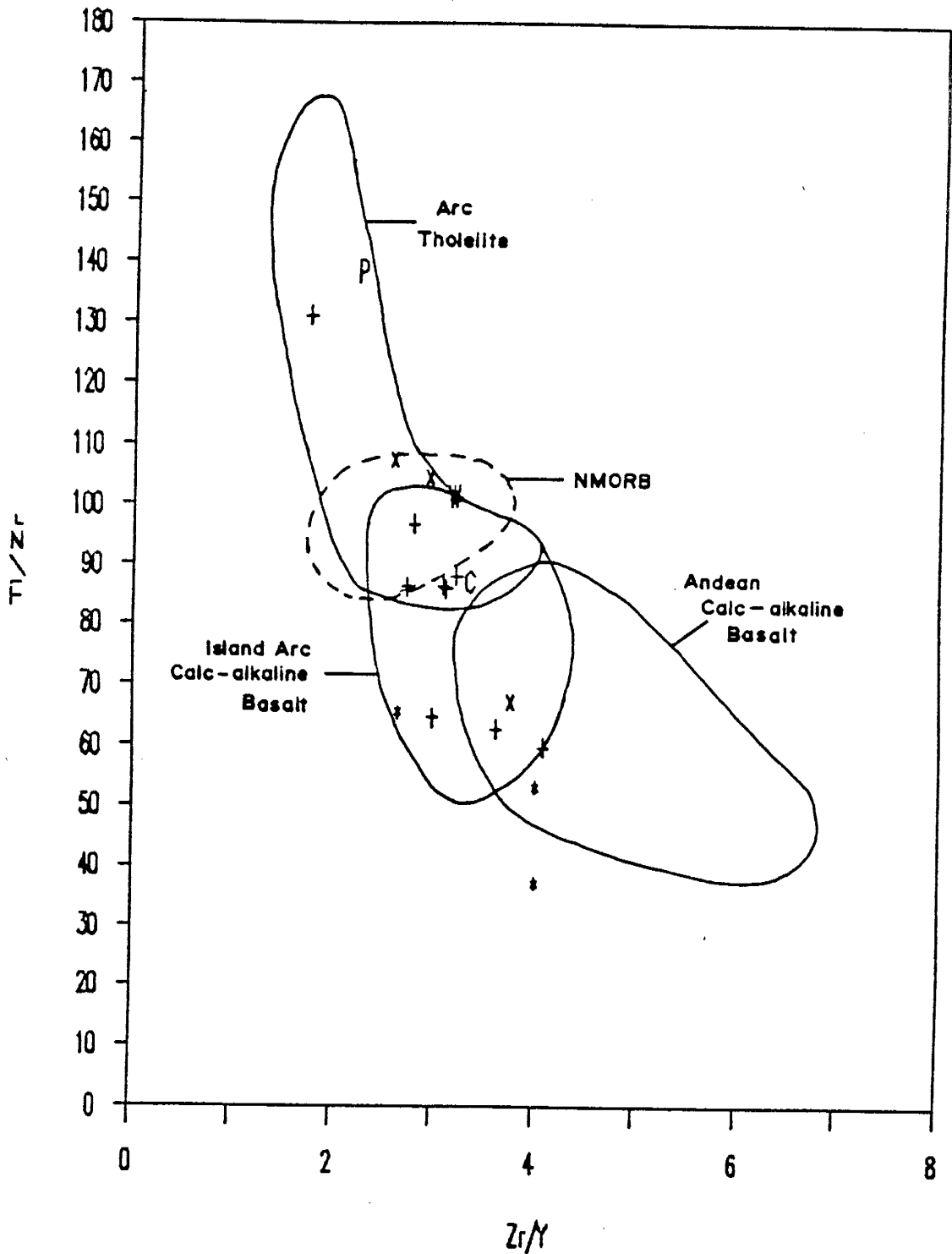
Figure 12
Ti/100-Zr-Y*3, BBC mafics. Fields of Pearce and Cann (1973).
Symbols as in Figure 3.
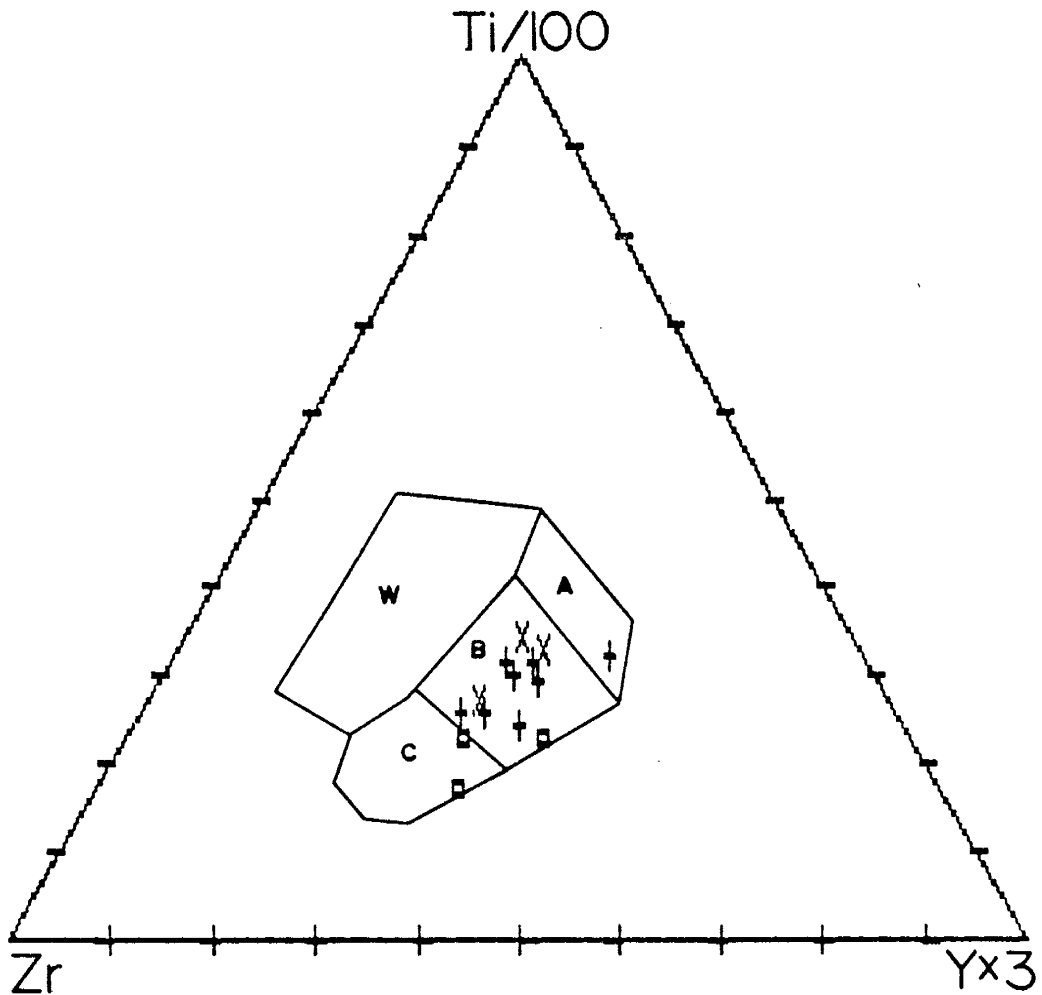
W = Within — Plate Basalts
A & B = Low — K Tholeiites
    B = Ocean Floor Basalts
B & C = Calc — alkaline Basalts

Figure 13
Nb*2-Zr/4-Y, BBC mafics. Fields of Meschede (1986).
Symbols as in Figure 3.
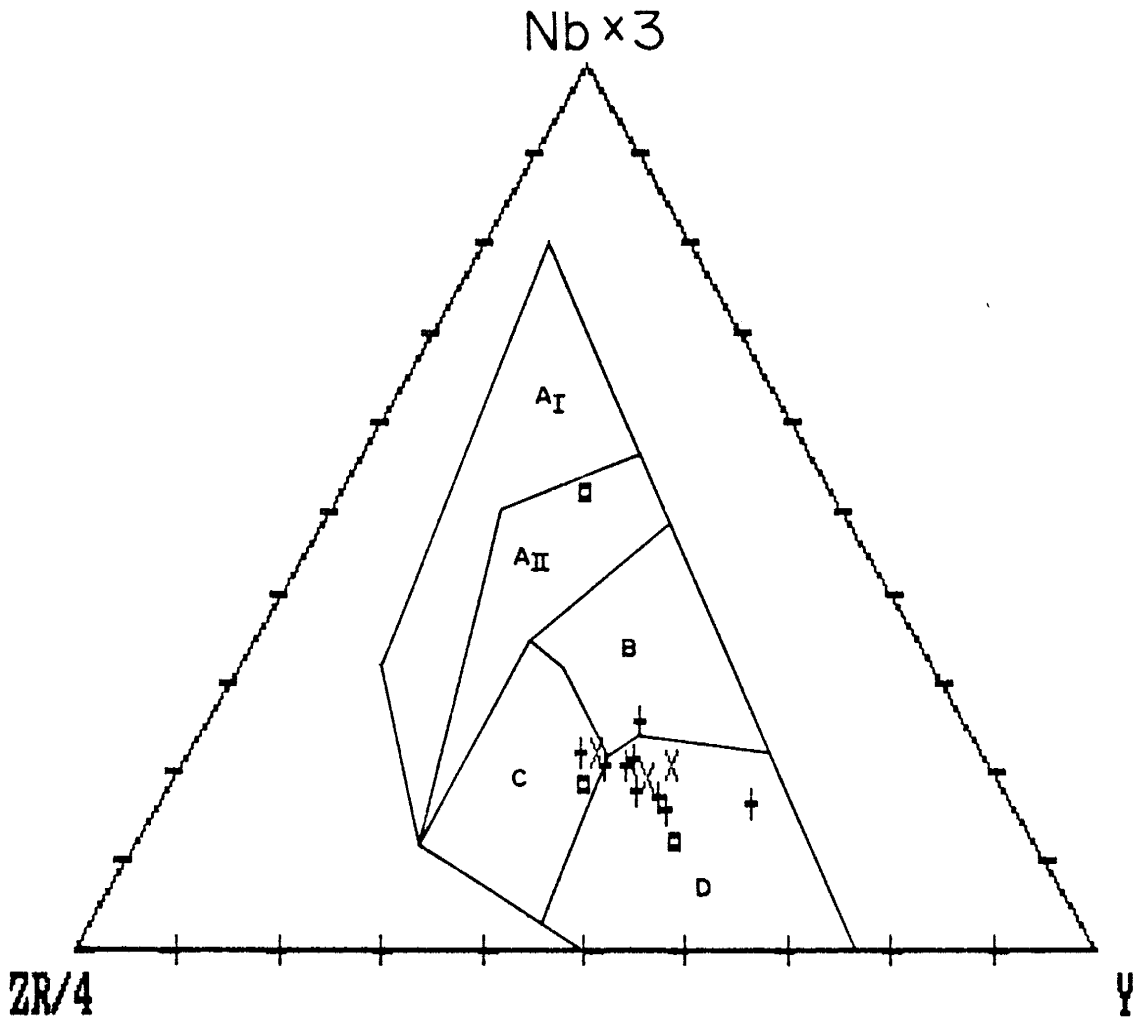
A_I, A_{II} = Within – Plate Alkaline Basalts

A_{II}, C = Within – Plate Tholeiites

B = Enriched MORB

C, D = Volcanic Arc Basalts

D = NMORB

Plots involving Th are designed to discriminate between arc-related and MORB-like rocks; however, Th has been mobilized in some of the rocks of this study. The bulk of the samples lie in arc-related fields on Pearce's (1983) Th/Yb vs. Ta/Yb diagram while a small group (the samples thought to have lost Th) lies close to the MORB field (Fig. 14). The same is true on the Th vs. Hf diagram and the ternary diagram involving Hf/3, Th, and Ta, both from Wood et al. (1979).

The MORB-normalized spidergram developed by Pearce (1983) is useful in identifying the possible components involved in the evolution of basalts. Pearce has argued that an enrichment in Sr, K, Rb, Ba, and Th and usually Ce, Sm, and P over Ta, Nb, Zr, Hf, Y, and Yb (all normalized values) is evidence for the presence of a subduction zone component (SZC) in basalts. High concentrations of Ta and Nb relative to Zr and Hf and of Zr and Hf relative to Y and Yb are suggestive of within-plate (WP) enrichment processes. Figures 16a-c show patterns of the two main groups (arc-like, Figures 16a and b, and altered and Th-depleted, Figure 16c), with concentrations normalized to average mid-ocean ridge basalt (NMORB). The plots for the unaltered amphibolites show variable LILE enrichments but the less mobile elements (Ta through Yb) have similar concentrations. There is a small within-plate enrichment and a strong SZC in the geochemical signatures of these rocks. The depletion of Ti may be explained by the fractionation of small amounts of magnetite. The relative depletion in P may be explained by apatite remaining in the source, but such a model does not support the slight overall enrichment in REE. The altered samples show similar signatures, but the patterns are too erratic to be meaningful.

Figure 14
Th/Yb vs. Ta/Yb (log scale), BBC mafics. Fields after Pearce (1983).
Symbols as in Figure 3.
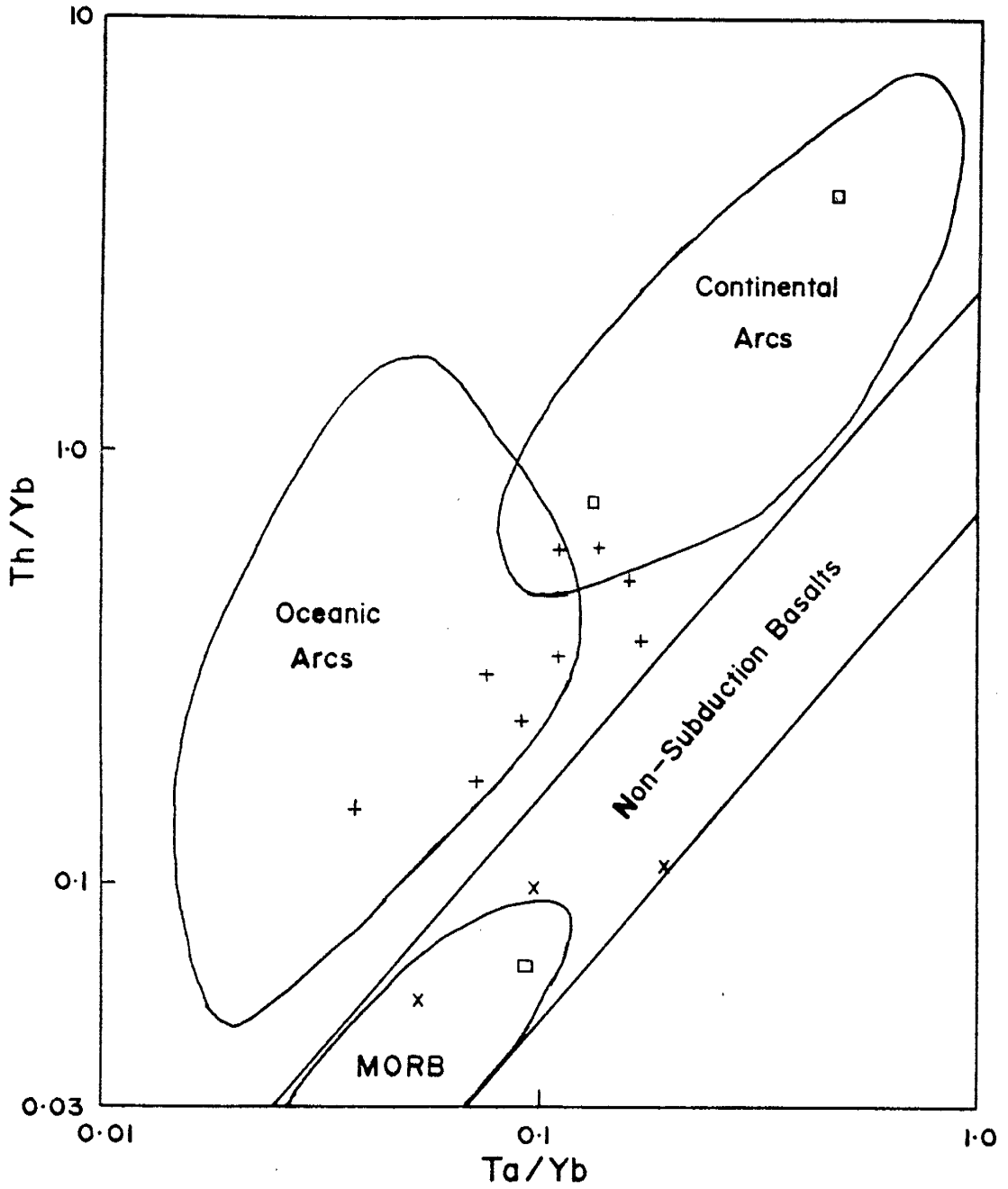
Figure 15
Hf/3-Th-Ta, BBC mafics. Fields after Wood et al. (1979).
Symbols as in Figure 3.
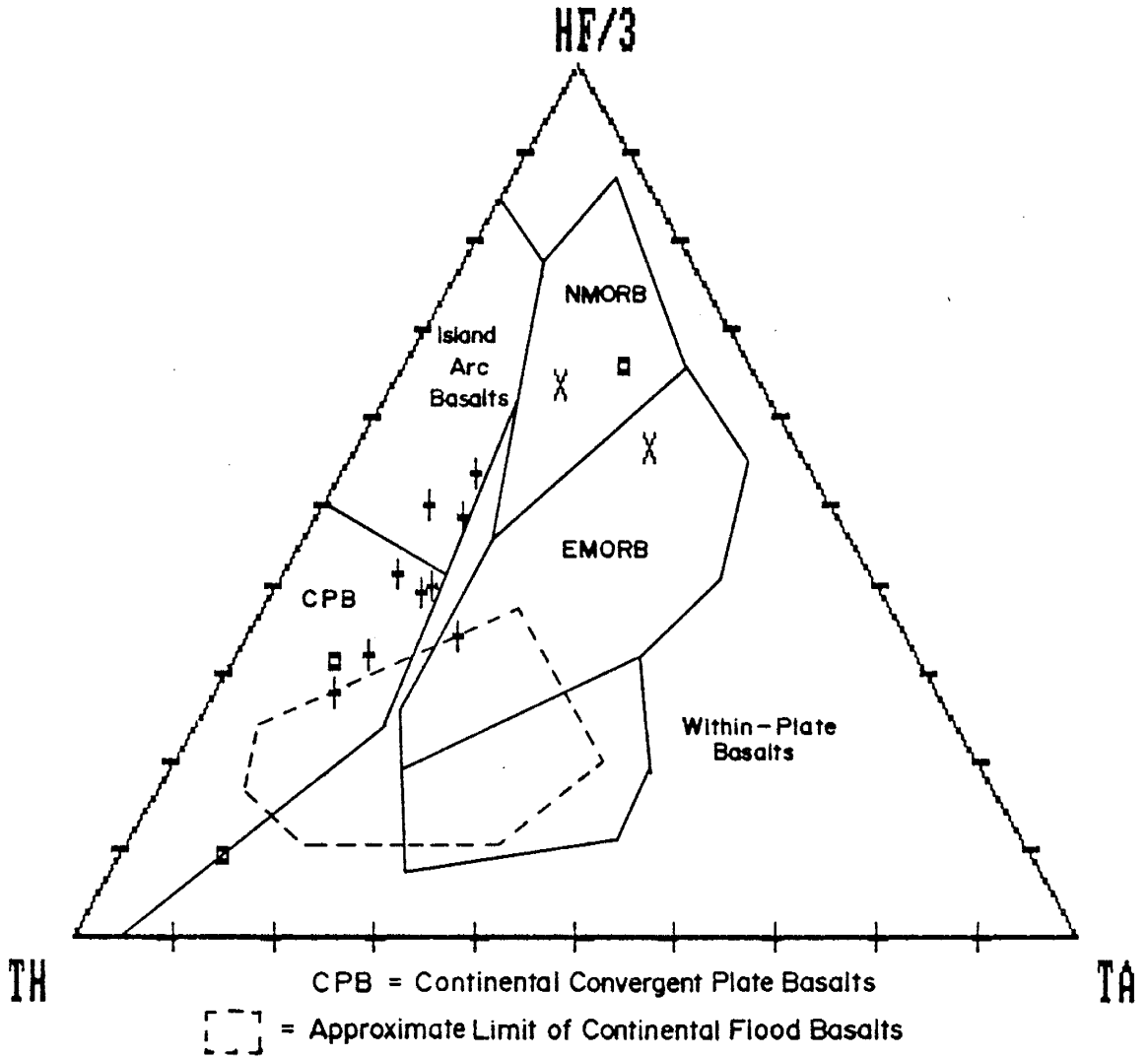
Figure 16a
Pearce's (1983) NMORB-normalized spidergram for BBC arc-like mafics.

□ LMP-1   + LMP-6   ◊ LMP-10   △ LMP-14
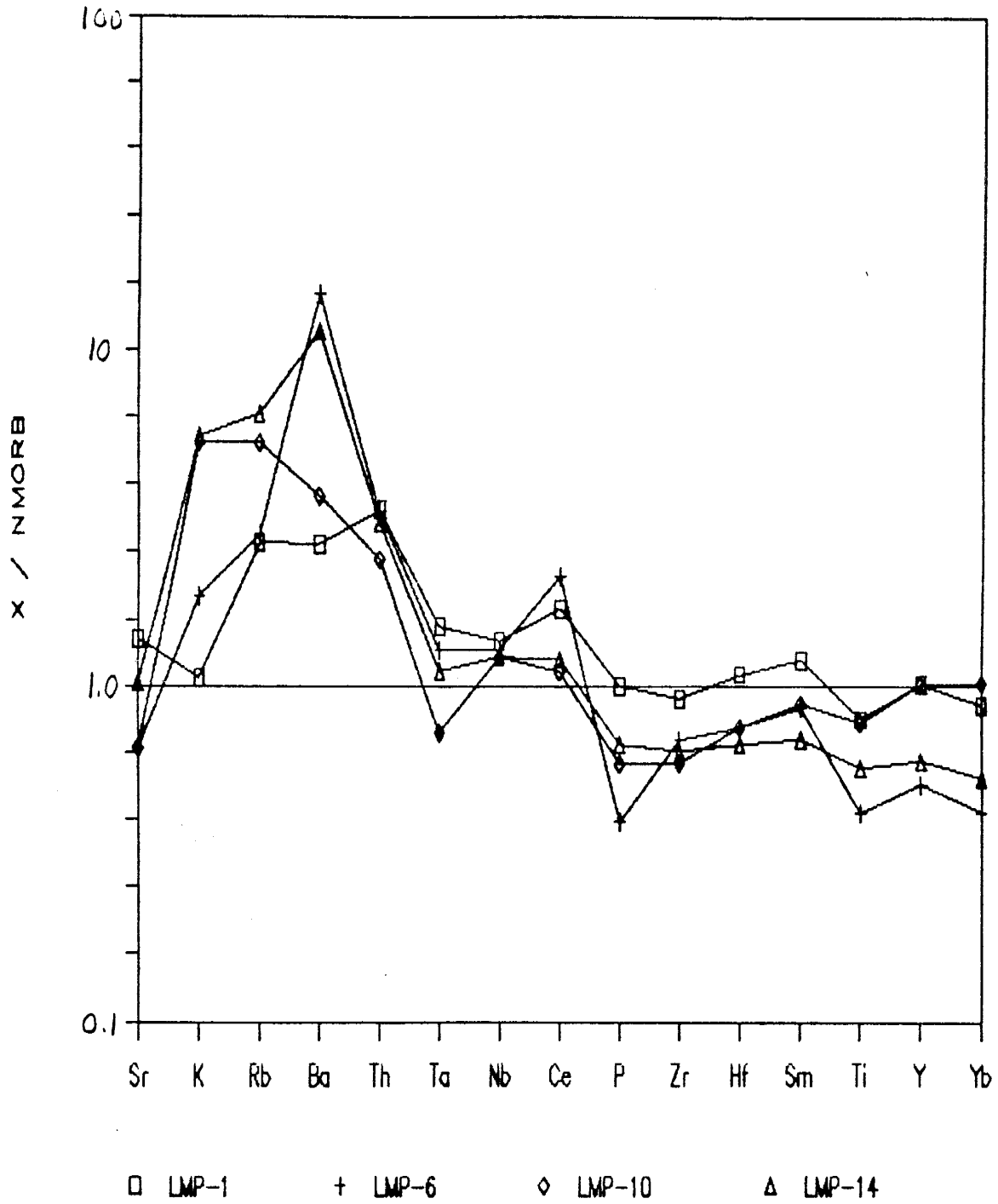
Figure 16b
Pearce's (1983) NMORB-normalized spidergram for BBC arc-like mafics.
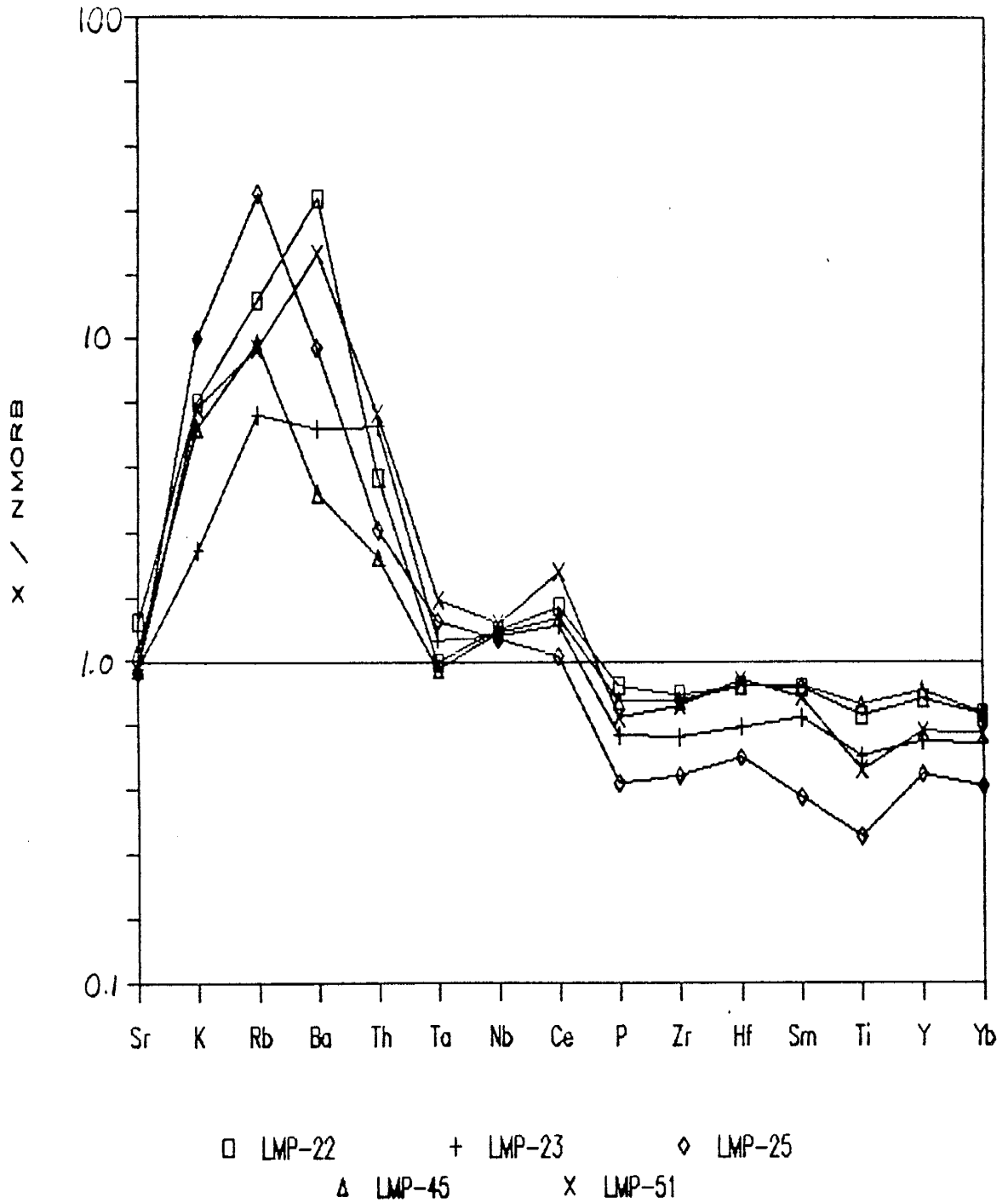
Figure 16c
Pearce's (1983) NMORB-normalized spidergram for BBC altered mafics.

Legend:
□ MS-5   + LMP-49   ◇ LMP-58
△ LMP-34   X LMP-47   ▽ LMP-54
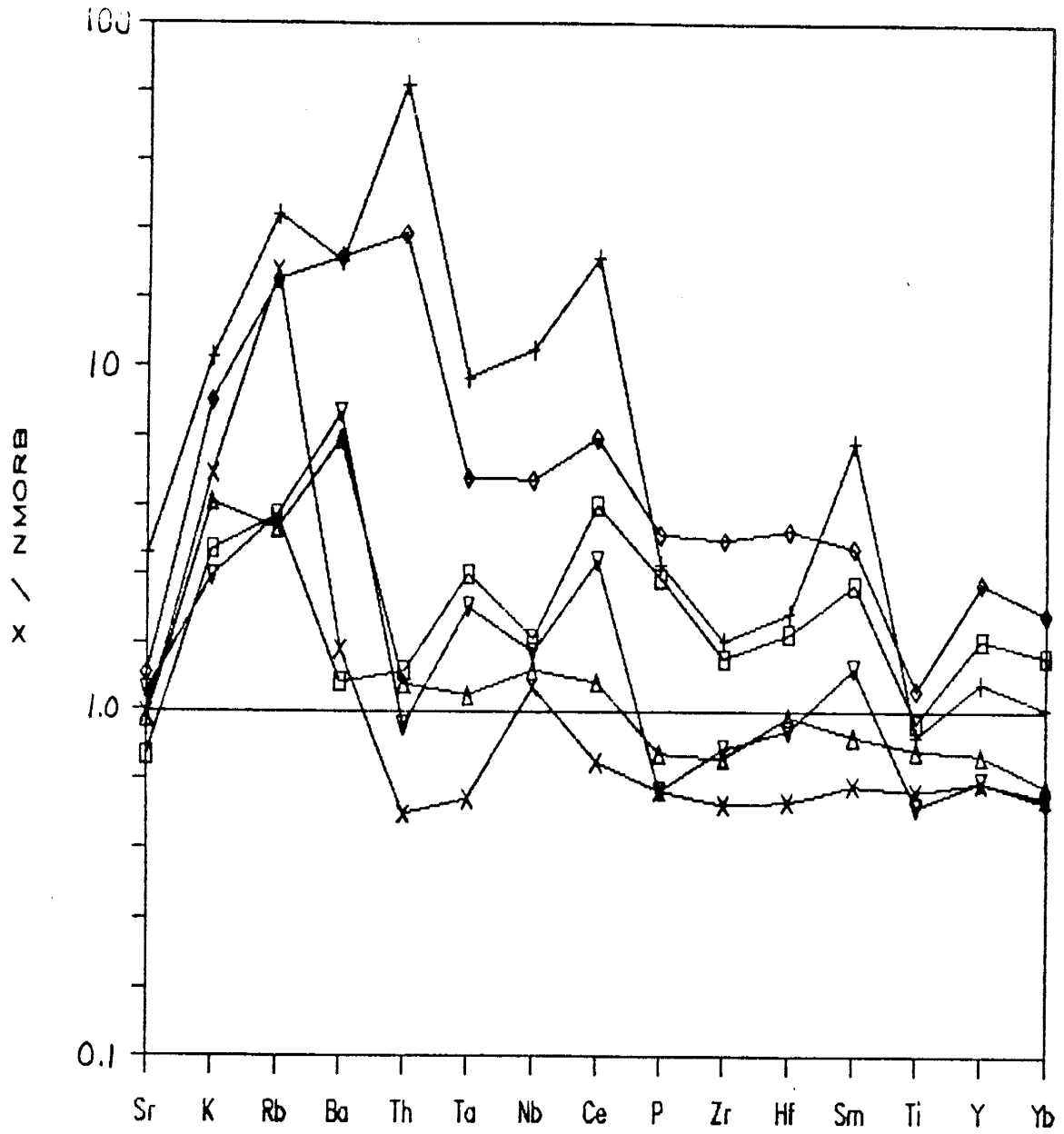
Average ratios of incompatible elements are compared with those of other basalts from known tectonic settings in Table III. The averages include a combination of all but two samples from the arc-like and Th-depleted groups for ratios which do not involve Th (i.e. n = 11); for the ratios which include Th the samples which are depleted in that element have been excluded from the average (n = 8). The other two samples (6 and 54) are averaged in a separate column because of their high MgO, Cr, and Ni contents. For the ratios involving Th, only the values for sample 6 are listed because sample 54 has lost Th.

Comparison of incompatible element ratios is perhaps more useful in this study than comparison of elemental abundances. This is because although elements may or may not be mobilized, their ratios may not vary significantly during metamorphism. Most of the ratios argue against a within-plate origin for the BBC mafic rocks (e.g. La/Yb, Ti/Y, Hf/Ta). The difference between NMORB and arc-related basalts is exemplified by ratios such as La/Yb, Ti/Y, Hf/Ta, Th/Yb, Zr/Nb, and Th/Ta; the BBC samples have values similar to arc-related basalts for these. The ratios form a continuum between island arc and continental arc basalts.

Modeling

The igneous fractionation-like trends discussed above suggest that the BBC amphibolites are genetically related. Therefore, an attempt may be made to relate these rocks to each other by magmatic processes.

The recrystallization into granulite facies and then retrograde amphibolite facies mineral assemblages has removed any evidence of

Table III
Incompatible Element Ratios for BBC Mafics and Average Basalts.

	Beit Bridge Complex		Island Arc Basalts	Cont. Arc Basalts	NMORB	Within-Plate Basalts
	Tholeiite	High-Mg Tholeiite				
n	$11^a(8)^b$	$2^c(1)^d$				
La/Yb	2.5	5.9	1-3	3-7	0.9-1.2	7-9
Zr/Y	2.9	3.9	2-3	3-6	2.5-3.0	4-7
Ti/Zr	89	64	90-120	40-90	90-105	75-90
Ti/Y	249	249	200-300	200-300	300-325	450-500
Hf/Ta	9.8	6.8	12-40	5-20	12-15	2-3
Th/Yb	0.34^b	0.46^d	0.2-0.5	0.5-1.0	0.05-0.1	0.8-1.2
Zr/Nb	19	14	15-35	15-35	28-35	6-10
Nb/La	0.64	0.52	0.2-0.6	0.2-0.6	0.9-1.1	1.0-1.5
Ta/Yb	0.1	0.18	0.05-0.2	0.05-0.2	0.05-0.08	0.6-0.7
Hf/Yb	0.85	1.2	0.5-1.0	0.5-1.0	0.7-1.2	1.6-1.8
Th/Ta	3.4^b	2.9^d	4-6	4-6	1.0-1.2	1-2

[a] includes samples 1, 10, 14, 22, 23, 25, 34, 45, 47, 51, and MS-5

[b] as in a, minus altered samples 34, 47 and MS-5.

[c] includes samples 6 and 54.

[d] as in c, minus altered sample 54.

Average basalt data compiled by K. C. Condie.

primary phases in the rocks. For this reason, the use of experimental crystallization assemblages in the modeling is appropriate; however, such assemblages could also be calculated in some systems using major element modeling programs. This approach may give one a rough idea of which phases and what proportions might be feasible starting assemblages.

The most primitive sample in the study set, based on high Ni and Cr content and Mg #, is picked as a starting material (sample LMP-10). The least primitive sample (LMP-58) is used for comparison with the calculated end product. Due to some mobilization of the major elements (especially possible silicification mentioned previously) this approach is unsuccessful because unreasonable fractionation assemblages are required to produce a relationship.

Trace element modeling proves to be somewhat more fruitful when mobile elements are not included. Again it is difficult to relate one sample to another, but it is possible to relate the entire suite to a viable source, at least in terms of a few elements.

A computer program is employed for trace element modeling calculations. This program, entitled MODULUS, was written by Mike Knoper at New Mexico Tech and incorporates batch melting (BM) and Rayleigh fractional crystallization (FXL) options. The FXL options include a closed system (CFXL) model, described by Allègre and Minster (1978), as well as two open system (OFXL) models, one by Cann (1982) and one by O'Hara and Mathews (1981). Distribution coefficients (K_d's) are built into the program and have been compiled from values in the literature. Temperature-sensitive K_d's are calculated from published

data. A temperature of $1200^{\circ}C$ is used as an average temperature of crystallization of the basaltic magmas. The K_d's used are presented in Table IV. By supplying the parent composition (C_0), the mineral assemblages, and appropriate modes (from the experiments of others), the resulting liquid (C_1) is calculated. The C_1 is then compared with the sample compositions by plotting elements against each other.

Four plots are used which involve seven elements (two plots are shown here). Concentrations of these elements vary widely in the samples, and these variations can be related to possible igneous fractionation trends. Two sources were tested using various assemblages of phases and modes. These tests suggest it is unlikely that a source which generates a typical NMORB (such as that of Condie, 1985 or of Wood, 1979) was the parent of the rocks of this study. The mafic rocks of the Central Zone are much too enriched in light REE and in Cr and Ni and depleted in HFSE to have been derived from a depleted mantle source. The two NMORB compositions mentioned above are plotted on the diagrams discussed below for comparison.

A primordial mantle (PM) source (Wood, 1979) is also tested. The modal assemblage of the parent is that of a lherzolite composed of 60% olivine, 25% orthopyroxene, and 15% clinopyroxene. From experimental data, this assemblage melts in proportions of 25:20:55, respectively. Clinopyroxene is the first mineral to disappear, at 27.3% melting. The batch melting trend is noted on the diagrams. On plots involving incompatible elements (I-I plots), the BM trend lies near the cluster of samples. In the plot of Th vs. Hf (Fig. 17), only those samples suspected of having lost Th lie far from the trend. A plot of La vs.

Table IV
Mafic Distribution Coefficients

	Olivine	Opx	Cpx	Plag	Amphibole	Gar	Mgt
Na	0.02000	0.02000	0.27000	50.000	0.75000	0.010	0.000
K	0.00700	0.01400	0.01100	0.17000	0.96000	0.020	0.000
Rb	0.01000	0.02000	0.02000	0.13000	0.20000	0.040	0.000
Sr	0.01500	0.02000	0.10000	2.00000	0.60000	0.012	0.000
Cs	0.00040	0.02000	0.01000	0.02500	0.10000	0.030	0.000
Ba	0.01000	0.01300	0.00500	0.25000	0.70000	0.020	0.000
Th	0.02000	0.13000	0.02000	0.05000	0.05000	0.001	0.000
U	0.04000	0.00700	0.05000	0.06000	0.15000	0.001	0.000
Pb				0.45000			
V	0.05000	0.30000	1.20000		3.50000	0.270	25.000
La	0.00001	0.00700	0.07000	0.15000	0.20000	0.030	0.000
Ce	0.00001	0.00800	0.10000	0.12000	0.26000	0.030	0.000
Nd	0.00007	0.01000	0.22000	0.08000	0.40000	0.087	0.000
Sm	0.00060	0.02000	0.40000	0.06700	0.70000	0.220	0.000
Eu	0.00100	0.02000	0.40000	0.35000	0.80000	1.000	0.000
Tb	0.00200	0.05000	0.50000	0.06000	0.80000	3.000	0.000
Yb	0.02000	0.15000	0.60000	0.07000	0.60000	5.000	0.000
Lu	0.01600	0.18000	0.60000	0.06000	0.50000	5.500	0.000
P	0.04300	0.01400	0.00900			0.150	
Sc	0.30000	1.00000	2.00000	0.04000	1.50000	5.000	2.000
Ti	0.02000	0.10000	0.40000	0.04000	1.50000	0.300	7.500
Y	0.01000	0.20000	0.50000	0.03000	1.00000	2.000	0.200
Zr	0.01000	0.03000	0.10000	0.01000	1.50000	0.300	0.100
Nb	0.01000	0.15000	0.10000	0.01000	0.80000	0.100	0.700
Hf	0.04000	0.04000	0.30000	0.01000	0.40000	0.150	0.300
Ta	0.03000	0.10000	0.06000	0.04000	0.40000	0.100	0.800
Cr*	1.00	2.34	0.77	0.00100	15.00	17.500	94.72
Mg*	2.27	8.12	1.28	0.00000	10.00		1.33
Mn*	0.59	2.00	1.01	0.00000	1.00		2.00
Fe*	0.74	0.86	0.25	0.00000	10.00		2.79
Co*	3.70	3.00	0.51	0.00100	7.00		10.00
Ni*	9.70	3.00	6.82	0.00100	7.00		10.00

* Temperature-dependent distribution coefficients interpolated from values found in the literature for 1200°C.

Ta is virtually a repeat of the Th-Hf plot except that the low-Th group is not distinct from the other samples.

The distribution of incompatible elements versus compatible elements (I-C plots, Figure 18), on the other hand, is not consistent with batch melting of PM in the form of a lherzolite. Either the source contained much lower relative abundances of compatible elements than the PM of Wood (1979) or the mafic rocks evolved in two stages, such as partial melting followed by fractional crystallization.

CFXL models involving the fractionation of 55% olivine, 37% clino-pyroxene and 8% magnetite are plotted along with the BM curves on Figures 17 and 18. The parent compositions for these calculations are 5% and 25% batch melting compositions of PM as discussed above. I-I plots demonstrate that up to 40% fractionation of this assemblage does not vary the composition of the melt beyond the range of the samples. The fractional crystallization trends coupled with the batch melting line on these plots encompass most of the samples if the PM source is variably enriched in incompatible elements, such as Th and La, as Tatsumi et al. (1986) suggest is common for subduction zone related magmas. Other lines of evidence supporting such enrichment in the source for these rocks were presented above (e.g. in NMORB-normalized spidergrams, all samples show the SZC).

On I-C plots, fractionation trends encompass a majority of the samples. The range can therefore be accommodated by 5% to 25% batch melts which subsequently undergo approximately 10% to 30% fractional crystallization of mostly olivine and clinopyroxene, with minor magnetite. The presence of magnetite in the fractionation assemblage

52

Figure 17
Th vs. Hf (I-I) modeling diagram for BBC mafics. Symbols as in Figure 9; tic-marks are in increments of 5% melting for BM curve and 5% fractionation for FXL curves. See text for details.
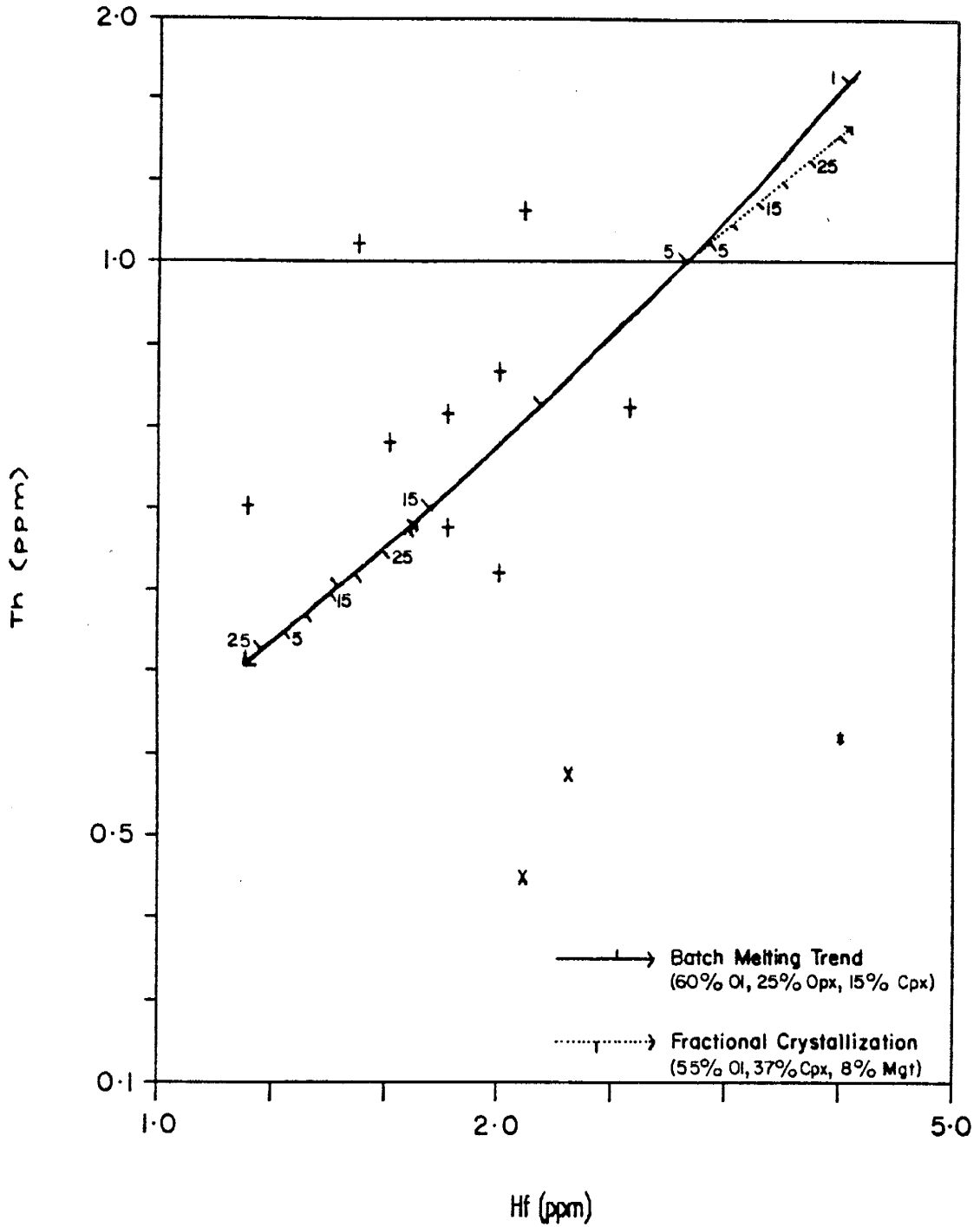
Figure 18
Cr vs. La (I-C) modeling diagram for BBC mafics. Symbols as in
Figure 9; tic-marks are in increments of 5% melting for BM curve
and 5% fractionation for FXL curves. See text for details.
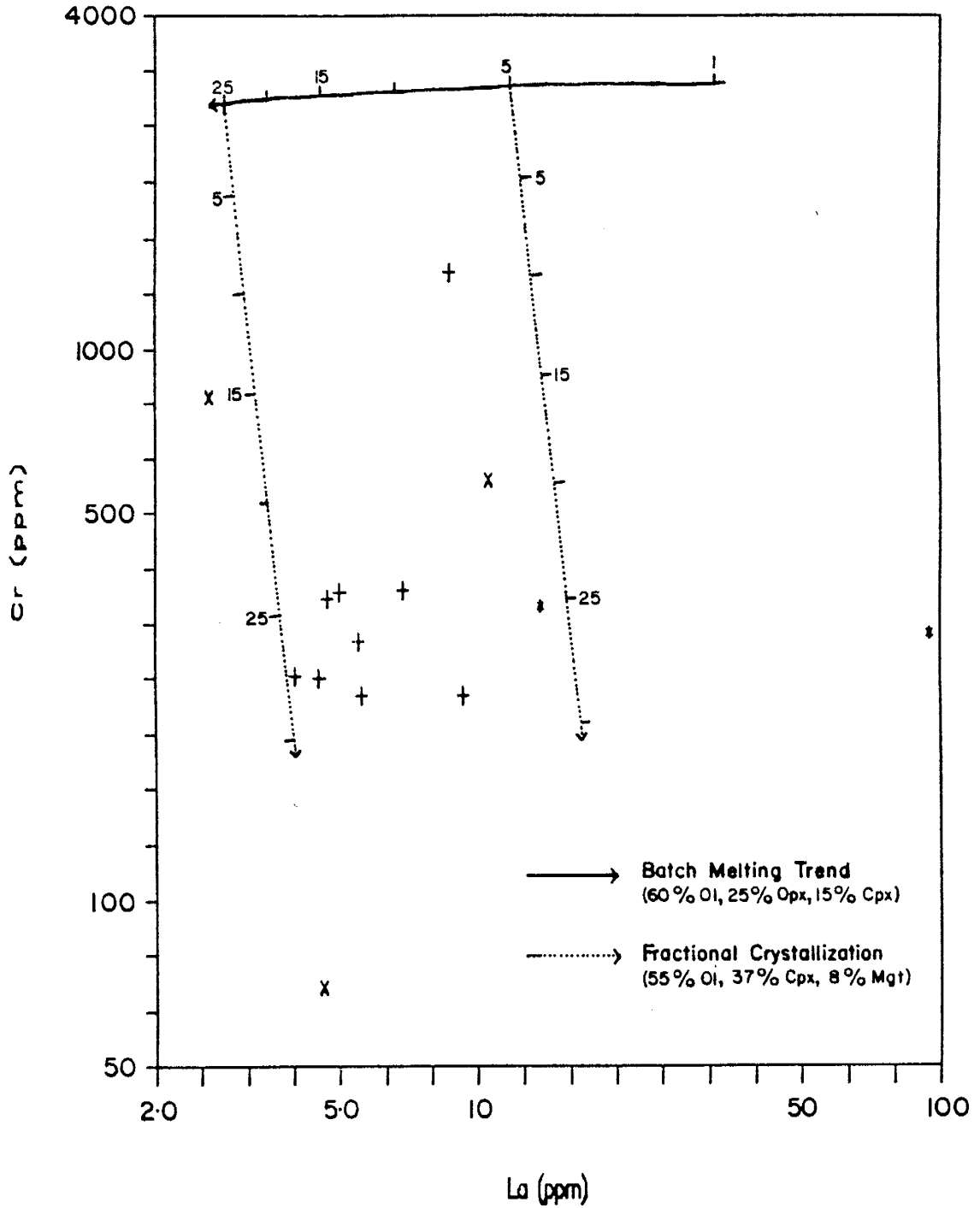
is necessary to explain the low levels of Ti in the samples as well as the abundances of Cr.

The same trends are apparent from modeling based on the OFXL system of O'Hara and Mathews (1981). Introduction of a small degree of leakage in OFXL models causes a much more significant variation in the concentrations of incompatible elements using smaller degrees of fractionation than the CFXL models.

Summary and Discussion

Any model for the tectonic setting of Limpopo mafic rocks must consider all geologic aspects, and any conclusions drawn at this time must rely on one basic assumption: that most of the mafic rocks are related to a common source. Three lines of evidence support this assumption: 1) the abundance of mafic rocks in the field, all probably of the same age based on field relations; 2) the igneous trends defined by many of the less mobile major and trace elements; and 3) the narrow fields defined by the samples on various discrimination diagrams.

It is evident that some of the LILE have been mobilized in some samples, probably as a result of metamorphism. Most affected are Ca, K, Rb, Ba, Th, and U. Because of their generally coherent relationships, the HFSE and REE are assumed to have remained relatively immobile throughout the metamorphic events.

Geochemical variation plots suggest that the mafic rocks are transitional between the calc-alkaline and tholeiitic suites. Island arcs are one of the only tectonic environments to which both calc-alkaline and tholeiitic rocks are common (Miyashiro, 1973).

Plots involving Ti, Zr, Nb, Hf, Ta and Y are the most sensitive in terms of characterizing the tectonic setting of the mafic rocks. These diagrams suggest that the BBC mafic rocks evolved in an arc-related setting. An interpretation of their NMORB-normalized distributions on the spidergram of Pearce (1983) is also consistent with the presence of a subduction zone component, which is characteristic of basalts from both island arc and continental arc settings. Ratios of incompatible elements demonstrate the similarity of these rocks to Phanerozoic arc-related rocks. Chondrite-normalized REE distributions of modern arc-related basalts also compare well with those of the BBC mafic rocks.

Most of the samples can be derived from a PM-like source which is enriched in incompatible elements, possibly by mantle metasomatism. Five to 25% batch melting of a lherzolite followed by about 10 to 30% closed system fractional crystallization of 55% olivine, 37% clinopyroxene and 8% magnetite yields a range of compositions similar to most of the samples presented. Open system FXL involving a small degree of leakage (5%) requires less fractionation than the CFXL model. A small degree of plagioclase fractionation is required to cause the slight Eu anomaly seen in the REE diagrams; however, significant amounts are ruled out because higher degrees of FXL would be required which is inconsistent with the low concentrations of HFSE. Several other options have been tested and are less acceptable. These include derivation from a source similar to that of NMORB, which is discounted because of the low HFSE concentrations for the BBC rocks relative to the NMORB source, and the involvement of amphibole in the melting or

fractionation assemblages, which results in heavy REE fractionation that is not observed in the rocks.

Three samples are anomalous (LMP-49, -58, and MS-5). Various lines of evidence suggest that they are contaminated or that a high degree of mobilization of many elements has occurred. These include high P_2O_5, HFSE and REE and variable LILE contents (Table II), inconsistent relationships on most diagrams, and highly irregular NMORB-normalized spidergrams.

For the reasons cited above, the BBC mafic rocks are interpreted as metamorphic equivalents of arc-related basalts which intruded the sedimentary rocks of the Beit Bridge Complex.

Granitic Rocks

Field Relationships

The granitic gneisses of the Beit Bridge Complex are the most abundant rock type exposed in the Messina area (Horrocks, 1983). Contacts between the granitic rocks and surrounding lithologies are usually sheared when exposed and thus do not allow positive determination of their igneous character (K. C. Condie, personal communication, 1986). Horrocks (1983) notes that some appear to be pegmatitic and form discrete layers and dike-like bodies which cross-cut the other lithologies. Massive as well as banded varieties (on a hand specimen scale) comprise a complete suite of tonalitic through granitic gneisses. Mason (1973) considers the banding to be often clearly due to original stratification, as opposed to the tectonic banding of the refoliated and reworked basement gneisses. He presents no evidence in support of his assumption, and admits that such a distinction cannot always be made.

Petrography

Two groups of granitic rocks can be distinguished by their mineral assemblages. One group has high (15 to 60%, averaging 40%) K-feldspar and very low (<1 to 10%, averaging 1%) biotite contents. Samples in the other group have low abundances of K-feldspar (all but two samples have less than 2%) and high biotite (5 to 10%, averaging 8%). The rocks of the first group are granites (*sensu stricto*) while those of the second range from tonalite to granodiorite or quartz monzonite.

Quartz contents range from 20 to 44% and average 33% for all of the granitic rocks; plagioclase comprises 8 to 70% (most samples contain 20 to 50%) and averages 34%, with anorthite contents ranging from An_7 to An_{40}. Garnet is present as a minor phase in all but three of the samples (LMP-27, -28, and -29), usually comprising $\leq$1%. LMP-35 is composed of 10% garnet while biotite is found only in trace amounts; in LMP-4, biotite is absent and garnet comprises about 5%. Muscovite is rare, if present, and pyroxenes are absent.

Accessory phases in all samples include opaques, zircon, apatite, sphene, rutile, allanite and epidote/zoisite. Two samples (LMP-28 and -29) contain a small amount of blue-green amphibole; in the latter sample the accessory phases comprise about 4%. One sample (LMP-9) contains trains of sillimanite needles which lie in planes parallel to the foliation; this sample is clearly a metasediment, and is presented here for comparison with the igneous samples.

K-feldspar and plagioclase are often intergrown with quartz, producing granophyric and myrmekitic textures. The K-feldspar is usually perthitic microcline with strained twinning. Plagioclase grains usually show strained pericline and albite twins. Grain boundaries vary from embayed and scalloped to curviplanar and straight within a single thin section. In many of the samples, 120° triple-junctions are found. Garnet appears to be skeletal, but no evidence of a replacement reaction is observed. Textures are generally polygonal equigranular and granoblastic, with some banding and foliation present. Grain sizes vary slightly between minerals and especially between

Table V
Chemical compositions of BBC granites

SAMPLE	LMP-8	LMP-11	LMP-15	LMP-24	LMP-26	LMP-27	LMP-35
SiO_2	74.74	75.49	75.74	75.35	78.29	80.21	75.60
TiO_2	0.21	0.09	0.09	0.19	0.12	0.10	0.26
Al_2O_3	14.50	13.71	14.27	13.94	12.53	11.22	13.52
Fe_2O_3T	1.88	1.19	1.09	1.73	1.01	0.94	2.42
MnO	0.04	< 0.02	< 0.02	< 0.02	< 0.02	< 0.02	0.06
MgO	1.09	0.47	0.45	0.62	0.55	0.55	0.53
CaO	2.20	1.12	1.33	1.43	0.91	0.37	1.23
Na_2O	4.14	2.56	3.88	3.40	3.80	2.92	2.65
K_2O	2.60	5.87	4.30	4.33	3.64	4.70	5.14
P_2O_5	0.09	0.04	0.06	0.06	0.06	0.02	0.05
LOI	0.42	0.08	0.00	0.00	0.15	0.13	0.00
Total	101.91	100.62	101.21	101.05	101.06	101.16	101.45
Rb	61.1	104	157	104	106	114	194
Cs	0.21	0.20	0.46	0.17	1.4	< 0.10	0.60
Sr	147	48.4	59.0	111	102	17.2	82.1
Ba	481	726	657	757	841	184	938
Th	8.8	38	16	41	23	29	23
U	1.8	2.4	3.2	3.4	1.5	2.2	3.0
Pb	29	48	34	41	27	25	34
Sc	3.4	2.0	1.7	3.9	1.0	0.5	5.5
Y	26.9	24.6	22.5	34.0	12.5	8.31	54.3
Zr	85	93	71	127	69	114	166
Hf	2.8	3.5	2.3	5.1	3.3	8.9	7.0
Nb	4.9	3.6	11	6.7	6.7	14	16
Ta	0.14	0.04	0.62	0.14	0.81	0.20	1.22
La	24.1	51.5	24.5	66.8	32.7	53.8	74.7
Ce	49.1	98.7	44.5	125	57.8	87.1	141
Sm	4.85	6.68	3.09	7.71	2.17	3.21	10.8
Eu	0.95	0.67	0.56	1.0	0.62	0.33	1.6
Tb	0.86	0.88	0.57	1.4	0.16	0.34	1.8
Yb	3.1	2.7	1.8	3.8	0.30	0.70	7.4
Lu	0.51	0.42	0.28	0.56	0.05	0.10	1.18
V	21	< 5.0	< 5.0	10	5.2	< 5.0	9.0
Cr	26	< 1.0	1.5	2.4	2.9	2.5	1.3
Co	3.9	0.8	1.4	2.2	4.0	0.7	2.4
Ni	17	12	9.8	7.9	9.5	6.5	12
Mg #	57	47	48	45	55	57	33
A/KNC	1.1	1.1	1.1	1.1	1.1	1.1	1.1
A/KN	1.5	1.3	1.3	1.4	1.2	1.1	1.4

Major elements in wt.%; trace elements in ppm. Fe_2O_3T = total Fe as Fe_2O_3. Mg # = [MgO/(MgO+FeO*)]*100 in mol. proportions.

Table V (continued)
Chemical compositions of BBC tonalites and granodiorites.

SAMPLE	LMP-7	LMP-28	LMP-29	LMP-30	LMP-39	LMP-59
SiO2	72.53	73.71	72.00	71.85	72.16	67.30
TiO2	0.46	0.39	0.54	0.49	0.56	0.69
Al2O3	14.81	14.34	14.78	14.32	14.35	16.94
Fe2O3T	3.41	2.17	2.69	3.14	3.28	4.07
MnO	0.06	0.04	0.05	< 0.02	0.03	< 0.02
MgO	1.51	1.29	1.35	1.42	0.98	1.86
CaO	2.91	3.25	3.20	2.39	2.37	3.57
Na2O	4.29	4.36	4.52	3.57	3.40	4.12
K2O	1.39	1.21	1.39	3.24	3.67	1.98
P2O5	0.11	0.06	0.11	0.07	0.13	0.16
LOI	0.49	0.65	0.24	0.36	0.13	0.28
Total	101.97	101.47	100.87	100.85	101.05	100.97
Rb	53.1	30.5	52.2	108	73.9	55.1
Cs	1.2	1.6	1.1	0.65	0.35	0.63
Sr	198	177	192	121	337	316
Ba	472	357	640	643	1782	1001
Th	35	0.32	17	59	47	52
U	1.5	0.30	1.2	2.2	3.9	1.5
Pb	18	14	12	26	28	22
Sc	6.7	5.2	6.1	5.0	3.7	3.8
Y	13.3	9.66	23.2	10.9	11.7	9.76
Zr	157	169	264	219	445	324
Hf	6.0	5.9	8.1	7.3	15	9.2
Nb	10	5.8	16	12	7.8	13
Ta	0.47	0.28	0.75	0.32	0.27	0.31
La	99.6	10.6	67.7	88.0	189	110
Ce	179	19.4	129	170	365	203
Sm	8.95	1.81	7.13	9.61	16.0	10.8
Eu	1.5	1.1	1.5	0.85	2.7	1.5
Tb	0.70	0.29	0.83	0.63	0.99	0.67
Yb	0.92	0.85	1.7	0.64	1.3	0.55
Lu	0.17	0.13	0.24	0.08	0.15	0.09
V	52	34	36	49	29	74
Cr	28	21	4.4	20	7.4	20
Co	9.1	4.6	4.1	6.7	4.2	8.9
Ni	17	17	12	17	9.8	14
Mg #	50	57	53	50	40	51
A/KNC	1.1	1.0	1.0	1.0	1.0	1.1
A/KN	1.7	1.7	1.7	1.5	1.5	1.9

Major elements in wt.%; trace elements in ppm. Fe_2O_3T = total Fe as Fe_2O_3. Mg # = [MgO/(MgO+FeO*)]*100 in mol. proportions.

Table V (continued)
Chemical compositions of other BBC granitic rocks

SAMPLE	LMP-9	LMP-17	LMP-4	LMP-5	LMP-33
SiO_2	74.13	75.42	76.50	72.33	76.67
TiO_2	0.38	0.88	< 0.02	0.04	0.02
Al_2O_3	13.65	11.48	14.00	16.66	14.15
Fe_2O_3T	2.75	3.57	1.06	0.73	0.45
MnO	< 0.02	0.03	< 0.02	0.04	< 0.02
MgO	2.39	1.62	0.69	0.55	0.67
CaO	2.26	2.60	1.29	1.63	1.69
Na_2O	2.24	2.75	3.56	3.49	3.80
K_2O	2.44	1.48	4.56	6.47	3.60
P_2O_5	0.03	0.20	0.06	0.05	0.04
LOI	0.63	0.56	0.02	0.10	0.45
Total	100.91	100.59	101.74	102.09	101.54
Rb	75.3	56.1	78.8	127	68.2
Cs	1.6	0.33	< 0.10	0.63	0.91
Sr	78.4	58.8	78.1	82.4	135.5
Ba	548	310	494	761	835
Th	14	10	1.4	0.48	0.73
U	2.4	2.6	0.51	0.36	1.4
Pb	21	18	55	57	43
Sc	5.1	13.4	5.1	2.2	0.70
Y	7.96	119	14.6	16.9	3.85
Zr	242	614	48	27	28
Hf	8.4	18	2.4	0.5	0.8
Nb	7.7	43	3.3	3.5	3.3
Ta	0.69	2.69	< 0.03	0.08	< 0.03
La	30.9	59.3	10.6	18.5	12.2
Ce	59.2	144	17.3	28.5	19.2
Sm	3.30	23.2	0.97	1.19	0.86
Eu	0.75	4.8	0.56	0.99	1.5
Tb	0.30	4.2	0.22	0.20	0.06
Yb	0.51	12	1.7	1.4	0.13
Lu	0.07	2.0	0.36	0.23	0.02
V	4.0	55	< 5.0	< 5.0	< 5.0
Cr	168	< 1.0	2.4	1.5	2.1
Co	9.9	2.2	0.6	1.9	0.9
Ni	37	9.6	8.9	11	12
Mg #	66	50	59	63	77
A/KNC	1.3	1.1	1.1	1.1	1.1
A/KN	2.2	1.9	1.3	1.3	1.4

Major elements in wt.%; trace elements in ppm. Fe_2O_3T = total Fe as Fe_2O_3. Mg # = [MgO/(MgO+FeO*)]*100 in mol. proportions.

bands, averaging about 2 mm. Detailed petrographic descriptions of the samples are given in Appendix C.

Chemical Composition

Major and trace element data for the felsic rocks are presented in Table V. As with the mafic rocks, the mobility of elements in the granitic series must be investigated before meaningful interpretations can be made.

Prabhu and Webber (1984) have devised a series of four tests, based on major element compositions, which can distinguish the proto- lith as sedimentary or igneous. No test is diagnostic by itself; that is, each sample must place consistently in several tests in order to be classified as a metasedimentary or metaigneous rock. Prabhu and Webber applied these tests to highly deformed amphibolite grade gneisses from the Grenville Province of Quebec. The tests are repeated below on the granitic rocks of this study, but it is emphasized that major element mobility has been suggested for the mafic rocks (especially SiO_2 and possibly Na_2O and K_2O), and may have occurred in the granitic rocks.

The first test of Prabhu and Webber (1984) is to plot the samples on the diagram devised by Garrels and MacKenzie (1971), which shows compositional characteristics of various igneous and sedimentary rocks on the basis of $\log(SiO_2/Al_2O_3)$ vs. $\log[(CaO + Na_2O)/K_2O]$ (Fig. 19). This diagram suggests that the BBC samples have igneous precursors because they generally fall on a trajectory parallel to the igneous differentiation trend.

The second test involves the use of a discriminant function introduced by Shaw (1972) which is calculated from the weight percents of oxides using the following equation:

$$DF = 10.44 - 0.21*SiO_2 - 0.32*Fe_2O_3T - 0.98*MgO$$
$$+ 0.55*CaO + 1.46*Na_2O + 0.54*K_2O$$

Positive DF values are characteristic of igneous rocks and negative values indicate sedimentary parentage. Greywackes and arkoses have values near zero which indicate their mixed parentage. The values for DF for the BBC samples are presented in Table VI; from this test, an igneous protolith is suggested for all but two samples (LMP-9 and 17).

Also in Table VI, normative quartz values are compared with those of other rock types. The average sediment and rhyolite data are taken from Prabhu and Webber (1984). In the fourth test of Prabhu and Webber (1984) the Niggli numbers si vs. mg are compared with those of sediments and fresh igneous volcanics (Fig. 20). For rocks of high metamorphic grade, or which show evidence for quartz veining, tests which rely on only one major element are less dependable than tests that combine several elements. Hence, the comparisons based on Niggli numbers or normative quartz should be viewed with caution. The results of the third test are consistent with igneous parentage for the BBC samples, but the Niggli number plot suggests that the samples are derived from sediments.

Results suggest an igneous origin for most of the granitic rocks when consideration is given to element mobilization. Two exceptions are samples 17 and 9, which are considered to be metasediments. In the first test, sample 17 plots nearer the sandstone field than the igneous

Figure 19
BBC samples on the diagram of Garrels and MacKenzie (1971).
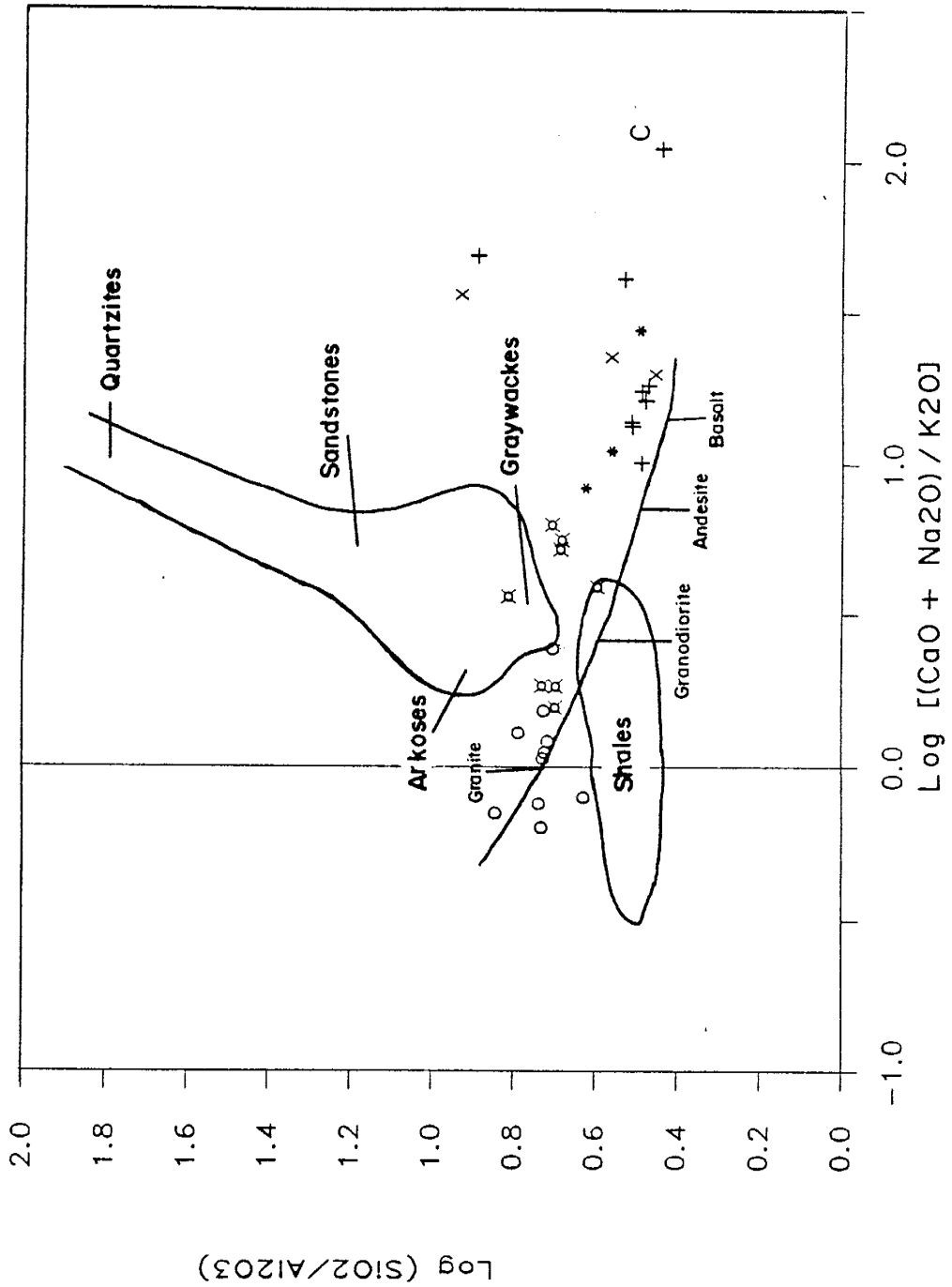Fields of original authors; symbols as in Figure 6a.

Figure 20
Niggli numbers si vs. mg, BBC samples. Fields of Prabhu
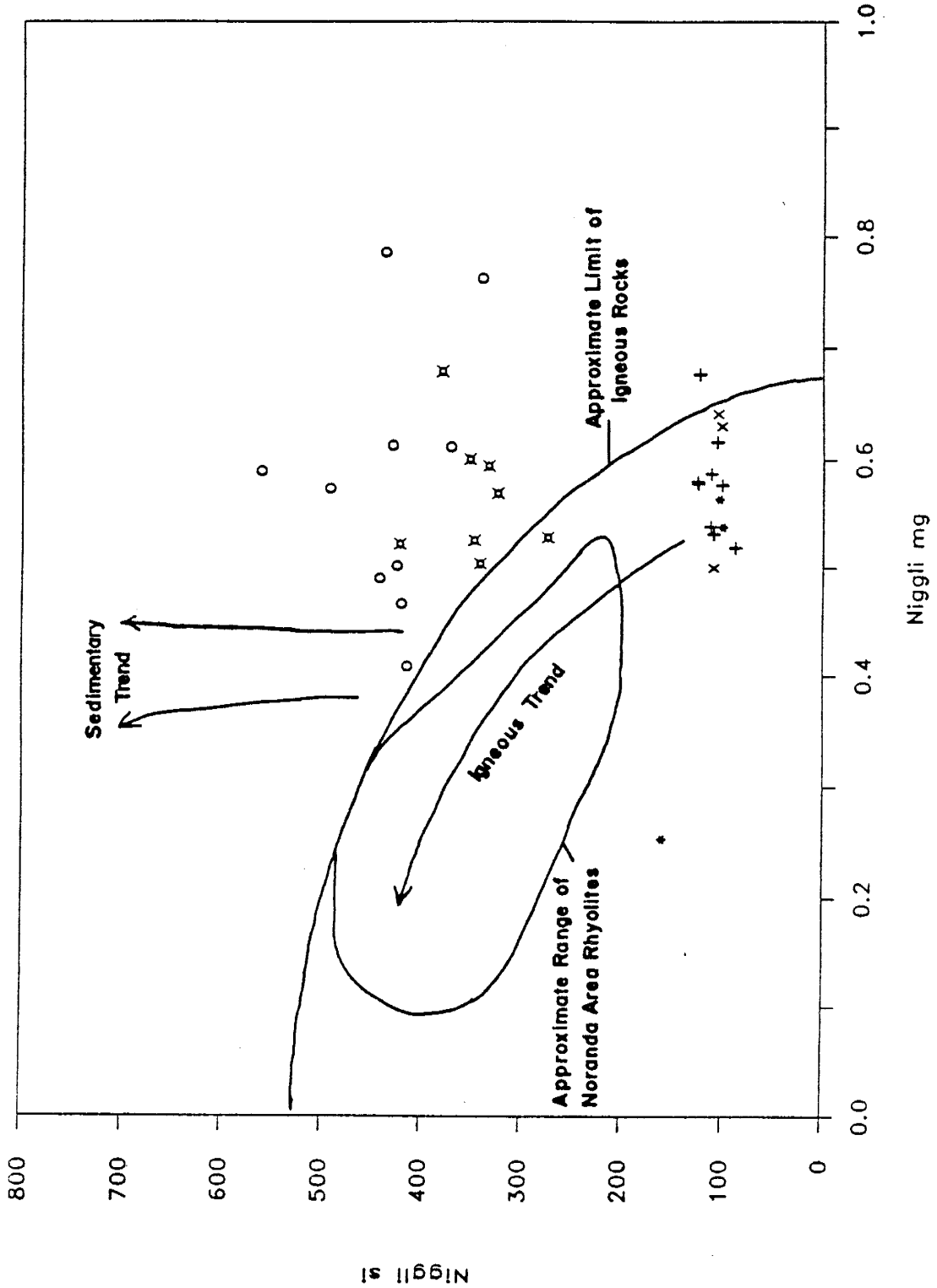and Webber (1984). Symbols as in Figure 6a.

Table VI
Comparison of BBC granitic rocks with tests of Prabhu and Webber (1984).

SAMPLE	Normative Quartz[a]	Shaw's DF[b]	Averages[c]	Normative Quartz	Shaw's DF
LMP- 8	31.75	1.73	Tertiary-Recent		
LMP-11	34.82	1.27	sialic volcanics	25.61 $\pm$ 7.06	+2.72
LMP-15	32.84	2.46			
LMP-24	34.66	1.54	Sandstones	52.28 $\pm$ 20.09	-4.22
LMP-26	39.23	1.15			
LMP-27	43.17	-0.24	Greywackes	36.11 $\pm$ 8.29	-0.05
LMP-35	35.89	0.59			
			Niranda area		
LMP- 7	31.84	1.25	Rhyolites	40.07 $\pm$ 7.12	+0.30
LMP-28	31.49	1.81	Rhy. pyroclastics	41.98 $\pm$ 9.79	-0.23
LMP-29	30.18	2.24			
LMP-30	31.29	1.23			
LMP-39	30.91	1.52			
LMP-59	25.33	2.23			
LMP- 9	43.26	-2.52			
LMP-17	46.43	-1.88			
LMP- 4	33.94	1.73			
LMP- 5	22.35	3.96			
LMP-33	36.68	1.96			

[a] CIPW norm.
[b] Discriminant Function of Shaw (1972), as described in text.
[c] Averages from Prabhu and Webber (1984), pp. 341 and 344.

trend (Fig. 19). Both 9 and 17 have strongly negative DF values and high normative quartz, although the quartz values are well within the range of Noranda area rhyolites (table VI). Also, sillimanite is present in sample LMP-9 and LMP-17 contains abundant apatite.

Sediments tend to scatter on variation plots which normally display igneous differentiation trends. Such diagrams include SiO_2 variation plots for the major elements, and others for the trace elements. Several plots that may distinguish between ortho- and

paragneisses are based on major elements (e.g. the ternary MgO-CaO-Al_2O_3 diagram of Leyreloup et al., 1977) and are applicable for rocks metamorphosed up to the amphibolite grade; however, felsic gneisses of igneous origin commonly lie in the sedimentary fields on such plots.

Figures 6a-g show the variations of the major elements relative to SiO_2. Most of the major elements show a covariation (notably TiO_2, Fe_2O_3T and CaO) but two oxides, Na_2O and K_2O, show considerable scatter. Such scatter is typical of fresh felsic igneous rocks and is therefore not necessarily a consequence of mobilization. Thus, mobilization of SiO_2 may have been minimal (±5%).

The granitic rocks are classified according to the diagrams of Winchester and Floyd (1977) (Fig. 3 and 4) and have been plotted on the alteration screen of Davis et al. (1979). The Winchester and Floyd diagrams and Table V suggest that the granitic rocks may be enriched in Nb (relative to Y), but according to the alteration screen they appear unaltered. On the ternary classification scheme of Bavington and Taylor (1980) (Fig. 5) and on the CaO-Na_2O-K_2O plot (Fig. 21) the samples show a continuous variation from tonalite to granite. Calc-alkaline trends are suggested by the classification schemes of Jensen (1976) (Fig. 7) and Irvine and Baragar (1971).

Because of the lack of scatter on the diagrams mentioned above, the granitic rocks (with the exception of samples 9 and 17) are thought to be ortho- rather than paragneisses. This hypothesis is supported by trace element variations which are typical of igneous rather than sedimentary rocks.

Figure 21
CaO-Na$_2$O-K$_2$O diagram, BBC granitic rocks. Filled squares,
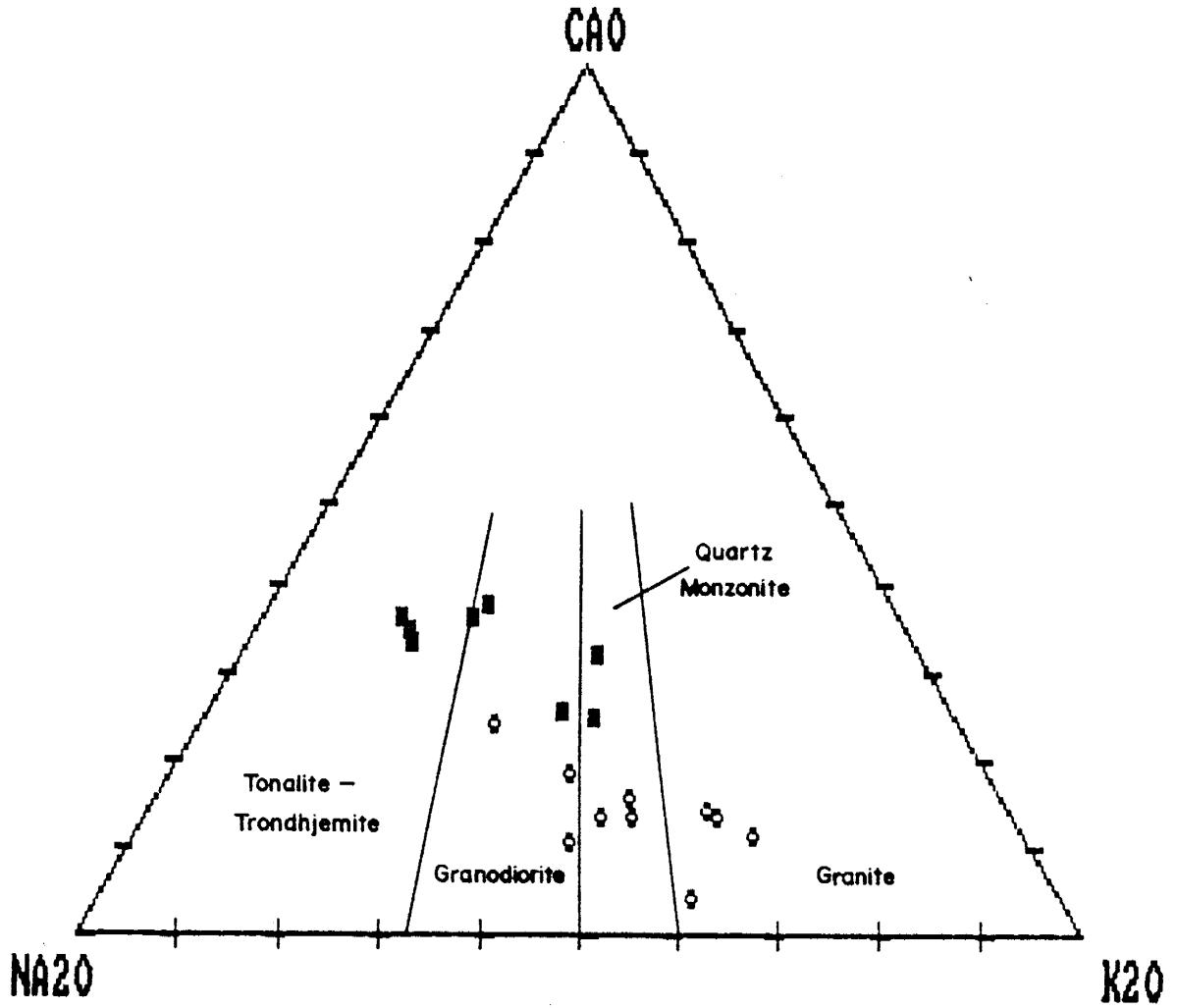tonalitic to granodioritic samples; open circles, granites.

Figure 22a and b
Chondrite-normalized REE distributions, BBC granites.
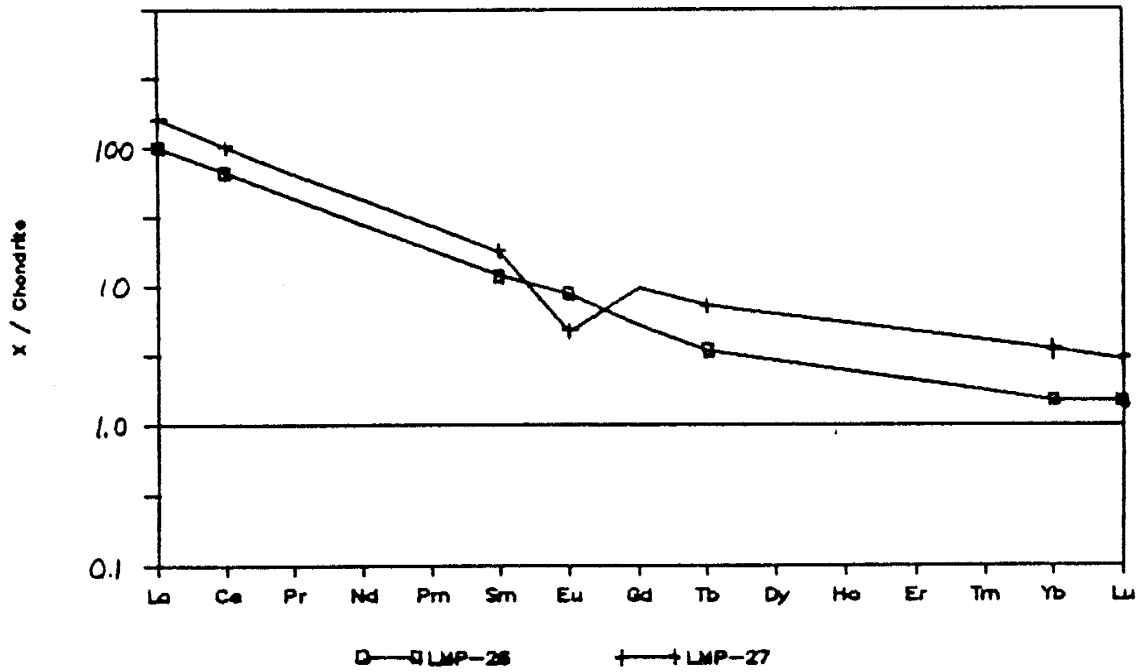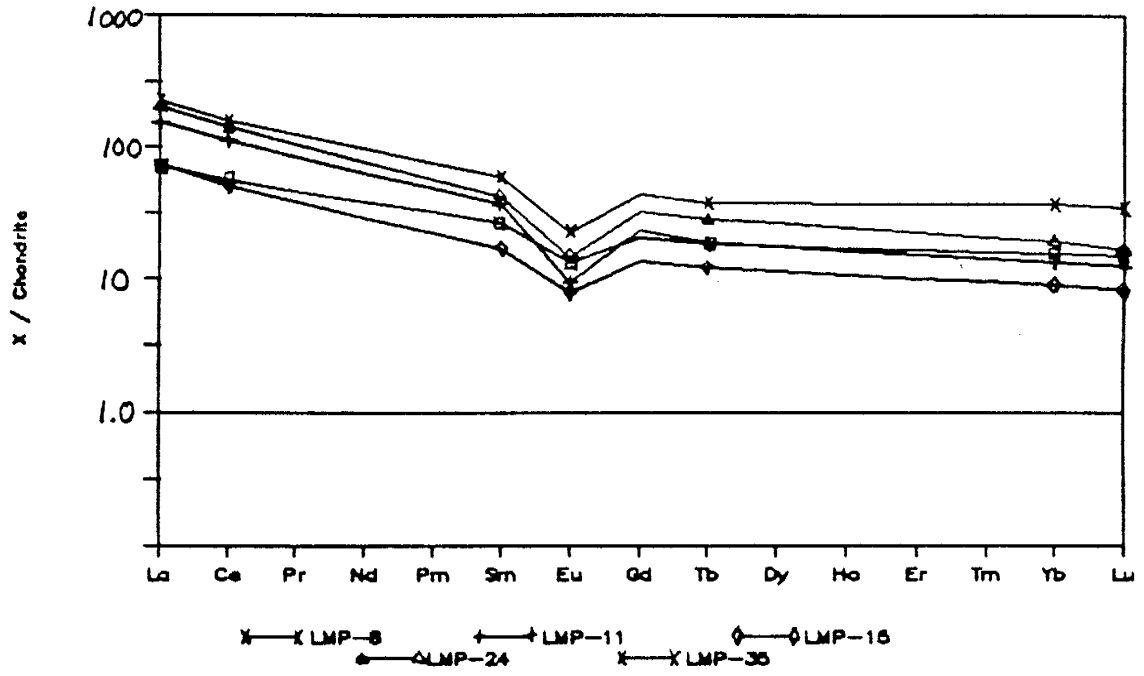
Figure 22c and d
Chondrite-normalized REE distributions, BBC tonalite-granodiorites, samples with positive Eu anomalies, and metasediments LMP-9 and -17.
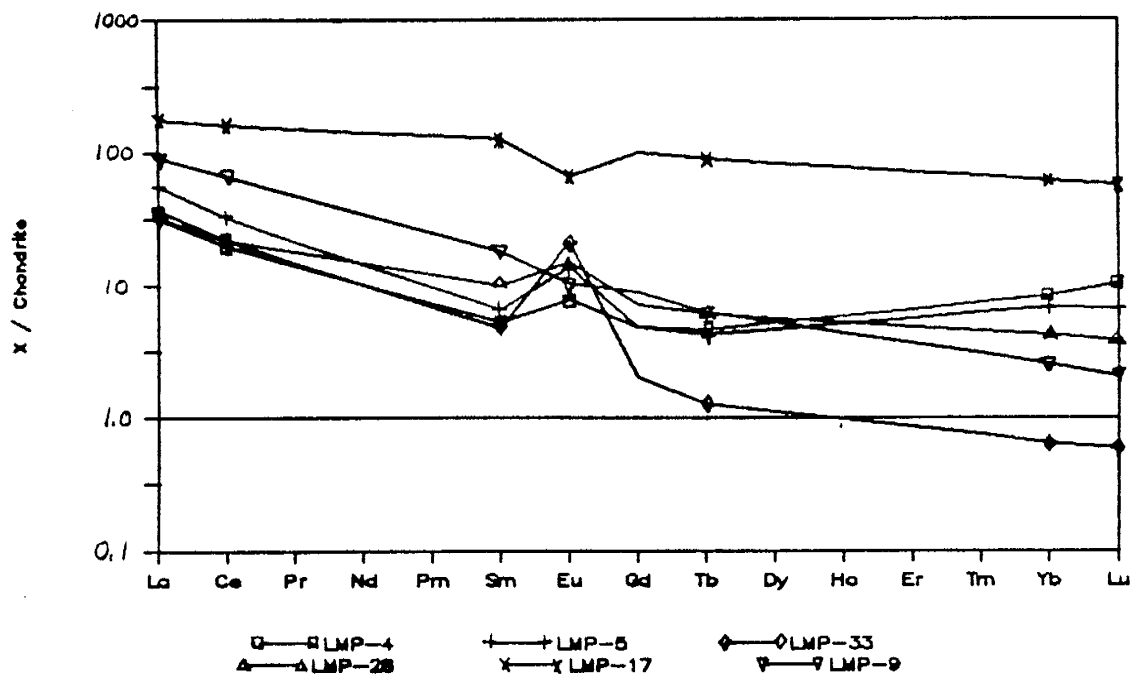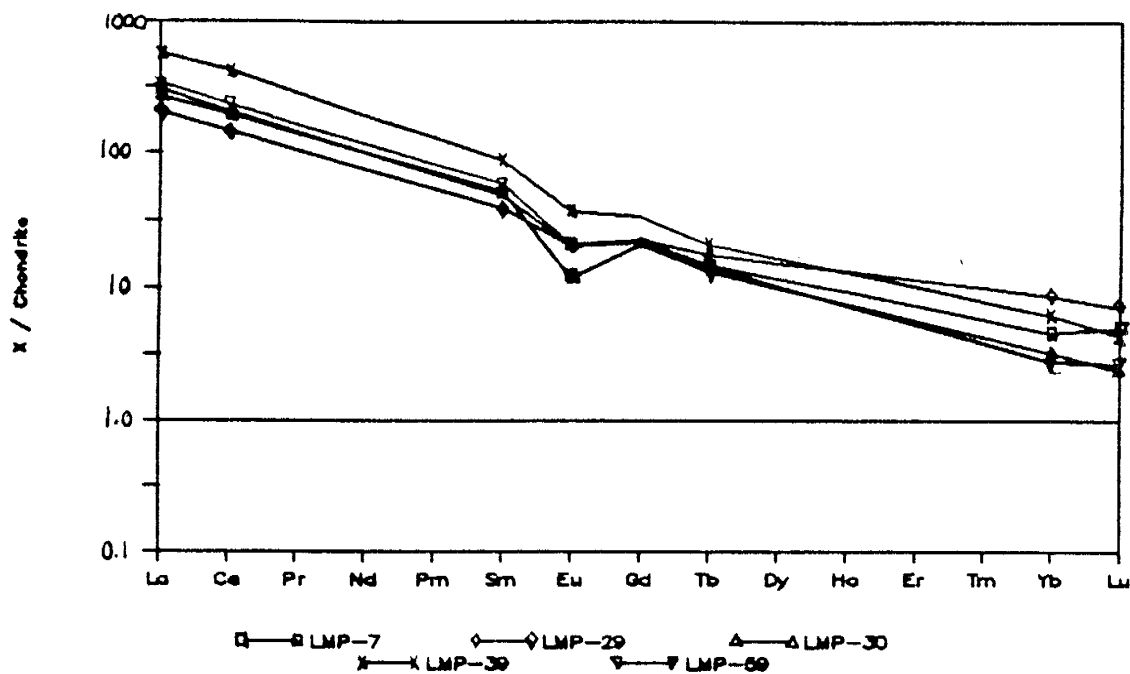
Figure 23a and b
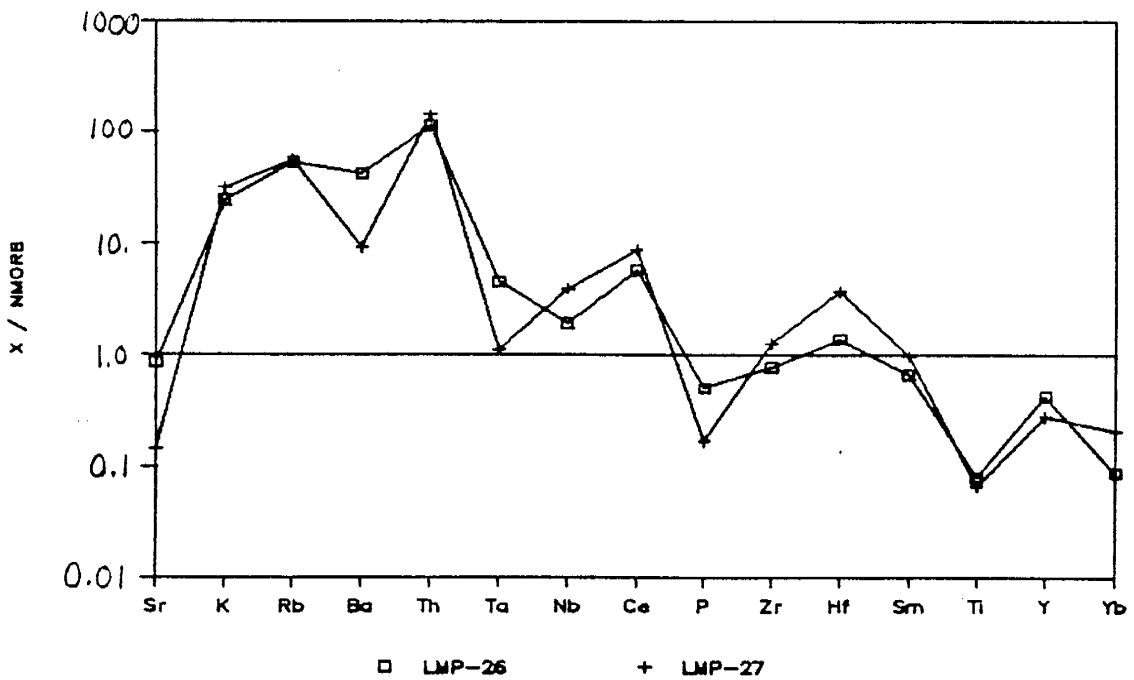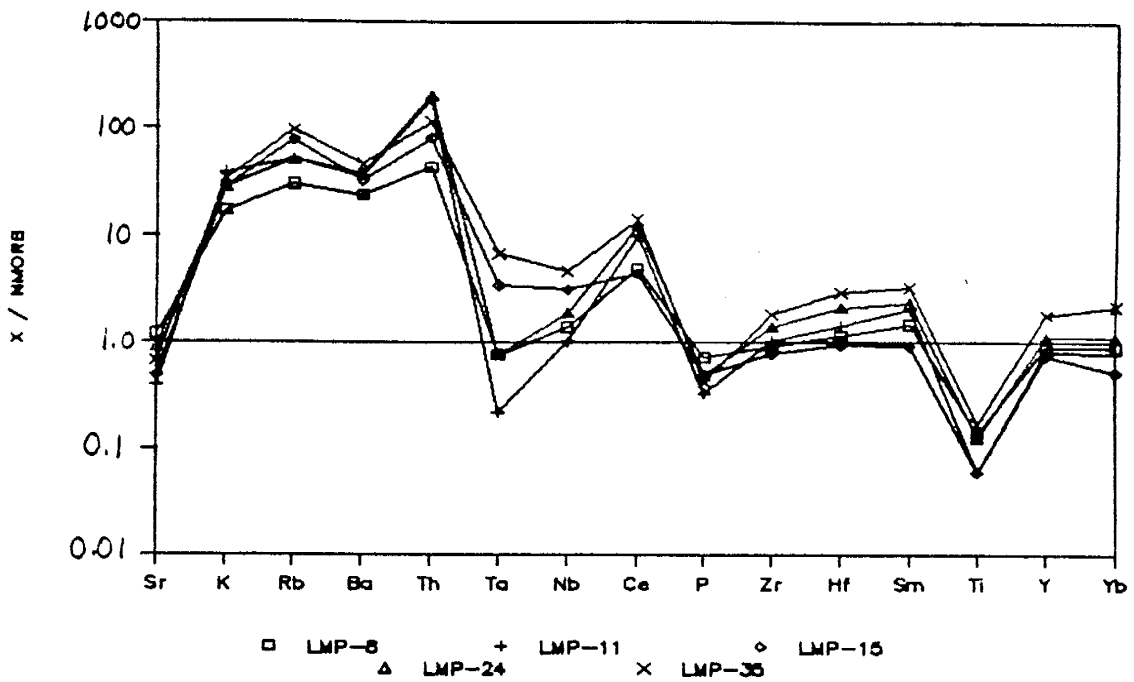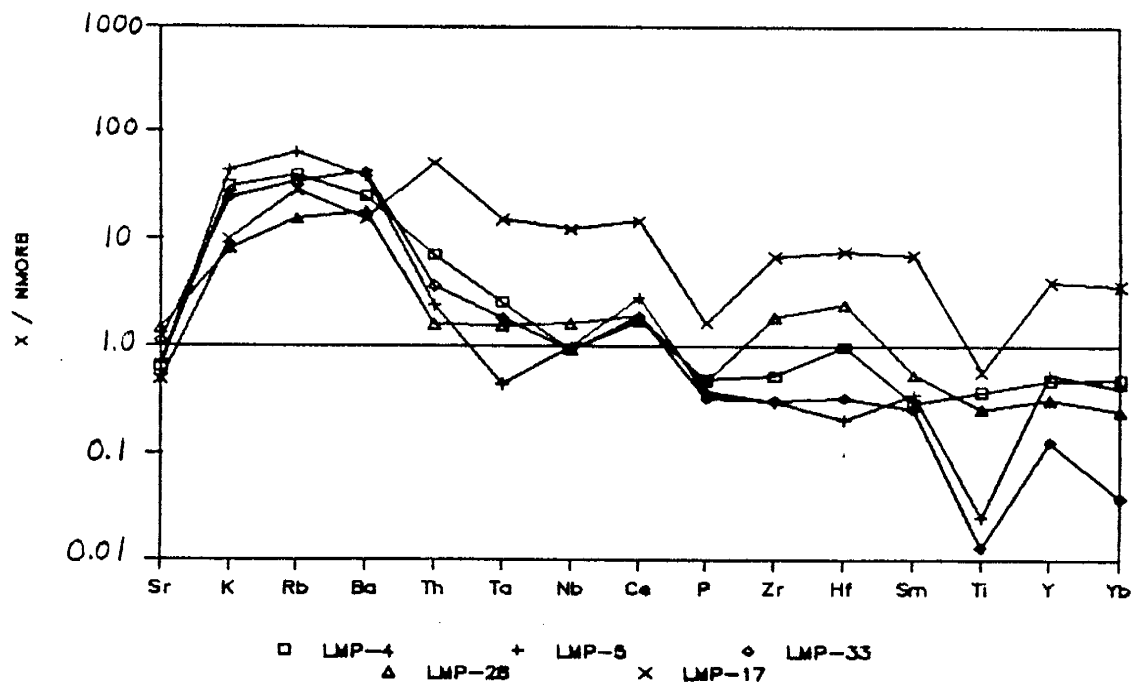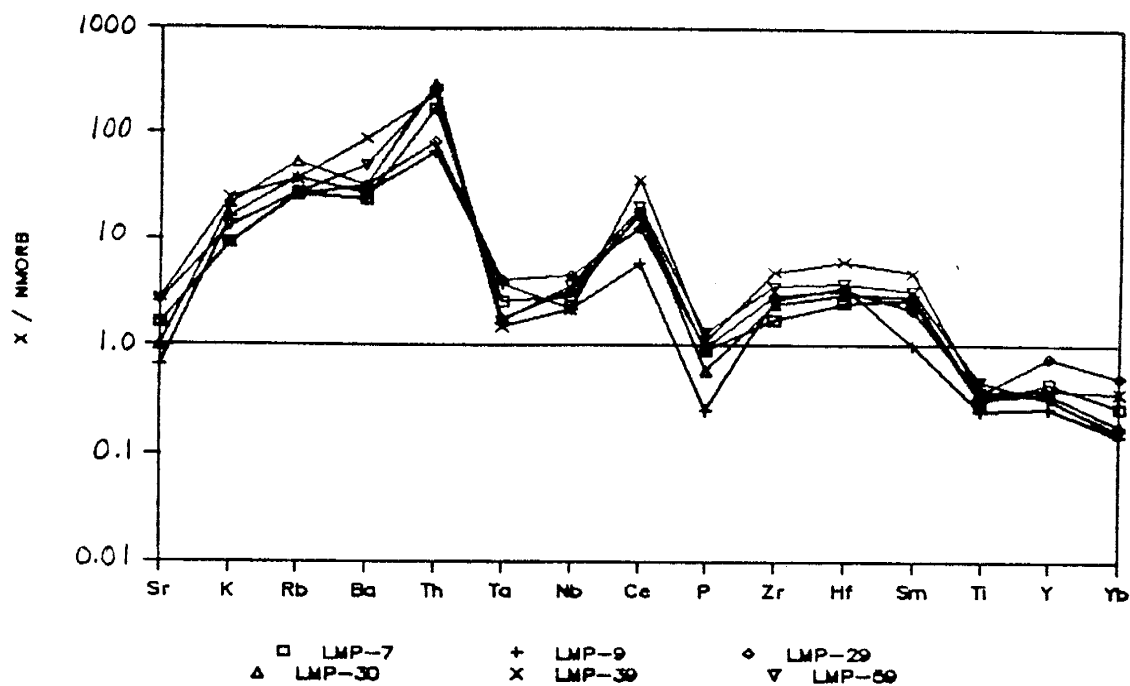NMORB-normalized spidergrams for BBC granites.

Figure 23c and d
NMORB-normalized spidergrams for BBC tonalitic to granodioritic samples
(c) and LMP-17 and samples with positive Eu anomalies (d).

Chondrite-normalized REE distributions are presented in Figure 22. The steep hREE-depleted patterns in the tonalitic to granodioritic gneisses are typical of Archean tonalites. These patterns are similar to, but slightly more fractionated than, dacites from modern continental volcanic arcs. The granite gneisses have less steep REE patterns with prominent negative Eu anomalies, and have relatively flat hREE patterns, similar to those of rhyolites from modern continental arc settings. The two samples in Figure 22b have been separated because they contain hornblende which may explain their slightly more fractionated patterns. The positive Eu anomalies of samples 28, 4, 5, and 33 may result from partial melting (anatexis) with these samples retaining plagioclase, but the U-shaped patterns of the latter three are difficult to explain. It is possible that they contain a phase rich in hREE (such as zircon or xenotime), but this is not evident in thin section. However, such phases are often very widely distributed in granites, and are not always encountered in thin section. Replicate INAA analyses of samples 4 and 5 confirm that the REE patterns are not the result of an analytical error.

The BBC granitic gneisses show a subduction zone component coupled with a within-plate signature on the NMORB-normalized spidergram of Pearce (1983) (Fig. 23). Depletions in P and Ti might be explained by fractionation of apatite and a Ti-bearing phase such as sphene or ilmenite.

The samples are similar to I-type granitic rocks from modern arc settings from several perspectives. On the NMORB-normalized diagram they tend to have greater normalized enrichments in Zr and Hf relative

Figure 24
Rb/30-Hf-Ta, BBC granitic rocks. Fields of Harris et al. (1986).
Symbols as in Figure 3.
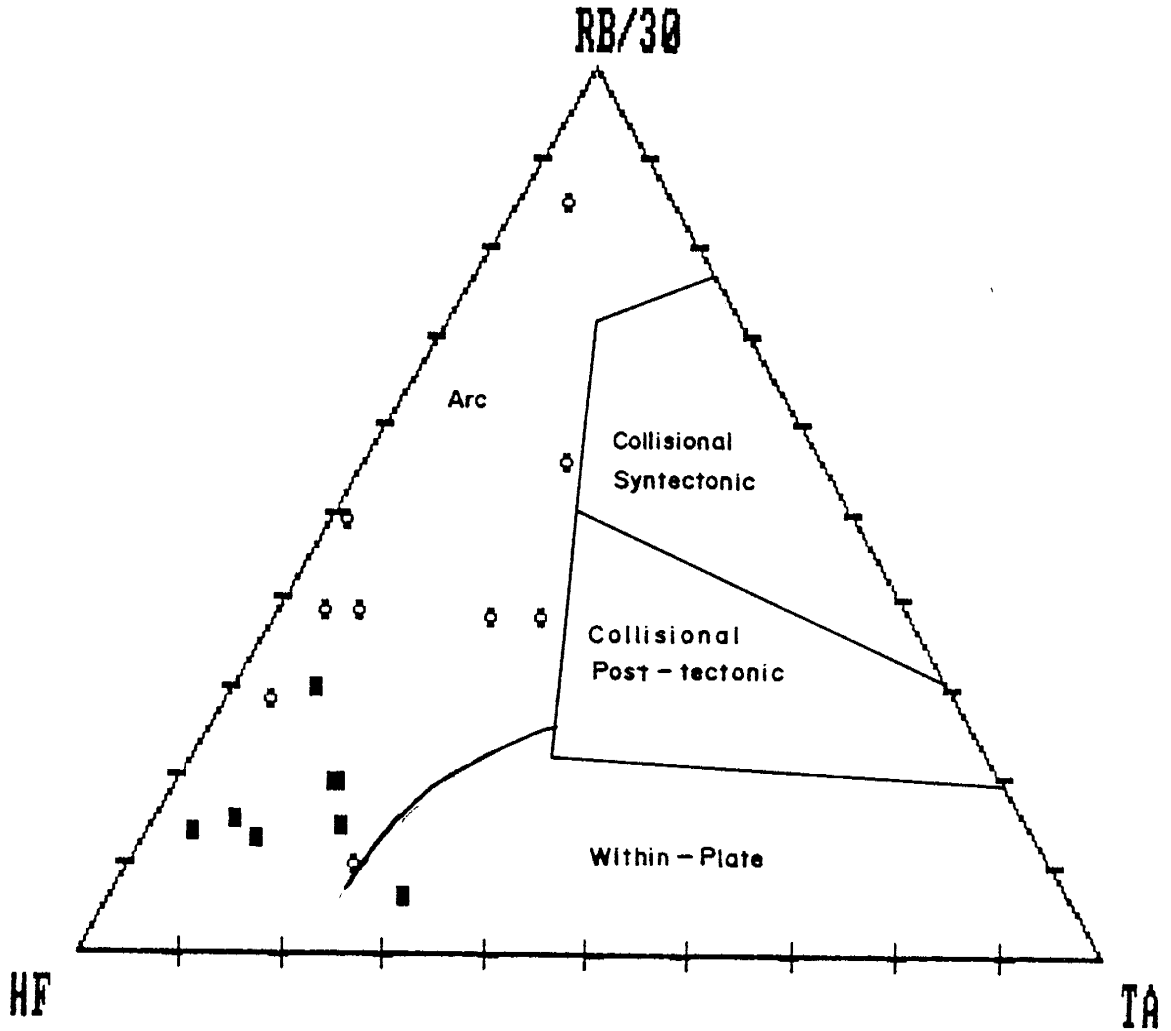
Figure 25
Rb vs. (Y + Nb), BBC granitic rocks. Fields of Pearce et al. (1984).
Symbols as in Figure 3.
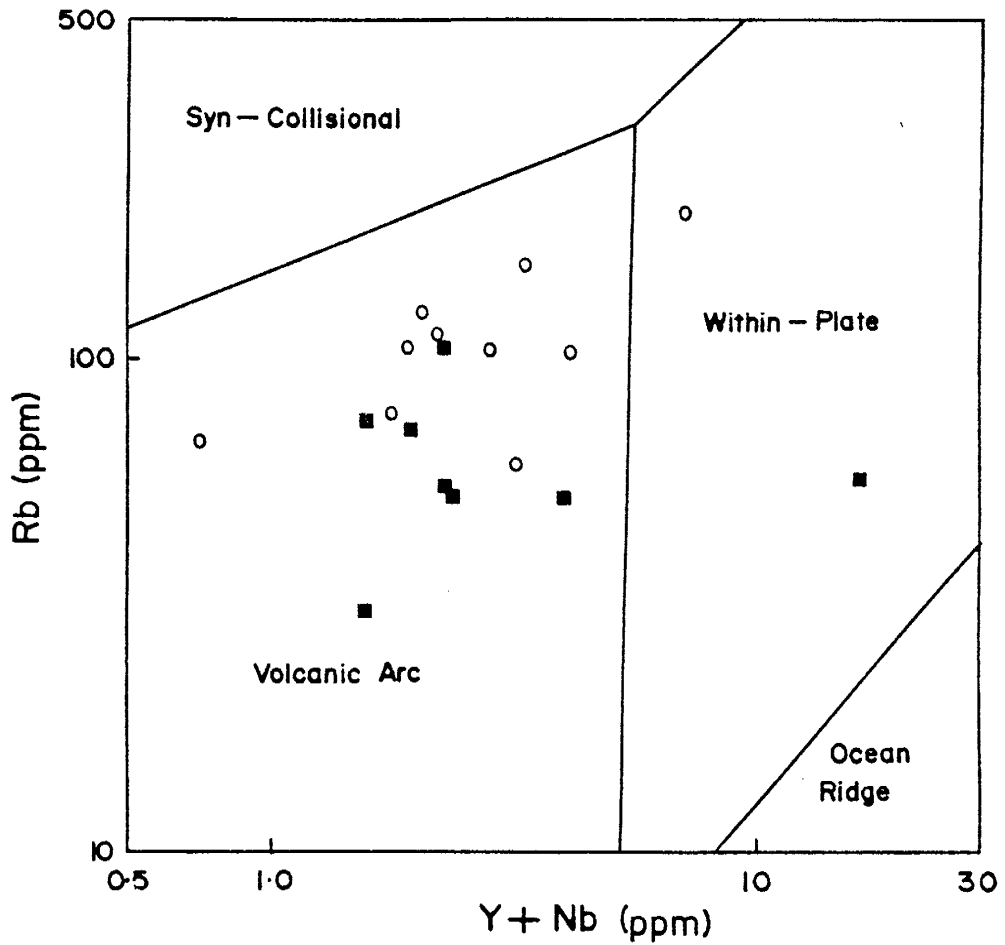
to Y and Yb than rift-related granitic rocks. The relative concentrations of Rb, Hf and Ta and Rb vs. Y+Nb (Fig. 24 and 25) are also suggestive of an origin in an arc-related environment. Other similarities with Phanerozoic I-type granitoids (Pitcher, 1983, p. 21) include the wide compositional range from tonalite to granite, the presence of biotite with hornblende but without muscovite, the presence of K-feldspar as interstitial material in the tonalites and granodiorites, and possibly an association with copper mineralization (Ryan et al., 1983). Other criteria have not been preserved, such as associated rock types, xenolith populations, proportions of alkalis and alkaline earths to aluminum, intrusive style, and duration of magmatism. These features could have been destroyed by the multiple high-grade metamorphic events, or they may never have been present due to subtle differences in geologic processes in the Archean; in the present case the latter may not be evaluated due to the former.

Summary

On the basis of major elements, many BBC granitic rocks appear to have derived from igneous precursors. The samples show a continuous trend from tonalite to granite. Major element variation diagrams suggest that only minor amounts of mobilization may have occurred for such oxides as Na_2O, K_2O and SiO_2. This mobilization has not obscured original compositions, so geochemical discrimination diagrams can be used to constrain the tectonic setting in which they formed.

Except for most LILE, trace elements also appear to have maintained their original distributions. Diagrams involving HFSE and REE

suggest that the granitic gneisses formed as igneous rocks in an arc-related environment.

Data from the BBC granitic rocks lead to an interpretation similar to that reached for the BBC amphibolites. Previous investigations maintain that the granitic rocks exposed in the Messina area are metasediments (e.g., Mason, 1973 and Brandl, 1983), based on their association with metamorphosed carbonates, quartzites, pelites and banded iron formations. Intrusive contacts between ortho- and paragneisses are not commonly preserved. The results of this study suggest that the metasediments in the area are much less widespread than previous authors indicate.

Discussion

The CZ of the Limpopo Belt contains a lithologic package distinct even from those in adjacent marginal zones. As the contact between the SRG and the BBC is not commonly exposed, it is possible that the two units have been tectonically juxtaposed; i.e. it is possible that the BBC has been thrust into its present position above the SRG.

The association of BBC lithologies (excluding the granitic gneisses) has been interpreted as a sea-floor depositional sequence (e.g., Shackleton, 1986; Burke et al., 1985). Because of their infolded nature, the granitic gneisses are assumed by these authors to be of sedimentary origin as well. However, as noted earlier, contacts between the granitic gneisses and metasediments do not preclude an intrusive relationship. If such contacts are found, the granitic rocks might be reinterpreted as felsic volcanics, which would alter the tectonic model proposed here only slightly.

The granitic gneisses of the BBC have not been studied by petrographers in as great detail as the metapelites because they do not contain mineral assemblages which record metamorphic P-T paths. Unless the conditions of the retrogressive metamorphism were more hydrous in the granitic gneisses than in the amphibolites, the granitic gneisses should record a granulite-facies event by preserving orthopyroxene (Condie and Allen, 1984). Orthopyroxene, however, is not observed in any of the felsic gneisses. The lack of both orthopyroxene grains and

syndepositional contact relationships with the surrounding lithologies suggests that the granitic gneisses are granitic magmas which intruded just after the peak of granulite-facies conditions. If this proves to be so, they might be regarded as I- (Caledonian) type rather than I- (Cordilleran) type (Pitcher, 1983); however, the geochemical data suggest the latter is more appropriate.

The amphibolites appear to be intrusive mafic dikes and sills (Condie, personal communication, 1986), but some could be extrusives. It is not possible to distinguish among these emplacement mechanisms due to metamorphic overprinting.

The MLI is infolded with all of the rocks above. Barton et al. (1979) suggest that it could represent the root zone of a greenstone-belt terrain which has been structurally interleaved with the metasediments of the BBC and the SRG. It is possible that the amphibolites of the BBC are related to the MLI by the mechanism proposed by Barton et al. (1979) (i.e., that the MLI is a remnant of the magma feeding the greenstone belt terrain), but data are not currently available to evaluate this problem further.

The Singlele Gneiss is probably the product of anatexis, which probably occurred during the peak of metamorphism. It is not known whether it was derived from any of the rock types studied here, although the presence of granitic rocks with positive Eu anomalies suggests that partial melting may have occurred, leaving behind residual plagioclase.

The Bulai Gneiss was emplaced into the BBC around 2690 Ma (Watkeys et al., 1983). It is significant that the source of this body must

have been at sufficient depth to have been isostatically unstable, and that at 2700 Ma the BBC was at the relatively shallow depth at which the Bulai gneiss equilibrated.

The CZ is bordered on either side by shear zones, suggesting that the CZ is an exotic block that has been tectonically emplaced between the NMZ and SMZ. This is supported by the uniqueness of the CZ relative to the surrounding marginal zones in terms of structural trends as well as lithologies and their ages. The timing of the various events affecting the CZ lithologies (including intrusions, deformations and metamorphisms) is loosely constrained at present.

The timing of deformation and metamorphism in the surrounding marginal zones is even more loosely constrained. The dominant structural trends are suggestive of N-S compression. Metamorphic events may be correlative with those in the CZ (especially those of the SMZ), but this has not been demonstrated.

Various models have been proposed for greenstone belts. One is that they formed at the edges of extensional basins (rifts and back-arc basins), and the other is that they may represent primitive oceanic arcs. There is at present no model for the tectonic environment in which the greenstone belts of the NMZ and SMZ formed, but most workers have called upon the presence of a subduction zone and related volcanism in their models for the evolution of the Kaapvaal and Zimbabwe craton margins bordering the Limpopo Belt. The geochemical characteristics of the BBC orthogneisses are consistent with the subduction zone model.

Toward a Tectonic Model

The importance of both felsic and mafic igneous rocks with subduction zone signatures has been overlooked in previous models for the tectonic reconstruction of the Limpopo Belt. Petrographic evidence presented here suggests that the BBC amphibolites have undergone the same metamorphic histories as the metasediments, but that the felsic igneous rocks may have intruded the metasediments during or after the peak of metamorphism. The peak of metamorphism (M_1p, Table I) occurred between 3270 and 3100 Ma, and may have lasted until about 3050 Ma (Barton, 1983b; Watkeys et al., 1983). The entire event may have been one of high pressure relaxing into slightly lower pressure, as a result of rapid erosion of an overthickened tectonic pile.

Previous models call upon collision of the Kaapvaal and Zimbabwe cratons at about 2700 to 2800 Ma (Light, 1982; Burke et al., 1986; Van Reenen et al., 1987). Such models are supported by most of the available data, but do not explain the geochemical features of the CZ. In the models of the first two authors, the BBC sediments are deposited in a marginal cratonic basin on the Zimbabwe plate and then subducted beneath the Kaapvaal plate during their collision at about 2700 Ma. Van Reenan et al. (1987), who base their model on extensive research in the SMZ, suggest that the Kaapvaal craton was on the underriding plate. The results herein presented suggest that both models are partly correct.

The two versions are reconcilable if one recalls the fact that the CZ lithologies had a unique pre-2700 Ma history. This new model (Fig. 26) is concerned with the events occurring between 3500 and 2700 Ma.

Figure 26
Proposed model for the tectonic evolution of the Limpopo Belt.
See text for detailed explanation.
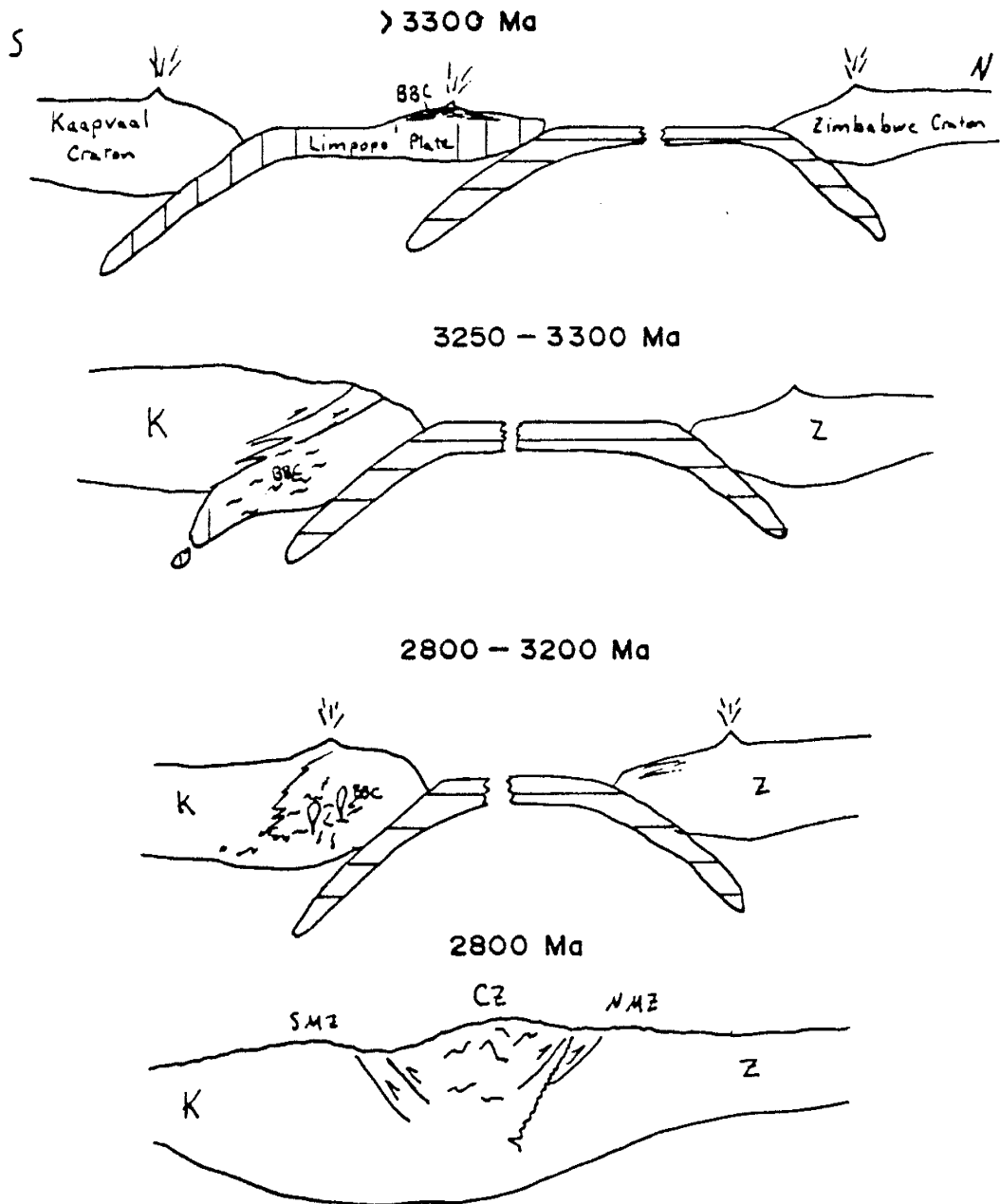
There are four plates involved: the Kaapvaal and Zimbabwe plates, an intervening Limpopo plate, which carries the CZ as an island arc or microcontinent, and an unpreserved section of oceanic crust. There are three subduction zones: one edge of the Limpopo plate is being consumed beneath the Kaapvaal plate, with arc volcanism appearing in the form of greenstone belts, and the other two dip both north (beneath the Zimbabwe craton, where greenstone belt successions can be traced into the NMZ) and south (beneath the CZ of the Limpopo plate). The Limpopo plate carries on its leading edge the beginnings of an island arc, represented by basaltic dikes, sills and possibly flows interlayered with the BBC metasedimentary succession. If the granitic gneisses are found to represent felsic volcanics, then they are extruded at this time.

At 3150-3200 Ma the Limpopo arc collides with the Kaapvaal craton, and is partially subducted along with the SMZ. The collision of the arc with the craton results in high-grade metamorphism and deformation of the SMZ (the leading edge of the Kaapvaal craton) and the BBC sediments and basalts, and causes subduction to cease. The event coincides with the M_1 and D_1 events of Watkeys et al. (1983) and Barton et al. (1983a). The M_1 event ends with partial uplift of the arc and SMZ, while mafic and felsic magmas are intruded into the CZ. The mafics are generated in the mantle wedge beneath the subducted arc and the felsics in the subducted oceanic plate, and therefore have subduction zone signatures. This is the model if the granitic gneisses are intrusive, which is the interpretation preferred here.

At about 2800 Ma, the Zimbabwe and Kaapvaal/Limpopo cratons col-

lide. This collision is marked by N-S directed compression resulting in crustal shortening via thickening in the CZ. The consequences of such an event are demonstrated by complex folding and interleaving of the felsic igneous rocks with the metasediments and amphibolites. The end results are isostatic uplift and outward thrusting, as suggested by Van Reenen et al. (1987), and finally intrusion of the Bulai gneiss and post-tectonic monzonites and related plutons of the Bandelierkop association (Table I). This latter sequence of plutons is at an angle to the sutures, and is continuous from the Kaapvaal craton into the CZ.

This model has advantages over the single-collision models of others which fail to account for the differing lithologies between the CZ and its surrounding marginal zones. Implications of this model raise several questions, however. How does the dual collision model explain the differing tectonic styles, if the deformations involve the surrounding terrains? How does the model account for the MLI, emplaced at 3270 Ma?

The differing tectonic styles might be the result of collisions which are at some angle to the trench. If the Limpopo arc were approaching the margin of the Kaapvaal from the northeast instead of the north, the arc might impose stress in a NE-SW direction. This is consistent with the observed isoclinal, recumbent folds formed during D_1 which have ESE to SE-dipping subhorizontal fold axes (Watkeys et al., 1983) and with the observed increase in metamorphic grade from west to east (Van Reenen et al., 1987).

The MLI was emplaced prior to the collision of the Limpopo arc and the Kaapvaal craton. Barton et al. (1979) have suggested that the MLI

may be a source magma chamber for basalts in a greenstone belt. This leaves open the possibility that the MLI may have been the magma chamber feeding the volcanic arc on the leading edge of the Kaapvaal plate. This is consistent with the MLI being tectonically emplaced and infolded with the BBC and SRG, as suggested by Barton et al. (1979).

Suggestions for Future Research

There is a preponderance of unsupported speculation concerning the early history of the Limpopo Belt. This is perhaps best epitomized by the tradition of assuming that the granitic rocks of the BBC are chiefly metasediments. If we are to understand clearly the interrelationships of the units, then several detailed surveys must be completed.

Isotopic work must be undertaken on all lithologies present in the CZ. Certain units have received considerable attention in the past (the SRG and MLI, studied by Barton et al., 1983c and Barton et al., 1979), and felsic samples from this study are currently being investigated by J. M. Barton (Department of Geology, Rand Afrikaans University, Johannesburg, Republic of South Africa). It is recommended that the metasediments also be analyzed in order to compare their isotopic characteristics with those of the igneous rocks of the terrain. This should enable better estimates of the relative abundances of ortho- and paragneisses. Such studies might also better constrain the timing of igneous, metamorphic and deformational events.

Isotopic work is meaningless without accompanying field mapping. Although minute sections of the zone have been mapped in sufficient

detail (e.g. Fripp, 1983), individual units must be traced unbroken until contact relationships can be decisively worked out. This is essential for all units present - the contact relationships of the SRG with the BBC may be tectonic rather than depositional, and the granitic and amphibolitic units may show intrusive or extrusive relationships with the surrounding lithologies.

Petrographic work on a variety of samples from the same lithologic unit may help to quantify mineralogic changes which may correlate with changes in chemical composition, sedimentary facies, etc. Analyses of this kind might elucidate the effects of metamorphism on the chemical compositions the granitic gneisses (including the metasediments). Furthermore, if such detailed work were coupled with equally detailed mapping, relationships to other areas of the CZ may become possible.

Clearly, there is an insignificant number of chemical analyses of rock units in the Messina area. In the past, geochemists have commonly not produced an extensive listing of trace element data, which can often demonstrate a rock's similarities to or differences from modern samples from known tectonic settings. Such data can also be used to further define the effects of metamorphism. Trace element data on rocks from the MLI might more clearly indicate its original composition, which in turn could be used to check the plausibility of the MLI as a parent material from which the amphibolites of the BBC were derived.

Conclusions

Chemical and petrographic analyses of important rock units of the Beit Bridge Complex of the Central Zone of the Limpopo Belt lead to the following conclusions:

1) Granulite facies metamorphism has not induced significant changes in the geochemical characteristics of a majority of the samples.

2) The amphibolite units appear to be intruded as dikes and sills and have geochemical characteristics similar to modern basalts from arc-related tectonic settings.

3) A considerable proportion of the (quartzofeldspathic or) granitic units are of igneous origin, and retain geochemical signatures most similar to modern granites and dacites from arc-related tectonic settings.

4) The amphibolites have two-pyroxene ± garnet assemblages indicating equilibration under granulite-facies conditions. The granitic gneisses do not preserve granulite-facies mineral assemblages. This evidence suggests that the amphibolites were probably associated with the sedimentary sequence of the BBC before the package was metamorphosed, while the felsic orthogneisses may have intruded the succession during the first metamorphic event. Alternatively, if the lack of granulite-facies assemblages in the granitic rocks is related to differences in water pressure during retrograde metamorphism and contacts are found that indicate an extrusive relationship with the metasediments, then the granitic gneisses can be interpreted as arc-

related felsic volcanics without significantly affecting the model.

A model based on these conclusions which incorporates all data bearing on the evolutionary history of the Limpopo Belt is presented. This model invokes the formation of the Limpopo Arc prior to 3150 Ma and involves two collisions: one at about 3150-3200 Ma, involving a collision of the Limpopo arc with the northern margin of the Kaapvaal province, and another at about 2700-2800 Ma, involving a collision of the Zimbabwe province with the Kaapvaal-Limpopo province.

Appendix A: Precision and accuracy data tables for XRF and INAA.

Precision and accuracy data for XRF and INAA analyses are represented in Tables A-1 and A-2. In these tables, n is the number of analyses of the standard, $\bar{x}$ is the mean, and s is the standard deviation. C.V. is the coefficient of variation, which measures, in percent, the deviation of s from $\bar{x}$; hence, the C.V. is a more relative measure of the precision of the data than s. $\overline{O_x}$ is the standard error of the mean, which is essentially an estimate of the significance of s. The % accuracy is a measure of how close the mean value is to the actual value.

For XRF, good to excellent results are obtained for the major elements (excluding MnO) and trace elements Y, Zr, Rb, Sr, Ba, and V. Concentrations of these elements are reproducible to within 5% and are within 5% of actual values for the standard. The other elements reported by XRF (except Ni at low concentrations) are reproducible to within 15% and are within 20% of the actual values. At higher concentrations of Ni (>15 ppm), XRF data are excellent.

For INAA, good to excellent results are obtained for all elements reported (Cs, Th, U, Sc, Cr, Co, Hf, Ta, La, Ce, Sm, Eu, Tb, Yb, Lu, and Ni). These are reproducible to within 10% and are within 10% of the actual values.

It is generally not possible to obtain Ni data from INAA; however, due to the high concentration of epithermal neutrons present in the nuclear reactor, determination of Ni concentrations are identical between XRF and INAA if concentrations are above 15 ppm.

The formulas used for calculating $\bar{x}$, s, C.V., $\sigma\bar{x}$, and % accuracy are given below.

$$\bar{x} = \frac{\sum x}{n}$$

$$C.V. = \frac{s}{\bar{x}} \times 100$$

$$\sigma\bar{x} = \frac{s}{n}$$

$$\% \text{ Accuracy} = 100 - \frac{\bar{x} - \text{Actual}}{\text{Actual}} \times 100$$

where

x = individual analysis

n = number of analyses

$\bar{x}$ = mean

s = standard deviation

The results shown in the tables demonstrate that the data presented in this paper are acceptable for the purposes of this study.

Table A-1

XRF Data for BCR-1[*]

Element	Accepted Values	n	$\bar{x}$	s	C.V.	$\sigma\bar{x}$	% Accuracy
SiO_2	54.53	21	54.59 ± 0.11		0.20	0.02	99.80
TiO_2	2.26	21	2.23 ± 0.03		1.36	0.01	98.65
Al_2O_3	13.72	21	13.65 ± 0.12		0.89	0.03	99.11
Fe_2O_3T	13.41	21	13.08 ± 0.34		2.61	0.07	97.46
MnO	0.18	21	0.18 ± 0.02		10.66	0.00	89.37
MgO	3.48	21	3.69 ± 0.30		8.04	0.06	91.46
CaO	6.97	21	6.99 ± 0.07		1.00	0.02	99.00
Na_2O	3.30	21	3.66 ± 0.14		3.84	0.03	95.74
K_2O	1.70	21	1.70 ± 0.03		1.62	0.01	98.38
P_2O_5	0.36	21	0.36 ± 0.01		3.59	0.00	96.42
Y	39	14	37.9 ± 1.8		4.88	0.49	95.26
Zr	191	13	190.1 ± 5.0		2.61	1.38	97.40
Nb	14	14	13.4 ± 1.7		12.87	0.46	87.69
Rb	47	14	51.3 ± 0.8		1.58	0.22	98.27
Sr	330	14	334 ± 4		1.31	1.17	98.67
Ba	680	11	686 ± 16		2.31	4.78	97.67
Pb	13.6	14	17.3 ± 2.2		13.00	0.60	83.51
V	420	6	430 ± 6		1.41	2.47	98.56
Ni	10	6	11.3 ± 2.7		24.26	1.12	72.58

[*] Compiled by M.D. Boryta, H.C. Crow, M. Knoper and D.J. Wronkiewicz.

Table A-2

INAA Data for BCR-1*

Element	Accepted Values	n	$\bar{x}$	s	C.V.	$\sigma\bar{x}$	Accuracy
Cs	0.96	10	0.95 +	0.06	6.21	0.02	93.84
Th	6.04	10	5.8 +	0.3	5.51	0.10	94.75
U	1.72	10	1.7 +	0.1	8.24	0.04	92.09
Sc	33	10	31.6 +	1.9	5.97	0.60	94.28
Cr	15.5	10	13.8 +	1.0	7.40	0.32	93.41
Co	37	10	36.8 +	2.0	5.42	0.63	94.62
Hf	5	8	5.0 +	0.3	5.34	0.10	94.62
Ta	0.83	8	0.78 +	0.02	3.12	0.01	97.05
La	24	10	24.5 +	1.7	7.01	0.54	92.83
Ce	53.45	10	53.2 +	3.1	5.86	0.98	94.17
Sm	6.6	10	6.80 +	0.31	4.52	0.10	95.34
Eu	1.96	10	1.89 +	0.11	5.95	0.04	94.27
Tb	1	10	1.07 +	0.08	7.66	0.03	91.79
Yb	3.38	10	3.36 +	0.19	5.68	0.06	94.36
Lu	0.51	10	0.52 +	0.03	5.91	0.01	94.04
Ni^{+}	267	3	272 +	13.1	4.80	7.60	98.13

* Compiled by M.D. Boryta, H.C. Crow, M. Knoper and D.J. Wronkiewicz.
+ Ni based on 3 INAA runs of standard BE-N.

Appendix B: Petrographic descriptions of mafic samples.

LMP-1

55% Plagioclase grains averaging 0.6 mm, with pericline and polysynthetic twins common, some bent; many are zoned with calcic cores. 25% Clinopyroxene as equant grains averaging 0.55 mm. 7% Garnet, usually fractured or broken anhedral grains 0.2 mm across. 6% Amphibole (reddish-brown Hornblende), replacing pyroxenes. 5% Orthopyroxene (Hypersthene) as equant grains about 0.55 mm across. 2% Biotite (reddish-brown), replacing pyroxenes. Trace minerals include sphene, zircon, apatite, and opaque minerals. Overall texture is polygonal equigranular granoblastic, massive.

LMP-6

30% Amphibole (brownish to olive-green Hornblende), possibly replacing pyroxenes; grains average 0.4 mm across and are stubby prisms. 25% Clinopyroxene, sometimes poikiloblastic around amphibole and plagioclase; these grains are up to 4 mm across; others average 1.7 mm. 20% Plagioclase (An55) with pericline more abundant than albite twins; zoning common; grains average 0.5 mm. 15% Orthopyroxene (Hypersthene), as poikiloblastic grains up to 3.8 mm across enclosing clinopyroxene, plagioclase, amphibole, and quartz; other grains about 1.5 mm across. 10% Quartz, most of which is a vein filling (grains up to mm), rest as equant grains highly variable in size but averaging 0.2 mm. Trace minerals are apatite, zircon, rare biotite, chlorite, and opaque minerals. Overall texture is polygonal equigranular granoblastic.

LMP-10

80% Amphibole (brown Hornblende) as equant grains with straight boundaries and 120° triple-junctions; average grain size is 2 mm, ranging up to 4 mm. 8% Plagioclase (An55?), commonly zoned, with pericline, albite, and polysynthetic twinning; two varieties: as small (0.4 mm) rounded grains mostly at amphibole triple-junctions, and as replacement (with symplectitic hypersthene) of garnet. 5% Orthopyroxene (Hypersthene) in two varieties: replacing garnet as symplectitic intergrowths with plagioclase and as "coatings" on clinopyroxene, and as equant grains 0.5 to 1.2 mm across with bent and broken cleavage traces. 5% Clinopyroxene generally as large (up to 5 mm) broken grains with bent cleavage traces. 2% Garnet being replaced by hypersthene + plagioclase; one small inclusion of quartz was observed; garnet grains probably were 0.6 to 4 mm across before replacement. Trace minerals include minor chlorite and sericite as alteration products of plagioclase. This sample preserves the reaction garnet + quartz + either clinopyroxene or hornblende going to plagioclase + hypersthene. Overall texture is polygonal equigranular granoblastic, with local symplectitic intergrowth.

LMP-25

60% Plagioclase (An40?), highly altered to sericite + epidote; average grain size is 0.4 mm. 10% Amphibole (olive brown and green Hornblende) as equant grains with straight boundaries, averaging 0.25 mm. 10% Clinopyroxene, averaging 0.25 mm, with bent cleavage traces, straight grain boundaries, and 120° triple-junctions. 10% Orthopyroxene

(Hypersthene), same as clinopyroxene. 9% Quartz, seriate (0.1 to 2.0 mm), disseminated equant grains. 1% Epidote + Sericite, as alteration products of plagioclase. Trace minerals include opaque minerals. Overall texture is polygonal inequigranular granoblastic, highly altered.

LMP-51

50% Amphibole (green-brown Hornblende) as elongate grains of variable size but averaging 0.8 mm, showing preferred orientation. 45% Plagioclase (An55-60), slightly altered to sericite, averaging 0.7 mm; albite twins common. 5% Quartz mostly as small (0.05 mm) rounded blebs. Trace minerals include opaque minerals and rare apatite, zircon, sericite, epidote, and biotite. Overall texture is seriate interlobate granoblastic.

LMP-47

55% Amphibole (reddish-brown to yellow Hornblende), seriate grains (0.2 to 4 mm), with straight boundaries and inclusions of other minerals, some of which are euhedral (but altered) plagioclase grains. 40% Plagioclase (An45?), moderately to highly altered seriate grains (0.4 - 2 mm), commonly with zoning. 5% Serpentine (± chlorite) especially along fractures; may have replaced some mafic mineral. Trace minerals include opaque minerals and possibly chlorite. Overall texture is polygonal seriate granoblastic.

LMP-54

40% Amphibole (brown to green - Cummingtonite?), elongate, grain size variable but averaging 0.8 mm long. 25% Clinopyroxene as equant grains averaging 0.75 mm across, with common fractures and bent cleavage traces. 25% Orthopyroxene (Hypersthene), a few of which are up to 5 mm across and poikiloblastic around clinopyroxene grains and quartz blebs; others are equant grains similar to clinopyroxene, averaging 0.75 mm across. 7% Quartz mostly as small (0.2 mm) blebs disseminated through-out sample; few larger grains (possibly a vein?) about 4 mm across with slightly undulose extinction. 1% Plagioclase (An30?) with very slight alteration; 1 large grain about 1 mm across, rest average about 0.2 mm. Trace minerals include opaque minerals, apatite, and biotite (as alteration of amphibole). Overall texture is intermediate between equigranular and seriate, polygonal and interlobate, granoblastic.

LMP-49

60% Clinopyroxene (deep green; some have a purplish tinge) as equant grains with straight boundaries and 120° triple-junctions; average grain size is 0.8 mm; concentrated into bands. 25% Amphibole (dark olive brown Hornblende) as elongate grains varying from 1.0 to 4.0 mm long; shows preferred alignment. 14% Plagioclase which is very highly altered to sericite + epidote, difficult to estimate grain size or An content. 1% Sphene as small (0.1 mm) grains dispersed throughout. Trace minerals include abundant apatite (averaging 0.12 mm across), quartz (mostly in veins but also dispersed throughout rock), calcite (in veins), zircon, and possibly zoisite (accompanying sericite as

alteration product of plagioclase). Overall texture is foliated

amphibolite.

LMP-58

53% Plagioclase (An55) with common polysynthetic and less abundant

albite twinning; zoned crystals show no twinning; grains are equant and

average 0.6 mm across and show perfect polygonal texture. 20% Ortho-

pyroxene (Hypersthene) with variable grain size averaging 0.4 mm,

disseminated throughout sample but more common in trains parallel to

the foliation. 15% Amphibole (greenish brown to light brown/yellow

Hornblende) with strong preferred alignment; grains are stubby prisms

averaging 0.3 mm across, may have replaced pyroxenes. 2% Quartz as

tiny (<0.1 mm) disseminated blebs. Trace minerals include abundant

(approaching 1%) opaque minerals and minor apatite. Overall texture is

seriate polygonal foliated granoblastic.

Appendix C: Petrographic descriptions of granitic samples.

LMP-4

45% K-feldspar (25% perthitic Microcline, 20% perthitic Orthoclase), often strained (bent twin lamellae and dislocation planes); grain size varies with banding: within K-feldspar-rich bands, grains average 1 to 2 mm across, otherwise average 0.5 to 1.0 mm. 25% Quartz in two occurrances: as rounded blebs averaging 0.2 mm across (unstrained, usually found within other minerals), and as highly irregular, anhedral grains about 0.5 mm across and which have undulose extinction and inclusion trains. 25% Plagioclase (variable An0-20) very slightly altered to sericite; twins are rare but commonly albite; average grain size is about 0.6 mm; K-feldspar-K-feldspar and plagioclase-K-feldspar boundaries show myrmekite, which totals about 1% of rock. 4% Garnet as small (0.10 to 0.15 mm), isolated, rounded to subhedral, fractured, inclusion-free grains which are commonly concentrated into trains parallel to K-feldspar layers. Trace minerals include rare metamict zircon and rarer apatite. Overall texture is hypidiomorphic equigranular and banded, and grain boundaries are curvilinear > straight > embayed.

LMP-5

(No thin section - probably similar to LMP-4)

LMP-33

(No thin section - probably similar to LMP-4)

LMP-8

35% K-feldspar (perthitic Microcline) with bent twin lamellae; grains average 0.6 mm across. 35% Plagioclase (An20-30), highly altered in one zone which is at a high angle to banding; most grains have unbent albite twins and average 0.5 mm across; there is a trace of myrmekite at K-feldspar-K-feldspar and plagioclase-K-feldspar boundaries, and plagioclase boundaries are often alteration- or inclusion-free. 27% Quartz in two occurrances: as small (0.2 mm) strain-free rounded blebs, especially within other grains and at triple-junctions, and as slightly undulose (<5° extinc-tion) crains averaging 0.5 to 0.6 mm across. 2% reddish-brown Biotite as stubby, ragged grains lying subparallel to banding; average dimensions are about 0.2 x 0.1 mm; 50% of total are altered to chlorite + opaque minerals. 1% skeletal Garnet with usually about 2% quartz inclusions; variable grain size (1.0 to 3.5 mm across). Trace minerals include abundant zircon (usually associated with biotite/chlorite), less abundant apatite, epidote (associated with chlorite as alteration product of K-feldspar and/or plagioclase), and rare sphene. Overall texture is banded hypidiomorphic granular, and grain boundaries are curved > straight ≥ embayed > cuspate; 120° triple-junctoions are common.

LMP-11

40% K-feldspar (perthitic Microcline) with strained twins; average grain size is 0.9 mm, with larger grains occurring in faint bands. 35% Quartz in two varieties: as small (0.3 mm), unstrained, rounded blebs and as slightly undulose (<5° extinction) grains averaging 0.7 mm

across. 25% Plagioclase (An10) averaging 0.5 mm across, slightly
altered to sericite and commonly with albite twins; trace of myrmekite
is found along K-feldspar-K-feldspar and K-feldspar-plagioclase
boundaries. <1% Garnet as allotriomorphic grains strung out in trains
roughly parallel to K-feldspar banding; grain size is variable but
averages 1.0 mm; quartz inclusions are common. Trace minerals include
opaque minerals, zircon, sphene, and epidote (as alteration of
feldspars). Overall texture is inequigranular granoblastic; 120°
triple junctions are common, and grain boundaries are straight -
curvilinear > embayed; K-feldspar exhibits a faint banding.

LMP-24

60% K-feldspar (perthitic Microcline) with bent twin lamellae and
highly irregular grain boundaries; grain size averages 1.0 mm. 30%
Quartz of which 80% is unstrained; rest is slightly undulose (<5°
extinction); grain size varies but averages 0.8 mm with a few rounded
blebs about 0.2 mm across. 8% Plagioclase (An<10), with albite twins
which are occasionally bent; average grain size is 1.0 mm; myrmekite is
minor; slightly altered. 1% Garnet, allotriomorphic and fractured
grains generally about 3.0 mm across, with inclusions of quartz,
chlorite, and zoisite. Trace minerals include (reddish-brown biotite +
chlorite (as stubby grains about 0.1 mm long), muscovite (a few large
flakes, 0.8 mm across), opaque minerals, and zoisite (?). Overall
texture is equigranular granoblastic; hand specimen appears to show
banding which is not evident in thin section.

LMP-26

45% K-feldspar (perthitic Orthoclase, minor Microcline) concentrated in coarse bands (10 mm wide); in K-feldspar-rich bands, grains average 2.5 mm across; in K-feldspar-poor bands grains average 0.6 mm; twin lamellae are often bent. 32% Quartz in two varieties: as strain-free rounded blebs about 1.0 mm across, and as 0.5 mm grains with slightly undulose extinction ($<5^{o}$). 20% Plagioclase (An17), slightlly to moderately altered; albite twins often bent; grains average 0.5 mm across. 2% dark red Biotite laths, subparallel to banding, averaging 0.2 mm long; dispersed throughout sample; mostly altered to chlorite; may contain large rutile needles. <1% skeletal or allotriomorphic Garnet, inclusions of quartz; three large grains in slide, averaging 2 mm across. Trace minerals include zircon, zoisite (?), opaque minerals and possibly rutile and allanite. Overall texture is coarsely banded equigranular granoblastic; triple-junctions approach 120°.

LMP-27

40% K-feldspar (perthitic Microcline) of variable grain size, averaging 0.8 mm across; twin lamellae are commonly bent. 39% Quartz, with variable grain size averaging 0.9 mm; slightly undulose extinction ($<5^{o}$), crush bands are common and boundaries are embayed. 20% Plagioclase (An24), moderately altered to sericite in cores, but rims are clear when in contact with K-feldspar; albite and pericline twin lamellae are commonly bent or fractured; grains average 0.8 mm across but size is variable; myrmekite is present but rare. 1% reddish-brown Biotite, in part altered to chlorite; stubby grains averaging 0.4 mm

across, appear to be randomly oriented and associated with trace
muscovite and epidote. Trace minerals include muscovite + chlorite
(intergrown with biotite), epidote, zircon, and opaque minerals; trace
minerals are rare in the thin section. Overall texture is seriate
banded, interlobate; grain boundaries are most commonly embayed.

LMP-35

44% Quartz in two varieties: as strain-free, rounded blebs averaging
0.28 mm across, and as variably-sized (averaging 0.8 mm) slightly
undulose grains. 30% Plagioclase (An20?), moderately altered to
sericite, with dominantly pericline twinning; grains average 1.0 mm
across. 15% K-feldspar (perthitic Microcline) with bent twin lamellae;
grains average 1.0 mm across. 10% Garnet with inclusions of quartz,
biotite, zircon, apatite, K-feldspar, and plagioclase; some is
skeletal, rest is subhedral; grain sizes vary but average 1.5 mm;
grains are concentrated in trains or bands. Trace minerals include
reddish-brown biotite (partly altered to chlorite) associated with
opaque minerals, apatite (approaching 1% of rock), zircon (about 0.5%
of rock), and opaque minerals. Overall texture is seriate granoblastic
with a faint banding; triple-junctions approach 120°.

LMP-7

49% Plagioclase (An15), slightly altered; albite and pericline twins
commonly bent; grain size averages 0.8 mm. 40% Quartz, undulose,
rarely flattened, with crush bands common and parallel to flattening;
grains average 1.6 mm across. 10% reddish-brown Biotite, randomly

oriented to subparallel to flattening of quartz; both laths and stubby

grains, 0.2 to 0.3 mm across, partly altered to chlorite. 1% Garnet

with inclusions of quartz, biotite, and zircon; grains average 1.0 mm

across. Trace minerals include abundant apatite, common zircon, and

rare muscovite. Opaque minerals are notably rare or absent. Overall

texture is seriate interlobate granoblastic.

LMP-28

50% Plagioclase (An20?), moderately altered; pericline twins generally

bent; dislocation planes are much more altered than rest of grains,

which average 1.4 mm across. 40% Quartz which is moderately undulose

and averages 0.8 mm across. 7% reddish-brown Biotite as laths 0.8 mm

long, showing preferred alignment; some contains abundant rutile

needles, and some is altered to chlorite. 1% K-feldspar (Microcline),

appears to be interstitial between other grains. Trace minerals

include amphibole (olive green hornblende), sphene, epidote + calcite,

rutile (in biotite), opaque minerals, apatite, zircon, and allanite.

Overall texture is foliated.

LMP-29

(is identical to LMP-28)

LMP-39

50% Plagioclase (An27), rarely myrmekitic, with albite, pericline, and

polysynthetic twinning; grains are slightly altered and average 1.0 mm

across. 20% Quartz as irregular grains of variable size but averaging

0.8 mm across; undulose extinction and crush bands are common. 19% K-feldspar (10% perthitic Microcline, 9% not perthitic) with dislocation planes common; highly irregular grain shapes, with average size of 0.6 mm. 10% reddish-brown Biotite as laths about 0.8 mm long, showing preferred orientation. 1% Opaque minerals as odd-shaped grains dispersed throughout sample, averaging 0.3 mm across. Trace minerals include abundant apatite, zircon, monazite, muscovite, and rare sphene. Overall texture is foliated, mosaic.

LMP-9

30% K-feldspar (perthitic Microcline, rare Orthoclase) as irregular grains averaging 0.6 mm across. 30% Plagioclase (An5); 10% of rock is myrmekite; albite, pericline and polysynthetic twins common; grains average 0.6 mm across. 30% Quartz in two varieties: as slightly undulose ($<5°$ extinction), irregular grains averaging 0.8 mm across and as strain-free rounded blebs averaging 0.08 mm across. 8% reddish-brown Biotite laths about 0.2 mm long, showing preferred orientation; some is altered to chlorite. 1% Garnet as elongate grains - up to 4.2 mm long by 0.5 mm wide - with inclusions of quartz and sillimanite needles; elongation is parallel to foliation. Trace minerals include up to 0.5% sillimanite needles in trains parallel to foliation and in garnet, zircon (commonly associated with sillimanite), apatite, and opaque minerals (associated with biotite and chlorite). Overall texture is strongly foliated equigranular, with many triple-junctions approaching 120°.

LMP-17

40% Plagioclase (An7), moderately to slightly altered; bent albite twins, often recrystallized; average grain size is 1.0 mm but variable. 40% Quartz as equant slightly undulose grains with ragged boundaries, averaging 0.9 mm across. 10% reddish-brown Biotite laths 0.4 mm long on average, showing preferred orientation; abundant zircon inclusions. Trace minerals include garnet (as elongate grains about 0.3 mm across), abundant apatite (approaching 1%, grains up to 0.1 mm across, often included in garnet), zircon, opaque minerals, rare muscovite, epidote and chlorite (as alteration products of plagioclase and biotite), possibly monazite and xenotime, and rare K-feldspar (as minute intergranular microcline). Overall texture is foliated equigranular mosaic.

References

Allègre, C. J. and Minster, J. F., 1978. Quantitative models of trace element behavior in magmatic processes. Earth Planet. Sci. Letter., 38: 1-25.

Barton, J. M., Jr., 1983a. Pb-isotopic evidence for the age of the Messina Layered Intrusion, Central Zone, Limpopo Mobile Belt. Spec. Publ. Geol. Soc. S. Afr., 8: 39-41.

----------, 1983b. Our understanding of the Limpopo Belt -- a summary with proposals for future research. Spec. Publ. Geol. Soc. S. Afr., 8: 191- 203.

----------, Fripp, R. E. P. and Ryan, B., 1977. Rb-Sr ages and geologic setting of ancient dykes in the Sand River area, Limpopo Mobile Belt, South Africa. Nature, 267: 487-490.

----------, Fripp, R. E. P., Horrocks, P. and McLean, N., 1979. The geology, age and tectonic setting of the Messina Layered Intrusion, Limpopo Mobile Belt, southern Africa. Am. J. Sci., 279: 1108-1134.

----------, Du Toit, M. C., Van Reenen, D. D. and Ryan, B., 1983a. Geochronologic studies in the southern marginal zone of the Limpopo Mobile Belt, southern Africa. Spec. Publ. Geol. Soc. S. Afr., 8: 55-64.

----------, Fripp, R. E. P. and Horrocks, P. C., 1983b. Rb-Sr ages and chemical composition of some deformed Archean mafic dikes, Central Zone, Limpopo Mobile Belt, southern Africa. Spec. Publ. Geol. Soc. S. Afr., 8: 27-37.

----------, Ryan, B. and Fripp, R. E. P., 1983c. Rb-Sr and U-Th-Pb isotopic studies of the Sand River Gneisses, Central Zone, Limpopo Mobile Belt. Spec. Publ. Geol. Soc. S. Afr., 8: 9-18.

Bavington, O. A. and Taylor, S. R., 1980. Rare earth element geochemistry of Archean metasedimentary rocks from Kambalda, western Australia. Geochim. Cosmochim. Acta, 44: 639-648.

Brandl, G., 1983. Geology and geochemistry of various supracrustal rocks of the Beit Bridge Complex east of Messina. Spec. Publ. Geol. Soc. S. Afr., 8: 103-112.

Burke, K., Kidd, W. S. F. and Kusky, T., 1985. Is the Ventersdorp rift system of southern Africa related to a continental collision between the Kaapvaal and Zimbabwe cratons at 2.64 Ga. ago? Tectonophysics, 115: 1-24.

Cahen, L., Snelling, N. J., Delhal, J. and Vail, J. R., 1984. The Geochronology and Evolution of Africa. Oxford: Clarendon Press. 512 pages.

Cann, J. R., 1982. Rayleigh fractionation with continuous removal of liquid. EPSL, 60: 114-116.

Condie, K. C., 1985. Secular variation in the composition of basalts: an index to mantle evolution. J. Petrol., 26: 545-563.

---------- and Allen, P., 1984. Origin of Archean charnockites from southern India. In: Kroner, A., Hanson, G. N. and Goodwin, A. M., (editors), Archean Geochemistry. New York: Springer-Verlag, pp. 182-203.

----------, Bowling, G. P. and Allen, P., 1985. Missing Eu anomaly and Archean high-grade granites. Geology, 13: 633-636.

Coward, M. P., 1983. Some thoughts on the tectonics of the Limpopo Belt. Spec. Publ. Geol. Soc. S. Afr., 8: 175-180.

----------, Graham, R. H., James, P. R. and Wakefield, J. 1973. A structural interpretation of the northern margin of the Limpopo orogenic belt, southern Africa. Phil. Trans. R. Soc. Lond. A., 273: 487-491.

----------, James, P. R. and Wright, L., 1976. Northern margin of the Limpopo mobile belt, southern Africa. GSA Bull., 87: 601-611.

Davis, P. A., Blackburn, W. H., Brown, W. R. and Ehunann, W. D., 1978. Trace element geochemistry and origins of late Precambrian-early Cambrian Catoctin greenstones of the central Appalachian mountains. Unpublished manuscript.

Du Toit, M. C., Van Reenen, D. D. and Roering, C., 1983. Some aspects of the geology, structure and metamorphism of the Southern Marginal Zone of the Limpopo Metamorphic Complex. Spec. Publ. Geol. Soc. S. Afr., 8: 121-141.

Fernandes, J. F., Iyer, S. S., Imakuma, K. and Choudhuri, A., 1987. Geochemical studies in the Proterozoic metamorphic terrane of the Guaxupe Massif, Minas Gerais, Brazil: A discussion on large ion lithophile element fractionation during high-grade metamorphism. Precamb. Res., 36: 65-79.

Finlow-Bates, T. and Stumpfl, E. F., 1981. The behavior of so-called immobile elements in hydrothermally altered rocks associated with volcanogenic submarine-exhalative ore deposits. Mineral. Deposita., 16: 319-328.
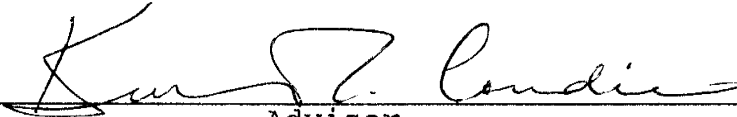
Fowler, M. B., 1986. Large-ion lithophile element characteristics of an amphibolite facies to granulite facies transition at Gruinard Bay, north-west Scotland. J. Metamorphic Geol., 4: 345-359.

Fripp, R. E. P., 1983. The Precambrian geology of the area around the Sand River near Messina, Central Zone, Limpopo Mobile Belt. Spec. Publ. Geol. Soc. S. Afr., 8: 81-87.

Garcia, M. O., 1978. Criteria for the identification of ancient volcanic arcs. Earth-Sci Rev., 14: 147-165.

Garrels, R. M. and Mackenzie, F. T., 1971. Evolution of Sedimentary Rocks. New York: Norton. 387 pages.

Harris, N. B. W., Pearce, J. A. and Tindle, A. G., 1986. Geochemical characteristics of collision-zone magmatism. In: Coward, M. P. and Ries, A. C. (editors), Collision Tectonics: Geol. Soc. Spec. Paper, 19: 67-81.

Hickey, R. L. and Frey, F. A., 1982. Geochemical characteristics of boninite series volcanics: implications for their source. Geochim. Cosmochim. Acta, 46: 2099-2115.

Horrocks, P. C., 1980. Ancient Archean supracrustal rocks from the Limpopo Mobile Belt. Nature, 286: 596-599.

----------, 1983. The Precambrian geology of an area between Messina and Tshipise, Limpopo Mobile Belt. Spec. Publ. Geol. Soc. S. Afr., 8: 81-88.

Irvine, T. N. and Baragar, W. R. A., 1971. A guide to the chemical classification of the common volcanic rocks. Can. J. Earth Sci., 8: 523-548.

Jacobs, J. W., Korotev, R. L., Blanchard, D. P. and Haskin, L. A. 1977. A well-tested procedure for instrumental neutron activation analysis of silicate rocks and minerals. J. Radioanal. Chem., 40: 93-114.

Jensen, L. S., 1976. A new cation plot for classifying subalkaline volcanic rocks. Ontario Division of Mines Misc. Paper, 66: 22 pp.

Jochum, K. P., Seufert, H. M., Spettel, B. and Palme, H., 1986. The solar abundances of Nb, Ta, and Y, and the relative abundances of refractory lithophile elements in differentiated planetary bodies. Geochim. Cosmochim. Acta, 50: 1173-1183.

Key, R. M., Ermanovics, I. F. and Skinner, A. C., 1983. The evolution of the southern margin of the Limpopo Mobile Belt in Botswana. Spec. Publ. Geol. Soc. S. Afr., 8: 169-173.

Korotev, R. L., 1987. National Bureau of Standards Coal Flyash (SRM-1633a) as a multielement standard for instrumental neutron activation analysis. J. Radioanal. and Nuclear Chem. (in press).

Lamb, R. C., Smalley, P. C. and Field, D., 1986. P-T conditions for the Arendal granulites, southern Norway: implications for the roles of P, T and CO_2 in deep crustal LILE-depletion. J. Metamorphic Geol., 4: 143-160.

Leyreloup, A., Dupuy, C. and Andriambololona, R., 1977. Catazonal xenoliths in French Neogene volcanic rocks: constitution of the lower crust. Contrib. Min. Petrol., 62: 283-300.

Light, M. P. R., 1982. The Limpopo Mobile Belt: a result of continental collision. Tectonics, 1.4: 325-342.

Lindstrom, D. J. and Korotev, R. L., 1982. TEABAGS: Computer programs for instrumental neutron activation analysis. J. Radioanal. Chem., 70: 439-458.

Mason, R., 1973. The Limpopo mobile belt - southern Africa. Phil. Trans. R. Soc. Lond. A., 273: 463-485.

Meschede, M., 1986. A method of discriminating between different types of mid-ocean ridge basalts and continental tholeiites with the Nb-Zr-Y diagram. Chem. Geol., 56: 207-218.

Miyashiro, A., 1972. Metamorphism and related magmatism in plate tectonics. Am. J. Sci., 272: 629-656.

---------- and Shido, F., 1975. Tholeiitic and calc-alkalic series in relation to the behaviors of titanium, vanadium, chromium and nickel. Am. J. Sci, 275: 265-277.

Muecke, G. K., Pride, C. and Sarkar, P., 1979. Rare-earth element geochemistry of regional metamorphic rocks. Phys. Chem. Earth, 11: 449-464.

Mullen, E., 1983. $MnO/TIO_2/P_2O_5$: a minor element discriminant for basaltic rocks of oceanic environments and its implications for petrogenesis. EPSL, 62: 53-62.

Norrish, K. and Hutton, J. T., 1969. An accurate X-ray spectrographic method for the analysis of a wide range of geologic samples. Geochem. Cosmochem. Acta, 33: 431-453.

---------- and Chappel, B. W., 1977. X-ray flourescence. In: Zussman, J. (editor), Physical Methods in Determinative Mineralogy. London: Academic Press, pp. 235-272.

O'Hara, M. J. and Mathews, R. E., 1981. Geochemical evolution in advancing, periodically replenished, periodically tapped, continuously fractionating magma chamber. J. Geol. Soc. Lond., 138: 237-277.

Pearce, J. A., 1983. Role of the sub-continental lithosphere in magma genesis at active continental margins. In: Hawkesworth, C. J. and Norry, M. J. (editors), Continental Basalts and Mantle Xenoliths. Nantwich, U.K.: Shiva Publishing Ltd., pp. 230-249.

---------- and Cann, J. R., 1973. Tectonic setting of basic volcanic rocks determined using trace element analyses. EPSL, 19: 290-300.

----------, Harris, N. B. W. and Tindle, A. G., 1984. Trace element discrimination diagrams for the tectonic interpretation of granitic rocks. J. Petrol., 25: 956-983.

Pharaoh, T. C. and Pearce, J. A., 1984. Geochemical evidence for the geotectonic setting of early Proterozoic metavolcanic sequences in Lapland. Precam. Res., 25: 283-308.

Pitcher, W. S., 1983. Granite type and tectonic environment. In: Hsu, K. J. (editor), Mountain Building Processes. London: Academic Press, 19-40.

Prabhu, M. K. and Webber, G. R., 1984. Origin of quartzofeldspathic gneisses at Montauban-les-Mines, Quebec. Can. J. Earth Sci., 21: 336-345.

Robertson, I. D. M., 1968. Granulite metamorphism of the basement complex in the Limpopo Metamorphic Zone. Trans. Geol. Soc. S. Africa Annex. to 81: Symposium on the Rhodesian Basement Complex: 125-134.

Ryan, B. D., Kramers, J. D., Stacey, J. S., Delevaux, M., Barton, J. M. Jr., and Fripp, R. E. P., 1983. Strontium and lead isotopic studies and K/Rb ratio measurements relating to the origin and emplacement of the copper deposits near Messina, South Africa. Spec. Publ. Geol. Soc. S. Afr., 8: 47-53.

Shackleton, R. M., 1986. Precambrian collision tectonics in Africa. In: Coward, M. P. and Ries, A. C. (editors), Collision Tectonics: Geol. Soc. Spec. Pub., 19: 329-349.

Shaw, D. M., 1972. The origin of the Apsley Gneiss, Ontario. Can. J. Earth Sci., 9: 18-35.

Sheraton, J. W., 1985. Chemical changes associated with high-grade metamorphism of mafic rocks in the east Antarctic Shield. Chem. Geol., 47: 135-157.
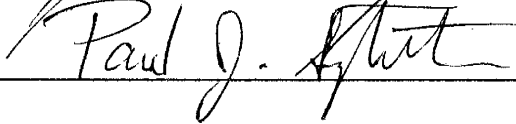
Tankard, A. J., Jackson, M. P. A., Eriksson, K. A., Hobday, D. K., Hunter, D. R., and Minter, W. E. L., 1982. Crustal Evolution of Southern Africa: 3.8 Billion Years of Earth History. Berlin: Springer-Verlag. 523 p.

Tatsumi, Y., Hamilton, D. L. and Nesbitt, R. W., 1986. Chemical characteristics of fluid phase released from a subducted lithosphere and origin of arc magmas: evidence from high-pressure experiments and natural rocks. In: Kushiro, I. (editor), M. Sakuyama and H. Fukuyama Memorial Volume: J. Volcanol. Geotherm. Res., 29: 293-309.

Vance, R. K. and Condie, K. C., 1987. Geochemistry of footwall alteration associated with the early Proterozoic United Verde massive sulfide deposit, Jerome, Arizona. Econ. Geol., 82: 571-586.

Van Reenan, D. D., Barton, J. M. Jr., Roering, C., Smith, C. A. and Van Schalkwyk, J. F., 1987. Deep crustal response to continental collision: The Limpopo belt of southern Africa. Geology, 15: 11-14.

Watkeys, M. K., Light, M. P. R. and Broderick, T. J., 1983. A retrospective view of the Central Zone of the Limpopo Belt, Zimbabwe. Spec. Publ. Geol. Soc. S. Afr., 8: 65-80.

Weaver, B. L. and Tarney, J., 1980. Rare earth geochemistry of Lewisian granulite-facies gneisses, northwest Scotland: implications for the petrogenesis of the Archaean lower continental crust. EPSL, 51: 279-296.

Winchester, J. A. and Floyd, P. A., 1977. Geochemical discrimination of different magma series and their differentiation products using immobile elements. Chem. Geol., 20: 325-343.

Windley, B. F., 1984. The Evolving Continents (2nd edition). New York: John Wiley and Sons. 399 pages.

Wood, D. A., 1979. A variably veined suboceanic upper mantle--Genetic significance for mid-ocean ridge basalts from geochemical evidence. Geology, 7: 499-503.

----------, Joron, J. -L. and Treuil, M., 1979. A re-appraisal of the use of trace elements to classify and discriminate between magma series erupted in different tectonic settings. EPSL, 45: 326-336.

This thesis is accepted on behalf of the faculty
of the Institute by the following committee:

_____
                    Advisor

_____

_____

_____

_____

_____7 June 1988_____
                    Date